



# THÈSE

En vue de l'obtention du

**DOCTORAT DE L'UNIVERSITÉ DE TOULOUSE**

Délivré par : *l'Université Toulouse 3 Paul Sabatier (UT3 Paul Sabatier)*

---

---

Présentée et soutenue le 11/07/2019 par :

**Sabrina HADJERAS**

**HYBRID CONTROL OF POWER CONVERTERS**

---

---

## JURY

LUIS MARTÍNEZ-SALAMERO	Professeur, U. Rovira i Virgili	Rapporteur
LAURENTIU HETEL	Chargé de Recherche, CNRS	Rapporteur
ROMAIN DELPOUX	M.D.C, INSA, Lyon	Membre du Jury
CORINNE ALONSO	Professeur, U. Paul Sabatier	Membre du Jury
CAROLINA ALBEA SANCHEZ	M.D.C, U. Paul Sabatier	Membre du Jury
GERMAIN GARCIA	Professeur, INSA, Toulouse	Membre du Jury

---

**École doctorale et spécialité :**

*EDSYS : Automatique 4200046*

**Unité de Recherche :**

*Laboratoire d'Analyse et d'Architecture des Systèmes du CNRS*

**Directeur(s) de Thèse :**

*Carolina ALBEA SANCHEZ et Germain GARCIA*

**Rapporteurs :**

*Luis MARTÍNEZ-SALAMERO et Laurentiu HETEL*



# Acknowledgments

---

Je tiens tout d'abord à remercier mes directeurs de thèse : Carolina Albea Sanchez et Germain Garcia pour m'avoir donné l'occasion de vivre cette expérience, pour leur présence, leur encadrement et leurs conseils.

Je suis reconnaissante envers Laurentieu Hetel et Luis Martinez-Sanamero pour avoir évalué mon manuscrit de thèse et pour leurs retours constructifs. Je remercie également mes examinateurs de thèse : Corinne Alonso et Romain Delpoux pour avoir évalué mes travaux.

Je remercie les autres membres de l'équipe MAC et toutes les personnes du laboratoire que j'ai pu côtoyer et plus particulièrement : Camille, Alex, Simo, Paolo, Matthieu, Flavien, Matteo, ...

Je remercie de tout cœur l'équipe pédagogique de l'université Paul Sabatier pour ses trois merveilleuses années partagés tous ensemble et plus précisément je tiens à dire un grand merci à Frédéric, Euriell, Pauline, Soheib, Emmanuel, Sylvain et toutes les personnes de l'équipe.

Je remercie vivement Catherine Stasiulis et la famille Bouvier qui nous ont soutenus et guidés durant ces cinq dernières années.

Je remercie Laura Sofía Urbina Iglesias pour le soutien moral qu'elle a pu m'apporter durant ses trois derniers années et pour toute sa gentillesse.

Je suis extrêmement reconnaissante envers Frédéric Gouaisbaut. Merci de m'avoir accompagnée depuis le master, pour toutes les choses que tu m'as apprises personnellement et scientifiquement et merci pour ton soutien sans faille.

Mes plus sincère remerciement à la famille Dumont et surtout Justin pour m'avoir soutenu jusqu'au bout de ce chemin. Désolée de t'avoir pris pour un punching ball, chose dont tu ne t'es jamais plaint. Merci énormément.

Pour finir et le plus important, je tiens à dire un grand merci à ma chère famille

---

pour leur soutien, un grand merci à Saïd pour sa présence dans les derniers jours de cette thèse et un grand merci à Lydia pour tout ce qu'elle m'a appris et pour son grand soutien.

# Abstract

---

This thesis proposes the design of hybrid control laws for power electronics converters. These new type of control laws are based on some hybrid models which capture the macroscopic dynamical behaviors of such electronic devices, essentially its hybrid nature. In the context of the regulation of DC-DC or AC-DC converters, applying the hybrid dynamical theory, the proposed control laws are proved to ensure the stability of the closed loop as well as some LQ performances. For a half-bridge inverter (DC-AC converter), a hybrid control law is proposed in order that the output voltage tracks a desired sinusoidal reference. In the case of unknown load, an adaptive control law is coupled to the hybrid control allowing the estimation of the load and therefore leading to a more precise regulation or tracking. Notice that in order to achieve a perfect regulation or tracking, an infinite frequency is often mandatory for the proposed control laws, which is inappropriate in practice. To tackle this problem, a space- or time-regularization are added to the hybrid closed-loop ensuring a dwell time between two consecutive jumps and reducing thus drastically the switching frequency.



# Résumé

---

Cette thèse propose la conception de lois de commandes hybrides pour les convertisseurs électroniques de puissance. Ce nouveau type de lois de commande est basé sur l'utilisation de modèles hybrides qui capturent les comportements dynamiques macroscopiques de ces dispositifs électroniques, essentiellement leur nature hybride. Dans le contexte de la régulation des convertisseurs DC-DC ou AC-DC, en appliquant la théorie des systèmes hybrides, il est ainsi prouvé que les lois de commandes proposées assurent la stabilité de la boucle fermée ainsi que certaines performances de type LQ. Pour un onduleur en demi-pont (convertisseur DC-AC), une loi de commande hybride est proposée afin que la tension de sortie suive une référence sinusoïdale souhaitée. Dans le cas d'une charge inconnue, une loi de commande adaptative est alors couplée à la commande hybride permettant l'estimation de la charge et donc une régulation ou un suivi de trajectoire plus précis. Notons que pour obtenir une régulation ou un suivi parfait, une fréquence infinie est souvent obligatoire pour les lois de contrôle proposées, ce qui est inappropriée en pratique. Pour résoudre ce problème, une régularisation de l'espace d'état ou du temps est ajoutée à la boucle fermée assurant un temps de maintien entre deux sauts consécutifs et réduisant ainsi considérablement la fréquence de commutation.





# Contents

---

<b>1</b>	<b>Introduction</b>	<b>1</b>
1.1	Introduction . . . . .	1
<b>2</b>	<b>Modeling of power converters</b>	<b>5</b>
2.1	Introduction . . . . .	5
2.2	Modeling some power converters . . . . .	6
2.2.1	DC-DC Converters: Boost converter . . . . .	6
2.2.2	AC-DC Converters: Three-phase three-level NPC Converter . . . . .	9
A	Modeling of the voltage input $v_{s\alpha}$ and $v_{s\beta}$ . . . . .	13
B	The NPC dynamical model based on instantaneous powers . . . . .	14
2.2.3	DC-AC Converters . . . . .	17
A	Half-bridge inverter . . . . .	17
2.3	Switched Affine System (SAS) . . . . .	19
2.4	Conclusions . . . . .	19
<b>3</b>	<b>Hybrid Dynamical System (HDS)</b>	<b>21</b>
3.1	Introduction . . . . .	21
3.2	Hybrid systems: modeling framework and basic notions . . . . .	22
3.2.1	Hybrid time domains . . . . .	23
3.3	Solutions to a hybrid system . . . . .	24
3.4	Basic assumptions on the hybrid data . . . . .	25
3.5	Hybrid system stability . . . . .	26
3.5.1	Singularly perturbed hybrid systems . . . . .	28
A	Manifold: . . . . .	29
B	Boundary layer system: . . . . .	29
C	Reduced system: . . . . .	30

---

3.6	Conclusions	30
<b>4</b>	<b>Hybrid control for DC-DC and AC-DC converters</b>	<b>31</b>
4.1	Introduction	31
4.2	DC-DC Converters: Boost converter	32
4.2.1	Problem formulation	33
4.2.2	Hybrid control for a boost converter	37
	A Optimality and parameters tuning	41
4.2.3	Hybrid adaptive control for a boost converter	43
	A Adaptation law	44
	B Hybrid model and proposed control law	46
4.2.4	Applications	53
4.2.5	Conclusions	60
4.3	AC-DC Converters: Three-phase three-level NPC Converter	62
4.3.1	The control objectives	64
4.3.2	Hybrid model and proposed control law	64
4.3.3	Applications	66
4.3.4	Conclusions	68
4.4	Conclusions	68
<b>5</b>	<b>Hybrid control for DC-AC converters</b>	<b>73</b>
5.1	Introduction	73
5.2	DC-AC Converters: Half-bridge inverter	74
5.2.1	Problem formulation	74
5.2.2	A reference model	75
5.2.3	Problem statement	76
	A Error dynamics model	77
5.2.4	Adaptation law	78
5.2.5	Hybrid model and proposed control law	79
5.2.6	Stability of the hybrid system	82
	A Singular perturbed form	83
	B Regularity of "manifold" and the fast sub-system	84
	C Stability for reduced system	85
	D Stability of the boundary layer	86
5.2.7	Applications	87
5.3	Conclusions	91
<b>6</b>	<b>Practical stabilisation of hybrid system with dwell-time guarantees</b>	<b>93</b>
6.1	Problem formulation	95
6.2	Practical global results using space- or time- regularization	96

---

CONTENTS

---

- 6.2.1 Space regularization . . . . . 99
- 6.2.2 Time regularization . . . . . 100
- 6.3 Illustrative example . . . . . 103
- 6.4 Conclusions . . . . . 108
  
- 7 Conclusions and perspectives 111**
- 7.1 Conclusions . . . . . 111
- 7.2 Perspectives . . . . . 112
  
- Bibliography 113**



# List of Figures

---

2.1	Illustration of the boost converter objective. . . . .	7
2.2	Boost converter circuit. . . . .	7
2.3	Boost converter circuit (ON). . . . .	8
2.4	Boost converter circuit (OFF). . . . .	8
2.5	Three-phase three-level neutral point clamped (NPC) rectifier. . . . .	10
2.6	Representation of a set (2.16) and the proposed polytope. . . . .	14
2.7	Half-bridge inverter. . . . .	18
3.1	Hybrid arc $\phi$ . . . . .	24
4.1	Attainable equilibrium points in sens of Fillipov. . . . .	35
4.2	Hybrid adaptive control scheme. . . . .	36
4.3	Hybrid adaptive control scheme. . . . .	36
4.4	Schematic representation of the flow and jump sets. . . . .	48
4.5	Voltage and current evolution of the boost converter. . . . .	55
4.6	Zoom of $u$ in the boost converter. . . . .	56
4.7	Evolution of the normalized switching frequency w.r.t. $\eta$ for different initial conditions in the boost converter. . . . .	57
4.8	Evolutions for $\gamma = 5 \cdot 10^{-4}$ of the voltage and current in a) and b) resp., $\check{x}_2$ in c) and, zoom of $u$ in d). . . . .	58
4.9	Evolutions for $\gamma = 50 \cdot 10^{-4}$ of the voltage and current in a) and b) resp., $\check{x}_2$ in c) and, zoom of $u$ in d) . . . . .	59
4.10	Evolutions for $\gamma = 0.1$ of the voltage and current in a) and b) resp., and zoom of $\check{x}_2$ and $u$ in c) and d) resp. . . . .	60
4.11	Evolutions for $\gamma = 1$ of the voltage and current in a) and b) resp., and zoom of $\check{x}_2$ and $u$ in c) and d) resp. . . . .	61
4.12	Evolution of the states for different values of sampling time $T_s$ . . . . .	69

---

4.13	Evolution of the phase currents for different values of sampling time $T_s$ and for $\eta = 0.1$ . . . . .	70
4.14	Evolution of the Lyapunov function. . . . .	71
5.1	Evolution of voltage and current for $\alpha = 200$ . . . . .	89
5.2	Evolution of voltage and current for $\alpha = 400$ . . . . .	90
5.3	Evolution of the estimation of $\beta$ and the error $\check{e}_2$ for $\alpha = 200$ and for $\alpha = 400$ . . . . .	91
6.1	Evolution of the states for different values of $\varepsilon$ . . . . .	103
6.2	Evolution of the states for different values of sampling time $T$ . . . . .	104
6.3	Top surfaces: evolution of the switching frequency with space regularization in the transient (left) and at the steady state (right). Bottom surfaces: evolution of the average switching frequency with time regularization in the transient (left) and at the steady state (right). . . . .	105
6.4	The chosen initial conditions. . . . .	106
6.5	Evolution of Lyapunov function for two values of $\varepsilon$ ( $\varepsilon=0.05$ and $\varepsilon=0.9$ ). . . . .	107
6.6	Lyapunov function $V(\tilde{x})$ with space regularization (left) and with time regularization (right). . . . .	108

# Notation

---

## List of symbols

- $\dot{x}$  : The derivative, with respect to time
- $x^+$  : The state of hybrid system after a jump
- $\mathbb{N}$  : The set of strictly positive integer numbers
- $\mathbb{R}$  : The set of real numbers
- $\mathbb{R}_{\geq 0}$  : The set of nonnegative real numbers
- $\mathbb{R}^n$  : The  $n$ -dimensional Euclidean space
- $\mathbb{R}^{n \times m}$  : The real  $n \times m$  matrices space
- $\mathcal{A} \cup \mathcal{B}$  : The union of sets  $\mathcal{A}$  and  $\mathcal{B}$
- $\mathcal{A} \cap \mathcal{B}$  : The intersection of sets  $\mathcal{A}$  and  $\mathcal{B}$
- $\mathcal{A} \subset \mathcal{B}$  : The set  $\mathcal{A}$  is a subset of  $\mathcal{B}$
- $\overline{\mathcal{A}}$  : The closure of set  $\mathcal{A}$
- $1_n$  : The identity matrix  $\mathbb{R}^{n \times n}$
- $\mathcal{S}^n$  : The set of symmetric positive definite matrices in  $\mathbb{R}^{n \times n}$
- $\langle \cdot, \cdot \rangle$  : denotes the standard Euclidean inner product
- $\otimes$  : define the Kronecker product
- $\text{diag}\{\alpha_1, \alpha_2, \dots, \alpha_n\}$  : The block-diagonal matrix whose diagonal elements are  $\alpha_1, \alpha_2, \dots, \alpha_n$

- $A^T$  : The transpose of a matrix  $A$
- $\text{Trace}(A)$  : The trace of a matrix  $A$
- $f : \mathbb{R}^n \rightarrow \mathbb{R}^m$  : This notation indicates that  $f$  is a function from  $\mathbb{R}^n$  to  $\mathbb{R}^m$
- $F : \mathbb{R}^n \rightrightarrows \mathbb{R}^m$  : This notation indicates that  $F$  is a set-valued mapping with  $F(x) \subset \mathbb{R}^m$  for each  $x \in \mathbb{R}^n$
- $|x|$  : The absolute value if  $x \in \mathbb{R}$ , the vector component-wise absolute value if  $x \in \mathbb{R}^n$
- $|x|_{\mathcal{A}}$  : The distance of  $x$  to a set  $\mathcal{A}$
- $|x|_P$  : related to the  $P$ -norm defined as  $x^T P x$ , where  $P$  is a matrix positive definite
- $\mathbb{B}$  : The closed unit ball, of the appropriate dimension, in the Euclidean norm
- $r\mathbb{B}$  : The closed ball of radius  $r$
- $\Re(x)$  : The real part of a complex number  $x$
- $\text{co}\{\mathcal{A}\}$  : The convex hull of the set  $\mathcal{A}$
- $\mathcal{K}_\infty$  : The class of functions from  $\mathbb{R}_{\geq 0}$  to  $\mathbb{R}_{\geq 0}$  that are continuous, zero at zero, strictly increasing, and unbounded
- $\text{argmin}(f)$  : stands for argument of the minimum of the function  $f$

## Acronym

- $AC$  : Alternating Current
- $DC$  : Direct Current
- $LMI$  : Linear Matrix Inequality
- $LQ$  : Linear Quadratic
- $NPC$  : Neutral Point Clamped converter
- $UGAS$  : Uniformly Globally Asymptotically Stable
- $SPAS$  : Semi-Globally Asymptotically Stable



# CHAPTER 1

## INTRODUCTION

---

### 1.1. Introduction

What does a mobile phone, an electrical household appliance or electric cars have in common? Of course, you answer me, electricity! Yes, all these devices use electricity as an energy source, an energy very useful but very difficult to store. Hence, it must be properly used and transformed according to our needs. Indeed, an electric oven or the display of our telephone does not require the same electrical power. Currently, we estimate that 15% of the energy produced must be converted and this is the role of electronic power converters. They allow to obtain from a DC or AC voltage source the desired shapes for the targeted application. We are talking about AC-AC, AC-DC (rectifier), DC-DC, DC-AC (inverter) converters. For several decades and the development of semiconductor technologies, designing such devices that are both accurate and efficient is a research challenge [1] [2] [3]. Roughly speaking, a power converter uses a number of uncontrolled (diodes) or controlled (transistors, for example) switches to manipulate signals issued (coming) from capacitors and inductors. The clever use of the different switches and the choice of their switching frequency allow to manage the energy transfer between the inductors and the capacitors in order to shape some output signal to some prescribed references, this last performance is indeed associated with this trajectory tracking, is the search for high energy efficiency (often over 90%), that effectively requires semiconductor-type components for switching devices. Indeed, these components are known to be lossless even if this last property related to the switching frequency and should be then chosen ingeniously. In general, an higher frequency increases the energy losses. However, reducing the switching frequencies leads to other problems such as the introduction of high frequency components on the output signal, limiting the accuracy of the devices [4][5][6].

A typical power converter is thus composed of switching devices, resistors, capacitors, inductors and transformers. Using classical assumptions (neglecting some

high frequency dynamics for instance) and circuit analysis, a non linear time varying dynamical model can be achieved, where the states are often the current flowing through the inductors and the voltages applied to the capacitors. The controlled input signals are booleans, representing if a switch is open and closed. From a theoretical point of view, this kind of system belongs to the broad class of hybrid systems and are known to be difficult to handle.

This is why many engineers and researchers have turned to models that are easier to handle. The first developed ideas are thus based on the development of an averaged model capturing only the macroscopic behaviors of the power electronic devices [1][6][7][8]. It calculates the evolution of average state space variables over a switching period neglecting the higher harmonics. This usually involves to set the switching frequency. For the point of view of the system, the control signal is thus averaged and considered to be a continuous time variable. One obtains therefore some time invariant non linear models for which classical control may be designed. This is how we will find the classical tools of linear and nonlinear systems (robust and adaptive control [9], feedback linearization [10], backstepping method [11] to cite a few).

The problem of such a model is the difficulty to control the quality of the approximation made. Thus, this model cannot explain a certain number of phenomena that may appear like ripples [12] or high frequency undesirable oscillations. Another problem is that it is often mandatory to fix the switching frequencies which may be a drawback for high quality power converters [3]. Then, in recent years, several studies have been carried out to take into account the original hybrid model. Indeed, the development of an increasingly comprehensive theory on the analysis and control of hybrid systems has removed a number of mathematical deadlocks. This approach has thus been at the heart of a number of studies that have allowed a more complex model to be taken into account.

This thesis explores this same vein and proposes a number of contributions listed below. In this thesis, we propose a control law based on the same idea than the ones presented previously. Hence, these controls are based on Hybrid Dynamical System (HDS) theory. As previously noted, in these strategies the real nature of the signals are considered, providing stability properties and LQ performances of the hybrid system.

## Contribution

The contribution we offer in this thesis aims to design hybrid control laws for several converters. Indeed based on the Hybrid Dynamical System (HDS), firstly, we propose a hybrid control law for the boost converter, whose system can be modeled by a non-linear system and then a hybrid adaptive control is developed for this system to deal

with the unknown parameter. Secondly, a control law is proposed for the NPC rectifier which is modeled by a nonlinear time-varying model, in the aim to regulate the output voltage to the desired reference. The last proposed hybrid control is devoted to the half-bridge converter, where the objective is track the desired sinusoidal signals.

### Organization of this thesis

This thesis is organized as follows.

- Chapter 2 gives the background needed to understand the roles of the chosen converters. In this part, a model of each converter is given in form of state-space and some properties of system are considered.
- The background about the Hybrid Dynamical System (HDS) is resumed in Chapter 3. The important definitions and theorems are recalled and the singular perturbed approach are described in the end of this chapter.
- In Chapter 4, hybrid control laws are proposed in order to regulate the output voltage of the converter to the desired constant reference. Stability and optimality properties are discussed and some simulations show the effectiveness of the proposed methodologies. As these converters are submitted to the parameters variations, a hybrid adaptive control is proposed to deal with the unknown parameters.
- Chapter 5 deals with the tracking problem. In this chapter a hybrid control law is proposed in order to make the states follow a desired sinusoidal signals. As in Chapter 4, the stability properties are checked and simulations are provided to illustrate the effectiveness of the proposed control.
- In Chapter 6, space- and time-regularization schemes are proposed to deal with the practical implementation problem, meaning to reduce the switching frequency. Using a hybrid systems approach, we have addressed the practical stabilization of operating points for switched affine systems, ensuring a minimum dwell time and an admissible chattering around the operating point. To this purpose, the proposed solutions induce uniform dwell time and provide useful tuning knobs to separately adjust the switching frequency during transients and at the steady state. The potentials of the method are illustrated by simulating a boost converter.
- Chapter 7 summarizes, discusses and puts into perspective the main results obtained during my thesis work.

## Publications

### Conference

- Sabrina Hadjeras, Carolina Albea Sanchez and Germain Garcia, Hybrid adaptive control of the boost converter, in 2017 IEEE 56th Annual Conference on Decision and Control (CDC), Me 5720–5725, Melbourne, AUSTRALIA. December 12–15, 2017.
- Sabrina Hadjeras, Jesse-James Prince Agbodjan, Carolina Albea Sanchez and Germain Garcia, Hybrid adaptive control for the half-bridge inverter, in 2019 American Control Conference (ACC), Philadelphia, USA. July 10–12, 2019.
- Sabrina Hadjeras, Carolina Albea Sanchez, Fabio Gómez-Estern, Francisco Gordillo and Germain Garcia, Hybrid Control Law for a Three-Level NPC Rectifier, in 2019 European Control Conference (ECC) (in cooperation with IFAC), Naples, ITALY. Jun 25–28, 2019.

### Journal

- Carolina Albea Sanchez, Germain Garcia, Sabrina Hadjeras, Maurice Heemels, Luca Zaccarian. Practical stabilisation of switched affine systems with dwell-time guarantees. In IEEE Transactions on Automatic Control (TAC). April 2019. IEEE.

# CHAPTER 2

## MODELING OF POWER CONVERTERS

---

### Sommaire

---

<b>2.1</b>	<b>Introduction</b>	<b>5</b>
<b>2.2</b>	<b>Modeling some power converters</b>	<b>6</b>
2.2.1	DC-DC Converters: Boost converter	6
2.2.2	AC-DC Converters: Three-phase three-level NPC Converter	9
2.2.3	DC-AC Converters	17
<b>2.3</b>	<b>Switched Affine System (SAS)</b>	<b>19</b>
<b>2.4</b>	<b>Conclusions</b>	<b>19</b>

---

### 2.1. Introduction

One of the main objective of power electronics is to achieve a conversion of electric energy from its available form, to a required one by using electronic devices as power converters. In order to get a high efficiency and reliability of this conversion, it is necessary to design advanced control laws that govern the switches of the converters. The common classification of these converters are [13]:

- DC-DC converter, where 'DC' (Direct Current) refers to constant voltage waveforms. It relates to a regulation problem in control purposes.
- AC-DC converter (called also rectifier), where 'AC' (Alternating Current) refers to a sinusoidal voltage waveforms. It relates to a regulation problem also.
- DC-AC converter (called also inverter). It is a matter of a tracking problem in control purposes.
- AC-AC converter is as the DC-AC converter, relates to a tracking problem.

Control circuits are key elements in the conversion operation and performance of power converters. Through the design of advanced controls, we can get a high efficiency level. For example, DC-DC converters are used in many devices such as cell phones, where the circuits require higher voltage than the one generated by a battery. Then DC-DC converters can be used to boost the voltage and yield the required voltage [13].

In order to analyze and control the power converters, the first step is to get a mathematical model. To this purpose, we will start by describing these electronic converters, understanding how they work in order to design a mathematical model.

## 2.2. Modeling some power converters

In order to control power electronic converters, it is necessary to get a mathematical model. To this end, the next section describes briefly the structure and the principal functionality of some basic power electronic converters. Furthermore, some models in the form of state-space representation are proposed.

### 2.2.1. DC-DC Converters: Boost converter

DC-DC converters are power electronic circuits that are able to convert a DC voltage input level to a different DC voltage output level, often providing a regulated output, which is a regulation problem. As fundamental DC-DC converters, we can cite, buck converter, boost converter and buck-boost converter. In this section, we focus only on the boost converter.

Boost converters are largely used in many kind of applications such as uninterruptible power supply (UPS) systems [14] [15], power factor correctors [16], photovoltaic arrays, fuel cells, battery energy storage systems [17] and thermoelectric energy harvesting systems [18] to cite few of them. A boost converter generates a DC output voltage,  $v_C$ , larger than its DC input,  $V_{in}$ , by manipulating the state of the switch, denoted by  $u$  (see Figure 2.1). As depicted in Figure 2.2, the boost converter is fed by a constant voltage source, denoted  $V_{in}$ , and composed by a load filter,  $L, C_0$ , a purely and resistive load,  $R_0$ , and a parasite resistance,  $R_{LS}$ , that encompasses switching energy dissipation and the power loss in the inductance.

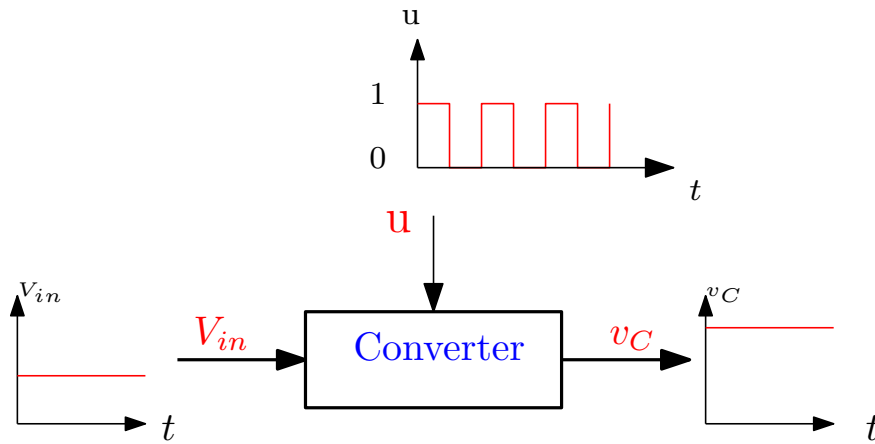


Figure 2.1: Illustration of the boost converter objective.

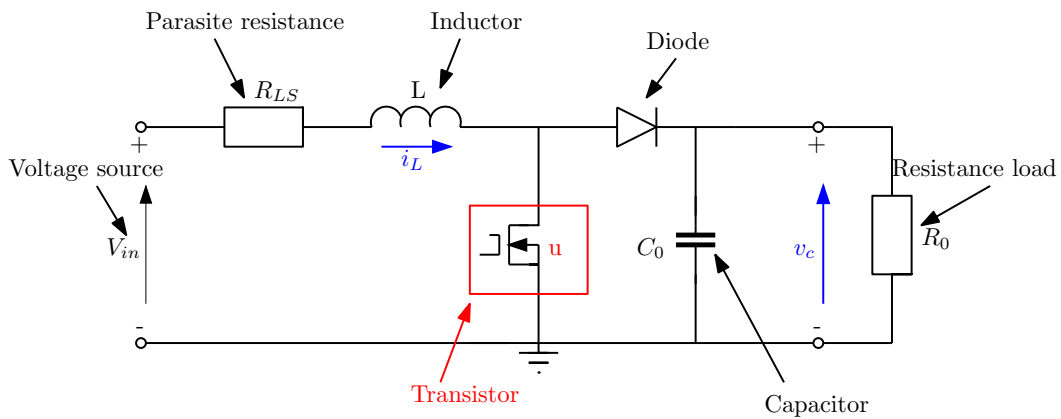


Figure 2.2: Boost converter circuit.

The system states are given by  $i_L \in \mathbb{R}$ , which is the inductor current and  $v_C \in \mathbb{R}$ , which is the capacitor voltage. Likewise, the control input manages the functioning mode of the switch  $u = \{0, 1\}$ , that corresponds to the case when the switch is ON ( $u = 1$ ) and when it is OFF ( $u = 0$ ).

**NOTE:**

*Boost converter system exhibits two kind of dynamics, the continuous-time dynamic, which is presented by the inductor current  $i_L$  and the capacitor voltage  $v_C$  and the discrete-time dynamic, which presents the dynamic of the state of the switch  $u$ .*

Depending on the functioning modes of the switch, the boost converter operates on two distinct phases, as follows:

**Switch ON ( $u = 1$ ):** When the transistor is turned ON ( $u = 1$ ) (See Figure 2.3), the boost converter circuit can be modeled by:

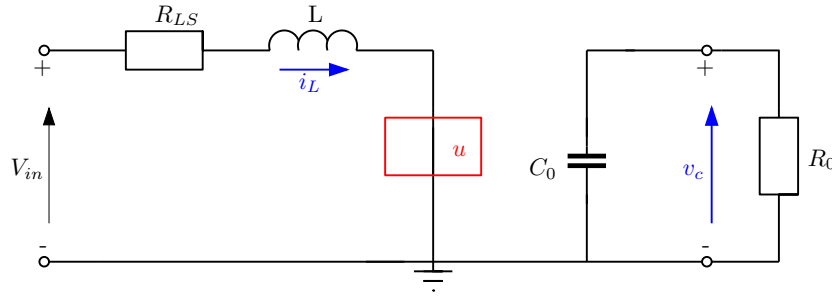


Figure 2.3: Boost converter circuit (ON).

In this configuration, the inductor  $L$  charges up, the inductor current  $i_L$  increases and the inductance stores a quantity of energy as magnetic energy. At the same time, the diode is reverse-biased and the capacitor discharges on the load  $R_0$ .

Applying the Kirchhoff's law, the system can be modeled by the following state-space model:

$$\frac{d}{dt} \begin{bmatrix} i_L(t) \\ v_C(t) \end{bmatrix} = \overbrace{\begin{bmatrix} -\frac{R_{LS}}{L} & 0 \\ 0 & -\frac{1}{R_0 C_0} \end{bmatrix}}^{A_1} \begin{bmatrix} i_L(t) \\ v_C(t) \end{bmatrix} + \overbrace{\begin{bmatrix} \frac{1}{L} \\ 0 \end{bmatrix}}^{B_1} V_{in}. \quad (2.1)$$

**Switch OFF ( $u = 0$ ):** When the transistor is turned OFF ( $u = 0$ ) (See Figure 2.4), the energy stored in the inductance  $L$  adds up with the given input energy feed the capacitor and the load. The diode becomes forward-biased to provide a path for the inductor current. Thus, the inductor current  $i_L$  ramps downward and this current flows through the diode to the capacitor, the capacitor voltage increases and capacitor stores energy as electrical energy.

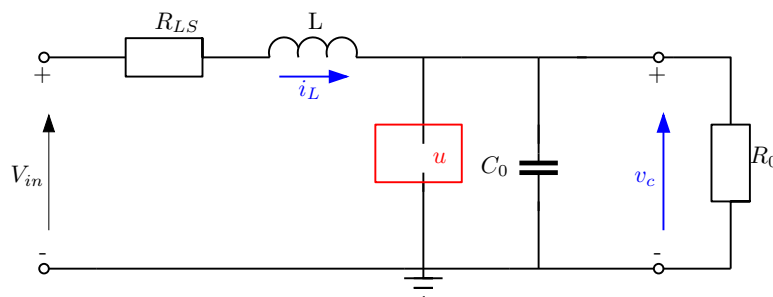


Figure 2.4: Boost converter circuit (OFF).

Applying the Kirchhoff's law, the state-space model of system described by Fig-



Figure 2.4 is given by:

$$\frac{d}{dt} \begin{bmatrix} i_L(t) \\ v_C(t) \end{bmatrix} = \overbrace{\begin{bmatrix} -\frac{R_{LS}}{L} & -\frac{1}{L} \\ \frac{1}{C_0} & -\frac{1}{R_0 C_0} \end{bmatrix}}^{A_0} \begin{bmatrix} i_L(t) \\ v_C(t) \end{bmatrix} + \overbrace{\begin{bmatrix} \frac{1}{L} \\ 0 \end{bmatrix}}^{B_0} V_{in}. \quad (2.2)$$

Note that, the model (2.1) and (2.2) can be rewritten in the compact form  $(\Sigma)$  given as:

$$(\Sigma) : \begin{cases} \dot{x}(t) = \overbrace{\begin{bmatrix} -\frac{R_{LS}}{L} & -\frac{1-u}{L} \\ \frac{1-u}{C_0} & -\frac{1}{R_0 C_0} \end{bmatrix}}^{A_u} x(t) + \overbrace{\begin{bmatrix} \frac{V_{in}}{L} \\ 0 \end{bmatrix}}^{B_u}, \\ y(t) = \overbrace{\begin{bmatrix} 0 & 1 \end{bmatrix}}^{C_u} x(t), \end{cases} \quad (2.3)$$

with  $x(t) = [i_L(t) \ v_C(t)]^T$  is the state vector,  $y(t)$  is the controlled output and  $u = \{0, 1\}$  is the control input.

To conclude, the boost converter can be modeled by a nonlinear time-invariant model given in equation (2.3). Furthermore, the obtained model contains a continuous-time dynamics, i.e; the dynamic of inductor current,  $i_L(t)$ , and the dynamic of capacitor voltage,  $v_C(t)$ . The control input of this model is the switching state  $u$ , which means that the dynamic of the control input are a discrete-time dynamics.

### 2.2.2. AC-DC Converters: Three-phase three-level NPC Converter

AC-DC converters are power electronic circuits that are able to generate a DC output from an AC input, which means it is a tracking problem. This converter is also considered as a multilevel power converter since they can generate different levels of the output voltage, The interest of the multilevel converters relies on the fact that by increasing the number of levels, the voltages generated by the converters have more possible steps to produce staircase waveforms. The sinusoidal waveforms can thus be approached and the total harmonic distortions can be reduced. In this work, we are interested specially in the three-phase three-level Neutral Point Clamped (NPC) converter.

The three-phase three-level NPC Converters have the advantage to improve the waveform quality and reduce voltage stress on the power devices. These converters are widely used in the field of high power industrial application such as photovoltaic (PV) system [19], fans, pumps and in the ones of wind energy conversion system [20].

The considered converter works as a rectifier [21], whose structure is depicted in Figure 2.5. This converter is connected to the grid through inductors of the same values,  $L$ , and parasitic resistances,  $R_{LS}$ . These parasitic resistances model not only the resistive components of the inductance, but also the dissipated switching energy. The phase voltages and the phase currents are denoted by  $v_{sa}, v_{sb}, v_{sc}$  and  $i_a, i_b, i_c$ , respectively. The  $dc$  link contains two capacitors  $C_1$  and  $C_2$ , which respective voltages are denoted by  $v_{c1}$  and  $v_{c2}$ , and their two parasitic resistances  $R_{p1}$  and  $R_{p2}$ , which model the parasitic imperfections of the capacitors  $C_1$  and  $C_2$ . This  $dc$  link is also connected to a pure resistive load  $R$ , and the voltage across this load is denoted by  $v_{dc}$ . This voltage is the sum of the capacitor voltages ( $v_{dc} = v_{c1} + v_{c2}$ ).

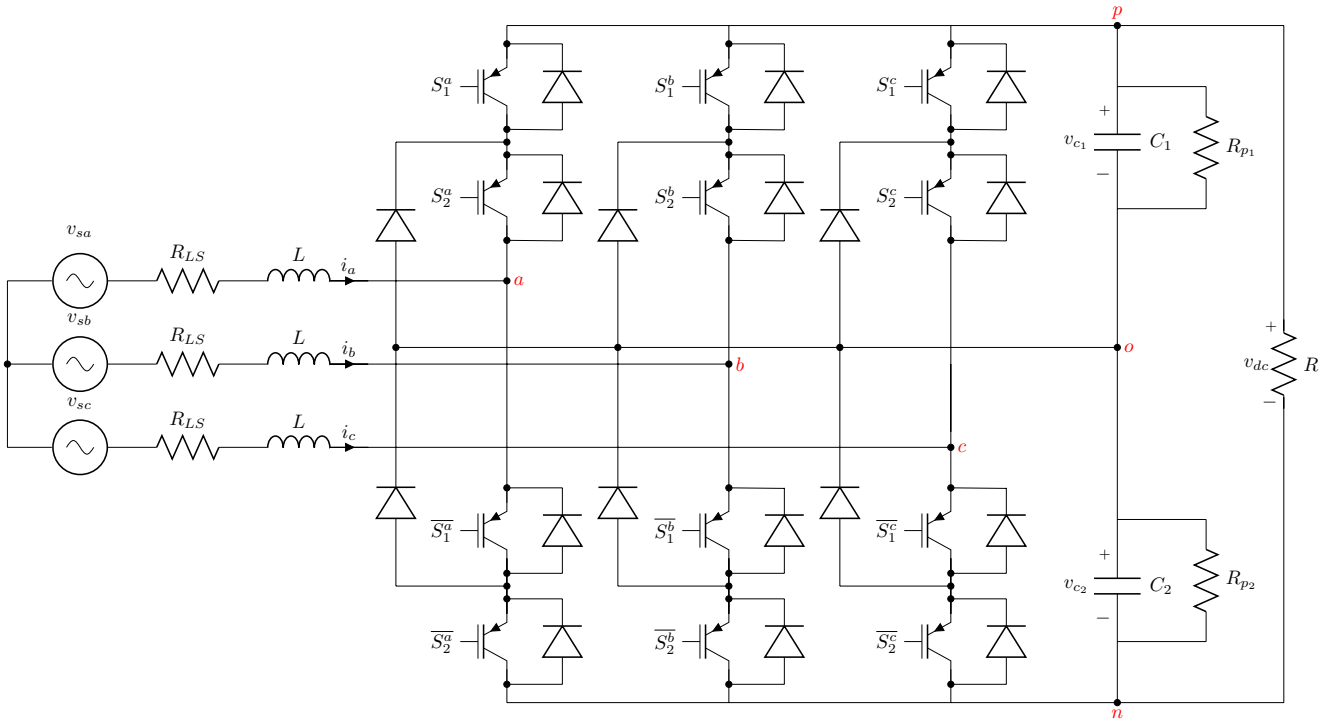


Figure 2.5: Three-phase three-level neutral point clamped (NPC) rectifier.

The circuit contains 6 complementary switches ( $S_l^i, \overline{S}_l^i$ ), with  $i = \{a, b, c\}$  and  $l = \{1, 2\}$ . The control inputs  $d_{ij} \in \{0, 1\}$ , with  $i = \{a, b, c\}$  and  $j = \{p, o, n\}$ , control the switches and they are assumed to be discrete variables:

$$d_{ij} = \begin{cases} 1, & \text{if phase } i \text{ is connected to level } j \\ 0, & \text{else.} \end{cases} \quad (2.4)$$

The phase  $i$  is connected to level  $j$  means that the switches between these two points are turned ON. The table 2.1 depicts when the control inputs are equal to 1.

Furthermore, they are equal to zero in other cases.  $X$  means ON or OFF, i.e; the position of the switch does not affect the value of the corresponding control input.

States =1	$S_1^a$	$S_1^b$	$S_1^c$	$S_2^a$	$S_2^b$	$S_2^c$	$\overline{S_1^a}$	$\overline{S_1^b}$	$\overline{S_1^c}$	$\overline{S_2^a}$	$\overline{S_2^b}$	$\overline{S_2^c}$
$d_{ap}$	ON	X	X	ON	X	X	OFF	X	X	OFF	X	X
$d_{ao}$	OFF	X	X	ON	X	X	ON	X	X	OFF	X	X
$d_{an}$	OFF	X	X	OFF	X	X	ON	X	X	ON	X	X
$d_{bp}$	X	ON	X	X	ON	X	X	OFF	X	X	OFF	X
$d_{bo}$	X	OFF	X	X	ON	X	X	ON	X	X	OFF	X
$d_{bn}$	X	OFF	X	X	OFF	X	X	ON	X	X	ON	X
$d_{cp}$	X	X	ON	X	X	ON	X	X	OFF	X	X	OFF
$d_{co}$	X	X	OFF	X	X	ON	X	X	ON	X	X	OFF
$d_{cn}$	X	X	OFF	X	X	OFF	X	X	ON	X	X	ON

Table 2.1: Relation between the control input and switches

At this stage, in order to control the whole system, we need 6 control inputs ( $d_{ij} \in \{0, 1\}$ ) presented in table 2.1. Moreover, according to the circuit presented in Figure 2.5 and since the switches are complementary, these control variables present the following constraint [22]:

$$d_{ip} + d_{io} + d_{in} = 1, \quad \text{for } i = \{a, b, c\}.$$

✦ **ASSUMPTION 1:**

Consider the following approximation of system depicted in Figure 2.5

- $C_1 = C_2 = C;$
- $R_{p1} = R_{p2} = R_p$

✦ **ASSUMPTION 2:**

The phase voltages and currents are balanced, that is:

$$\begin{aligned} v_{sa}(t) + v_{sb}(t) + v_{sc}(t) &= 0, \\ i_a(t) + i_b(t) + i_c(t) &= 0. \end{aligned}$$

If Assumption 2 is verified, then, the model of the NPC rectifier (Figure 2.5) in  $abc$  coordinates can be expressed as:

$$L \frac{di_a(t)}{dt} = v_{sa}(t) - R_{LS}i_a(t) + \frac{2d_{an} - 2d_{ap} - d_{bn} + d_{bp} - d_{cn} + d_{cp}}{6} v_{dc}(t) + \frac{-2d_{an} - 2d_{ap} + d_{bn} + d_{bp} + d_{cn} + d_{cp}}{6} v_d(t) \quad (2.5)$$

$$L \frac{di_b(t)}{dt} = v_{sb}(t) - R_{LS}i_b(t) - \frac{d_{an} - d_{ap} - 2d_{bn} + 2d_{bp} + d_{cn} - d_{cp}}{6} v_{dc}(t) + \frac{d_{an} + d_{ap} - 2d_{bn} - 2d_{bp} + d_{cn} + d_{cp}}{6} v_d(t) \quad (2.6)$$

$$L \frac{di_c(t)}{dt} = v_{sc}(t) - R_{LS}i_c(t) - \frac{d_{an} - d_{ap} + d_{bn} - d_{bp} - 2d_{cn} + 2d_{cp}}{6} v_{dc}(t) + \frac{d_{an} + d_{ap} + d_{bn} + d_{bp} - 2d_{cn} - 2d_{cp}}{6} v_d(t) \quad (2.7)$$

$$C \frac{dv_{dc}(t)}{dt} = (d_{ap} - d_{an})i_a(t) + (d_{bp} - d_{bn})i_b(t) + (d_{cp} - d_{cn})i_c(t) - \left( \frac{2}{R} + \frac{1}{R_p} \right) v_{dc}(t) \quad (2.8)$$

$$C \frac{dv_d(t)}{dt} = (d_{ap} + d_{an})i_a(t) + (d_{bp} + d_{bn})i_b(t) + (d_{cp} + d_{cn})i_c(t) - \frac{1}{R_p} v_d(t), \quad (2.9)$$

where  $v_d$  represents the dc-link capacitor voltage difference ( $v_d(t) = v_{c_1}(t) - v_{c_2}(t)$ ). Notice that,  $v_{sa}(t)$ ,  $v_{sb}(t)$ ,  $v_{sc}(t)$  are the grid voltage in the so-called  $abc$  coordinates. In order to take into account the balanced phase voltages and currents, we propose this change of variables [23]:

$$\begin{bmatrix} i_\alpha(t) \\ i_\beta(t) \\ i_\gamma(t) \end{bmatrix} = T_{abc \rightarrow \alpha\beta\gamma} \begin{bmatrix} i_a(t) \\ i_b(t) \\ i_c(t) \end{bmatrix}. \quad (2.10)$$

$$\begin{bmatrix} v_{s\alpha}(t) \\ v_{s\beta}(t) \\ v_{s\gamma}(t) \end{bmatrix} = T_{abc \rightarrow \alpha\beta\gamma} \begin{bmatrix} v_{sa}(t) \\ v_{sb}(t) \\ v_{sc}(t) \end{bmatrix}. \quad (2.11)$$

$$\begin{bmatrix} d_{ip} \\ d_{lo} \\ d_{in} \end{bmatrix} = T_{abc \rightarrow \alpha\beta\gamma} \begin{bmatrix} d_{ip} \\ d_{io} \\ d_{in} \end{bmatrix}, \quad (2.12)$$

with  $l = \{\alpha, \beta, \gamma\}$ ,  $i = \{a, b, c\}$  and  $T_{abc \rightarrow \alpha\beta\gamma}$  is given as:

$$T_{abc \rightarrow \alpha\beta\gamma} = \sqrt{\frac{2}{3}} \begin{bmatrix} 1 & -\frac{1}{2} & -\frac{1}{2} \\ 0 & \frac{\sqrt{3}}{2} & -\frac{\sqrt{3}}{2} \\ \frac{1}{\sqrt{2}} & \frac{1}{\sqrt{2}} & \frac{1}{\sqrt{2}} \end{bmatrix}. \quad (2.13)$$

This transformation is named the Clarke Transformation [23]. Considering the variables change given in equations (2.10)–(2.12), then the model of the rectifier in  $\alpha\beta\gamma$  coordinates can be written as:

$$\begin{cases} L \frac{di_\alpha(t)}{dt} = v_{s\alpha}(t) - R_{LS}i_\alpha(t) - (d_{\alpha p} - d_{\alpha n})\frac{v_{dc}(t)}{2} - (d_{\alpha p} + d_{\alpha n})\frac{v_d(t)}{2} \\ L \frac{di_\beta(t)}{dt} = v_{s\beta}(t) - R_{LS}i_\beta(t) - (d_{\beta p} - d_{\beta n})\frac{v_{dc}(t)}{2} - (d_{\beta p} + d_{\beta n})\frac{v_d(t)}{2} \\ C \frac{dv_{dc}(t)}{dt} = (d_{\alpha p} - d_{\alpha n})i_\alpha(t) + (d_{\beta p} - d_{\beta n})i_\beta(t) - \left(\frac{2}{R} + \frac{1}{R_p}\right)v_{dc}(t) \\ C \frac{dv_d(t)}{dt} = (d_{\alpha p} + d_{\alpha n})i_\alpha(t) + (d_{\beta p} + d_{\beta n})i_\beta(t) - \frac{1}{R_p}v_d(t), \end{cases} \quad (2.14)$$

where the control inputs  $d_{\alpha p}$ ,  $d_{\alpha n}$ ,  $d_{\beta p}$  and  $d_{\beta n}$  are the transformed of the control inputs  $d_{ij} \in \{0, 1\}$ , with  $i = \{a, b, c\}$  and  $j = \{p, o, n\}$ , given in (2.4). Notice that the control inputs  $d_{\gamma j}$  and  $d_{io}$  do not appear in this model.

The voltage variables,  $v_{s\alpha}(t)$  and  $v_{s\beta}(t)$ , and the current variables,  $i_\alpha(t)$  and  $i_\beta(t)$ , are the transformations in  $\alpha\beta\gamma$  of the phase voltages and phase currents, respectively. Notice that, according to Assumption 2, as the phase voltages and phase currents are assumed to be balanced, then the last transformation leads to:


$$\begin{aligned} v_{s\gamma}(t) &= 0 \\ i_\gamma(t) &= 0. \end{aligned}$$

#### A. Modeling of the voltage input $v_{s\alpha}$ and $v_{s\beta}$

The grid voltages in  $\alpha\beta\gamma$  coordinates are expressed as follows:

$$\begin{cases} v_{s\alpha}(t) = V_{s\alpha} \sin(wt) \\ v_{s\beta}(t) = V_{s\beta} \cos(wt), \end{cases} \quad (2.15)$$

where  $V_{s\alpha}$ ,  $V_{s\beta}$  and  $w$  are, respectively, the amplitude and the frequency of the grid voltage. We assume in the following that  $V_{s\alpha} = V_{s\beta} = V_s$ .

 **REMARK 1.** Note that from (2.15), it is simple to deduce that

$$v_{s\alpha}^2(t) + v_{s\beta}^2(t) = V_s^2.$$

We can therefore define the following set

$$\Phi = \{(v_{s\alpha}(t), v_{s\beta}(t)) \in \mathbb{R}^2, v_{s\alpha}^2(t) + v_{s\beta}^2(t) = V_s^2\}. \quad (2.16)$$

As depicted in Fig. 2.6, the set (2.16) can be embedded into a polytope described as:

$$\Omega := \sum_{j=1}^4 \nu_j \Omega_j \quad \text{for } 0 \leq \nu_j \leq 1 \quad \text{and} \quad \sum_{j=1}^4 \nu_j(t) = 1,$$

where  $\Omega_j$  ( $j = 1, 2, 3, 4$ ) represents the vertices of the polytope in the  $(v_{s\alpha}, v_{s\beta})$ -plane:

$$\Omega_1 = \begin{bmatrix} V_{s\alpha} \\ V_{s\beta} \end{bmatrix}, \quad \Omega_2 = \begin{bmatrix} -V_{s\alpha} \\ V_{s\beta} \end{bmatrix}, \quad \Omega_3 = \begin{bmatrix} V_{s\alpha} \\ -V_{s\beta} \end{bmatrix}, \quad \Omega_4 = \begin{bmatrix} -V_{s\alpha} \\ -V_{s\beta} \end{bmatrix}.$$

The evolution of system (2.15) is depicted by a green circle in Figure 2.6, and its evolution dynamical can be included into a polytope, surrounded by a red square, defined by four vertices (1, 2, 3, 4).

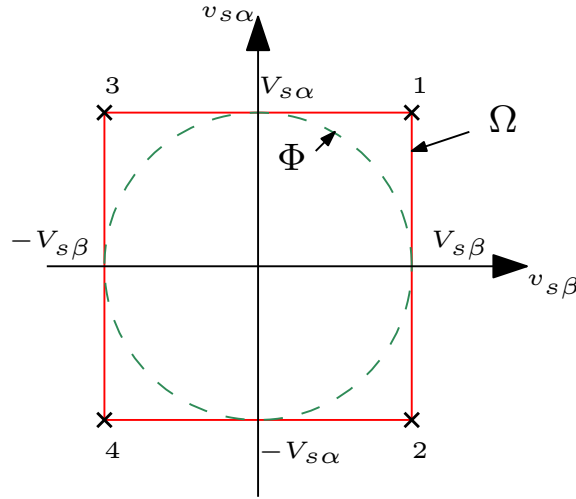


Figure 2.6: Representation of a set (2.16) and the proposed polytope.

### B. The NPC dynamical model based on instantaneous powers

The control algorithm is easier to express using instantaneous powers instead of current variables [24]. Furthermore, phase currents  $i_\alpha$  and  $i_\beta$  can be also expressed in terms of instantaneous active and reactive powers [25]:

$$i_\alpha(t) = \frac{1}{V_s^2} (v_{s\alpha}(t)p(t) - v_{s\beta}(t)q(t)) \quad (2.17)$$

$$i_\beta(t) = \frac{1}{V_s^2} (v_{s\beta}(t)p(t) + v_{s\alpha}(t)q(t)) \quad (2.18)$$

where  $p$  and  $q$  represent the instantaneous active and reactive powers of the system, respectively.

Then, model (2.14) can be rewritten according to the new state variable  $x = [p(t) q(t) v_{dc}(t) v_d(t)]^T$ :

$$(\Sigma) : \left\{ \begin{array}{l} \dot{x}(t) = \overbrace{\begin{bmatrix} -\frac{R_{LS}}{L} & 2\pi f & -\frac{\xi_1(t)}{2L} & -\frac{\xi_3(t)}{2L} \\ -2\pi f & -\frac{R_{LS}}{L} & \frac{\xi_2(t)}{2L} & \frac{\xi_4(t)}{2L} \\ \frac{\xi_1(t)}{CV_s^2} & -\frac{\xi_2(t)}{CV_s^2} & -(\frac{2}{RC} + \frac{1}{R_p C}) & 0 \\ \frac{\xi_3(t)}{CV_s^2} & -\frac{\xi_4(t)}{CV_s^2} & 0 & -\frac{1}{R_p C} \end{bmatrix}}^{A_u(t)} x(t) + \overbrace{\begin{bmatrix} \frac{V_s^2}{L} \\ 0 \\ 0 \\ 0 \end{bmatrix}}^{B_u}, \\ y(t) = \overbrace{\begin{bmatrix} 0 & 0 & 0 & 1 \end{bmatrix}}^{C_u} x(t), \end{array} \right. \quad (2.19)$$

where,  $f$  is the frequency of the phase voltages, and

$$\begin{aligned} \xi_1(t) &= u_1 v_{s\alpha}(t) + u_2 v_{s\beta}(t), & \xi_2(t) &= u_1 v_{s\beta}(t) - u_2 v_{s\alpha}(t), \\ \xi_3(t) &= u_3 v_{s\alpha}(t) + u_4 v_{s\beta}(t), & \xi_4(t) &= u_3 v_{s\beta}(t) - u_4 v_{s\alpha}(t). \end{aligned}$$

These equations can be rewritten as follows:

$$\xi(t) = \begin{bmatrix} \Gamma & 0 \\ 0 & \Gamma \end{bmatrix} u. \quad (2.20)$$

with  $\xi(t) = [\xi_1(t) \ \xi_2(t) \ \xi_3(t) \ \xi_4(t)]^T$  and  $\Gamma(t) = \begin{bmatrix} v_{s\alpha}(t) & v_{s\beta}(t) \\ v_{s\beta}(t) & -v_{s\alpha}(t) \end{bmatrix}$ .

$u = [u_1 \ u_2 \ u_3 \ u_4]^T$  is a vector containing the control variables

$$\begin{aligned} u_1 &= d_{\alpha p} - d_{\alpha n} & u_2 &= d_{\beta p} - d_{\beta n} \\ u_3 &= d_{\alpha p} + d_{\alpha n} & u_4 &= d_{\beta p} + d_{\beta n}. \end{aligned}$$

At this stage, let consider vector  $u = [u_1 \ u_2 \ u_3 \ u_4]^T$  with  $u \in U$ , where  $U$  is a set of all possible combinations for the control inputs. For the considered synchronous rectifier, there are 27 possible combinations of the switches [23], but as there are three redundant zero switching states, it suffices to consider 25 combinations, meaning that  $u \in \{u^{(1)}, \dots, u^{(25)}\}$  with  $u \in \mathbb{R}^4$ . Note that, the model (2.19) is a nonlinear time-variant system.

To ease the stability analysis, a new formulation of this nonlinear time-varying system is proposed, based on a polytopic presentation. First of all, notice that the matrix

$\Gamma$  defined in (2.20) can be written as a polytope:

$$\Gamma = \sum_{j=1}^4 \mu_j(t) \Gamma_j,$$

where  $\mu_j(t) \in [0, 1]$  is a function satisfying  $\sum_{j=1}^4 \mu_j(t) = 1$  and  $\Gamma_j$  are defined as

$$\begin{aligned} \Gamma_1 &= \begin{bmatrix} V_{s\alpha} & V_{s\beta} \\ V_{s\beta} & -V_{s\alpha} \end{bmatrix}, & \Gamma_2 &= \begin{bmatrix} -V_{s\alpha} & V_{s\beta} \\ V_{s\beta} & V_{s\alpha} \end{bmatrix} \\ \Gamma_3 &= \begin{bmatrix} V_{s\alpha} & -V_{s\beta} \\ -V_{s\beta} & -V_{s\alpha} \end{bmatrix}, & \Gamma_4 &= \begin{bmatrix} -V_{s\alpha} & -V_{s\beta} \\ -V_{s\beta} & V_{s\alpha} \end{bmatrix}. \end{aligned}$$

Then, equation (2.20) can be written as:

$$\xi = \sum_{j=1}^4 \mu_j(t) \begin{bmatrix} \Gamma_j & 0 \\ 0 & \Gamma_j \end{bmatrix} u.$$

Matrix  $A_u(t)$  defined in system (2.19), can also be written as follows:

$$A_u(t) = \sum_{j=1}^4 \mu_j(t) \tilde{A}_u(j), \quad (2.21)$$

where

$$\tilde{A}_u(j) = \begin{bmatrix} M_1 & M_2 & M_3 & M_4 \end{bmatrix} \left( \begin{bmatrix} \Gamma_j & 0 \\ 0 & \Gamma_j \end{bmatrix} u \right) \otimes 1_4 + M_0 \quad (2.22)$$

and

$$\begin{aligned} M_0 &= \begin{bmatrix} -\frac{R_{LS}}{L} & 2\pi f & 0 & 0 \\ -2\pi f & -\frac{R_{LS}}{L} & 0 & 0 \\ 0 & 0 & -(\frac{2}{RC} + \frac{1}{R_p C}) & 0 \\ 0 & 0 & 0 & -\frac{1}{R_p C} \end{bmatrix} \\ M_1 &= \begin{bmatrix} 0 & 0 & -\frac{1}{2L} & 0 \\ 0 & 0 & 0 & 0 \\ \frac{1}{CV_s^2} & 0 & 0 & 0 \\ 0 & 0 & 0 & 0 \end{bmatrix}, & M_2 &= \begin{bmatrix} 0 & 0 & 0 & 0 \\ 0 & 0 & \frac{1}{2L} & 0 \\ 0 & -\frac{1}{CV_s^2} & 0 & 0 \\ 0 & 0 & 0 & 0 \end{bmatrix}, \end{aligned}$$



$$M_3 = \begin{bmatrix} 0 & 0 & 0 & -\frac{1}{2L} \\ 0 & 0 & 0 & 0 \\ 0 & 0 & 0 & 0 \\ \frac{1}{CV_s^2} & 0 & 0 & 0 \end{bmatrix}, \quad M_4 = \begin{bmatrix} 0 & 0 & 0 & 0 \\ 0 & 0 & 0 & \frac{1}{2L} \\ 0 & 0 & 0 & 0 \\ 0 & -\frac{1}{CV_s^2} & 0 & 0 \end{bmatrix}.$$

Consequently, the original nonlinear model (2.19) can be rewritten as a polytopic system as follows:

$$\dot{x}(t) = \sum_{j=1}^4 \mu_j(t) \tilde{A}_u(j)x(t) + B, \quad (2.23)$$

with  $x = [p(t) \ q(t) \ v_{dc}(t) \ v_d(t)]^T$  is the state vector and  $u = [u_1 \ u_2 \ u_3 \ u_4]^T$  is a vector containing the control variables.

The three-phase three-level NPC rectifier can be modeled by a nonlinear time-varying model given in (2.19). The model contains a continuous-time dynamics, i.e; the dynamic of inductor currents and the dynamic of capacitor voltages. The control input of this model is the switching state  $u$ , taking its value in the discrete set  $U$ , which means that the dynamic of the control input are a discrete-time dynamics.

### 2.2.3. DC-AC Converters

This section deals with inverters that produce an AC output from a DC input. Inverters are used in applications such as adjustable-speed AC motor drives, Uninterruptible Power Supplies (UPS), and running AC appliances from an automobile battery. In this work, we are interested specially in the half-bridge inverter and the boost inverter.

#### A. Half-bridge inverter

We consider a half-bridge inverter depicted in Figure 2.7. This inverter is fed by a dc input,  $2V_{in}$ , and generates an ac output. This inverter is composed by a load filter,  $L, C_0$ , a purely resistive load,  $R_0$ . The parasite resistance  $R_{LS}$  models not only the switching energy dissipated, but also the resistive component of the inductance.

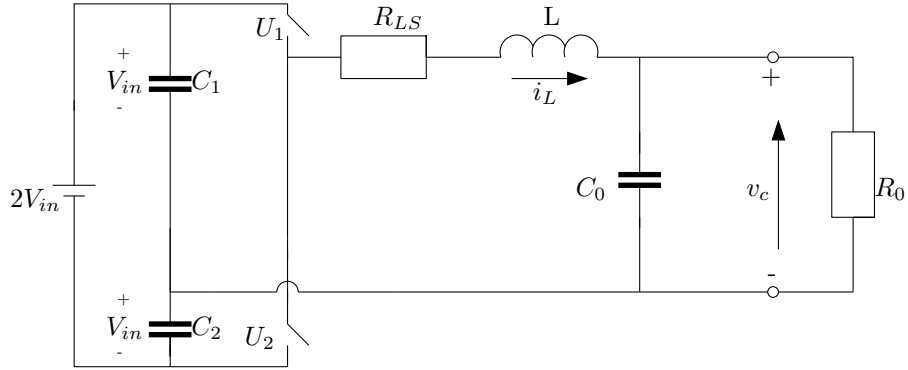


Figure 2.7: Half-bridge inverter.

the variable  $i_L(t)$  is the inductance current,  $v_C(t)$  is the capacitor voltage and these two states are considered as the continuous-time state variables.  $u := U_1 - U_2$  is the control input and it is assumed to be a discrete variable:

$$\begin{cases} u = -1, & \text{if } U_1 = \text{OFF and } U_2 = \text{ON.} \\ u = 1, & \text{if } U_1 = \text{ON and } U_2 = \text{OFF.} \end{cases}$$

In this circuit, the number of the switches is reduced to 2 by dividing the dc source voltage into two parts with the capacitors. Each capacitor will be the same and will have voltage  $V_{in}$  across it. When  $U_1$  is ON, the output voltage is  $v_C = -V_{in}$ , when  $U_2$  is ON, the output voltage is  $v_C = +V_{in}$

The dynamic behavior of this system can then be described by the following model:

$$(\Sigma) : \begin{cases} \dot{x}(t) = \underbrace{\begin{bmatrix} -\frac{R_{LS}}{L} & -\frac{1}{L} \\ \frac{1}{C_0} & -\frac{1}{R_0 C_0} \end{bmatrix}}_{A_u} x(t) + \underbrace{\begin{bmatrix} \frac{V_{in}}{L} \\ 0 \end{bmatrix}}_{B_u} u, \\ y(t) = \underbrace{\begin{bmatrix} 0 & 1 \end{bmatrix}}_{C_u} x(t), \end{cases} \quad (2.24)$$

with  $x(t) = [i_L(t) \ v_C(t)]^T$  is the state vector,  $y(t)$  is the controlled output and  $u = \{-1, 1\}$  is the control input.

The particularity of this model compared to the model of the Boost converter (Equation (2.3)) and the model of the rectifier (Equation (2.19)), is that, the control input takes place in the command matrix  $B$  and acts as a perturbation.

## 2.3. Switched Affine System (SAS)

All these systems can be modeled by a switched affine system with parameters that can change or vary periodically and can be rewritten under this formulation:

$$\begin{aligned}\dot{x} &= A_u x + B_u, & x(0) &= x_0 \\ y &= C_u x,\end{aligned}\tag{2.25}$$

where the control input  $u : \mathbb{R}_{\geq 0} \rightarrow \mathcal{N} := \{1, 2, \dots, N\}$  is the switching signal, assigning a specific desired mode among  $N$  possible ones at each time. Moreover, in dynamics (2.25),  $x \in \mathbb{R}^n$  is the state,  $y \in \mathbb{R}^p$  is a performance output, and  $A_i$ ,  $B_i$  and  $C_i$  have suitable dimensions for all  $i \in \mathcal{N}$ .

We aim to provide feedback strategies determining  $u$  such that practical stabilisation of an operating point  $x_e \in \mathbb{R}^n$  for switched affine systems is achieved, with guaranteeing some LQ performances.

## 2.4. Conclusions

This chapter has described and modeled some converters for which we will design some control laws in the next chapters. The obtained models are either a nonlinear time-invariant systems or a nonlinear time-varying systems. A particularity of this kind of system is that, the control input can take values in a discrete set. Further, as the dynamics of the states are a continuous-time dynamics then, a natural way to model these systems is to use the hybrid dynamical systems presented in the next chapters.



## CHAPTER 3

# HYBRID DYNAMICAL SYSTEM (HDS)

---

### Sommaire

---

<b>3.1</b>	<b>Introduction</b>	<b>21</b>
<b>3.2</b>	<b>Hybrid systems: modeling framework and basic notions</b>	<b>22</b>
3.2.1	Hybrid time domains	23
<b>3.3</b>	<b>Solutions to a hybrid system</b>	<b>24</b>
<b>3.4</b>	<b>Basic assumptions on the hybrid data</b>	<b>25</b>
<b>3.5</b>	<b>Hybrid system stability</b>	<b>26</b>
3.5.1	Singularly perturbed hybrid systems	28
<b>3.6</b>	<b>Conclusions</b>	<b>30</b>

---

### 3.1. Introduction

Dynamical systems that are described by an interaction between continuous-time and discrete-time dynamics are usually called hybrid systems.

Some notions about hybrid dynamical systems [26], are presented in this section, in particular, the notion of hybrid time domain and the notion of solutions which are essential in this framework. Furthermore, the stability properties need to be characterized.

The aim of this chapter is to provide only the basic concepts of this framework and the definitions needed in the rest of this dissertation.

## 3.2. Hybrid systems: modeling framework and basic notions

According to the formalism developed in [26], any hybrid system can be represented by a quadruple  $\mathcal{H} = (\mathcal{C}, F, \mathcal{D}, G)$ . In particular, we consider hybrid system in the following form:

$$\begin{cases} \dot{x} \in F(x), & x \in \mathcal{C} \\ x^+ \in G(x), & x \in \mathcal{D} \end{cases} \quad (3.1)$$

where  $x$  is the state of the hybrid system,  $\dot{x}$  represent the derivative and  $x^+$  indicates te value of the state after an instantaneous change.

Equation (3.1) shows the combination of continuous and discrete behaviors of the hybrid system. These evolutions are represented by four data and are detailed in the sequel:

- $\mathcal{C}$  is the flow set, otherwise, it indicates the set where the system evolves according to a continuous evolution (flow), meaning that, the continuous evolutions are allowed. Such an evolution is specified by the differential inclusion  $\dot{x} \in F(x)$ ;
- The set-valued mapping  $F$  is the flow map;
- $\mathcal{D}$  is the jump set. In other words, it indicates the set where the system evolves according to a discrete evolution, meaning that, the discrete evolutions are allowed. Such an evolution is determined by te difference inclusion  $x^+ \in G(x)$ ;
- The set-valued mapping  $G$  is the jump map.

In particular, a hybrid system with the data as above will be represented by the notation  $\mathcal{H} = (\mathcal{C}, F, \mathcal{D}, G)$ , or briefly by  $\mathcal{H}$ .

In the next, we present some definitions, which are important for the rest of this chapter.

◆ **DEFINITION 3.2.1:** (*Domain of a set-valued mapping*). For the set-valued mapping  $F : \mathbb{R}^n \rightrightarrows \mathbb{R}^n$  (respectively domain of  $G : \mathbb{R}^n \rightrightarrows \mathbb{R}^n$ ), the domain of  $F$  (respectively  $G$ ) is the set

$$\text{dom } F = \{x \in \mathbb{R}^n : F(x) \neq \emptyset\} \quad (\text{respect, } \text{dom } G = \{x \in \mathbb{R}^n : G(x) \neq \emptyset\})$$

◆ **DEFINITION 3.2.2:** (*Compact set*). A set  $\mathcal{A}$  is a compact set if and only if  $\mathcal{A}$  is closed and bounded.

In the following, we are focused on hybrid systems with state in  $\mathbb{R}^n$ . In that case, the data of the hybrid system  $\mathcal{H}$  can be defined as below.

•❖ **DEFINITION 3.2.3:** *The data of the hybrid system  $\mathcal{H} = (\mathcal{C}, F, \mathcal{D}, G)$  are defined as follows:*

- $\mathcal{C} \subset \mathbb{R}^n$
- $F : \mathbb{R}^n \rightrightarrows \mathbb{R}^n$ , with  $\mathcal{C} \subset \text{dom } F$
- $\mathcal{D} \subset \mathbb{R}^n$
- $G : \mathbb{R}^n \rightrightarrows \mathbb{R}^n$ , with  $\mathcal{D} \subset \text{dom } G$ .

### 3.2.1. Hybrid time domains

The solutions are parametrized by different ways depending in the nature of the system, meaning continuous-time or/and discrete-time systems. Thus,

- The continuous dynamics, the solutions are parametrized by a real scalar variable  $t \in \mathbb{R}_{\geq 0}$ , that is, by the ordinary time.
- The discrete dynamics, the solutions are parametrized by an integer scalar variable  $j \in \mathbb{N}$ , that defines the number of jumps or of the elapsed discrete steps.

Only some certain subsets of  $\mathbb{R}_{\geq 0} \times \mathbb{N}$  can parametrize the solutions of hybrid systems. Such sets are called hybrid time domains, whose the definition is given:

•❖ **DEFINITION 3.2.4:** *(Hybrid time domain). A subsets  $E \subset \mathbb{R}_{\geq 0} \times \mathbb{N}$  is a compact hybrid time domain if*

$$E = \bigcup_{j=0}^{J-1} \{[t_j, t_{j+1}], j\}$$

for some finite sequences of time  $0 = t_0 \leq t_1 \leq t_2 \leq \dots \leq t_J$ . It is a hybrid time domain if for all  $(T, J) \in E$ ,  $E \cap ([0, T] \times \{0, 1, 2, \dots, J\})$  is a compact hybrid time domain.

For a given  $(t, j), (t', j') \in E$ , we have  $(t, j) \leq (t', j')$  if  $t + j \leq t' + j'$ . Furthermore, for a given hybrid time domain  $E$ , then the supremum of the  $t$  and  $j$  coordinates are given, respectively, as:

$$\sup_t E = \sup\{t \in \mathbb{R}_{\geq 0} : \exists j \in \mathbb{N} \text{ such that } (t, j) \in E\},$$

$$\sup_j E = \sup\{j \in \mathbb{N} : \exists t \in \mathbb{R}_{\geq 0} \text{ such that } (t, j) \in E\}.$$

•❖ **DEFINITION 3.2.5:** *(Hybrid arc). A function  $\phi : E \rightrightarrows \mathbb{R}^n$  is a hybrid arc if:*

1.  $E$  is a hybrid time domain;
2. for each  $j \in \mathbb{N}$ , the function  $t \mapsto \phi(t, j)$  is locally absolutely continuous on the interval  $I^j = \{t : (t, j) \in E\}$ .

Figure 3.1 shows an example of a graph of a hybrid arc  $\phi$  with the associated hybrid time domain  $\text{dom } \phi$ .

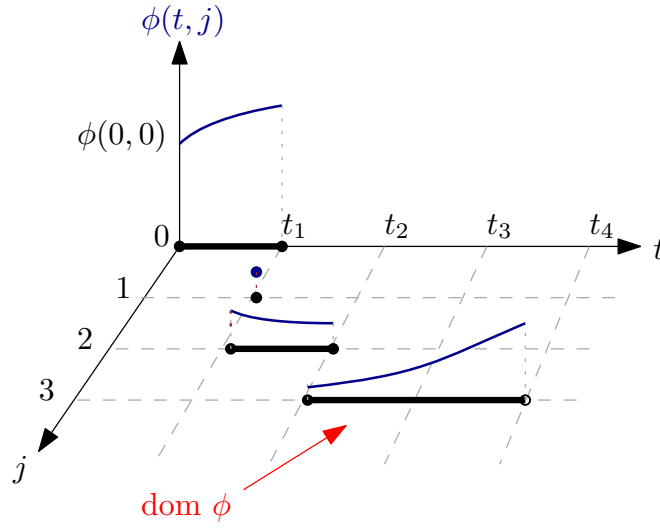


Figure 3.1: Hybrid arc  $\phi$ .

◆ **DEFINITION 3.2.6:** (Types of hybrid arc). A hybrid arc  $\phi$  is called:

- Nontrivial, if  $\text{dom } \phi$  has at least two points.
- Complete, if  $\text{dom } \phi$  is unbounded.
- Zeno, if it is complete and  $\sup_t \text{dom } \phi < \infty$ .

Here, we have only mentioned those that are relevant within this thesis. For more specifications, the reader is referred to [26].

Now that we have defined and established the principals definitions, we are able to define the notion of solution to hybrid systems used throughout this work.

### 3.3. Solutions to a hybrid system

◆ **DEFINITION 3.3.1:** (Solutions to a hybrid system). A hybrid arc  $\phi$  is a solution to hybrid system  $\mathcal{H}$  if:



1. the initial condition  $\phi(0, 0) \in \bar{\mathcal{C}} \cup \mathcal{D}$ , where  $\bar{\mathcal{C}}$  denotes the closure of  $\mathcal{C}$ ;
2. (S1) for all  $j \in \mathbb{N}$  such that  $I^j = \{t : (t, j) \in \text{dom } \phi\}$  as nonempty interior:

$$\phi(t, j) \in \mathcal{C} \quad \text{for all } t \in \text{int}(I^j),$$

$$\dot{\phi}(t, j) \in F(\phi(t, j)) \quad \text{for almost all } t \in I^j,$$

3. (S2) for all  $(t, j) \in \text{dom } \phi$  such that  $(t, j + 1) \in \text{dom } \phi$ ,

$$\phi(t, j) \in \mathcal{D},$$

$$\phi(t, j + 1) \in G(\phi(t, j)),$$

•◆ **DEFINITION 3.3.2:** (Maximal solutions). The solution  $\phi$  is maximal if there does not exist another solution  $\psi$  to  $\mathcal{H}$  such that:

- $\text{dom } \phi$  is strict subset of  $\text{dom } \psi$
- $\phi(t, j) = \psi(t, j), \forall (t, j) \in \text{dom } \phi$ .

🔗 **REMARK 2.** The complete solutions are maximal, but the converse statement is not true.

## 3.4. Basic assumptions on the hybrid data

Before to give the required assumptions to ensure that a given hybrid system is well-posed in the sense specified in [26, Theorem 6.5]. Let start by given some basics definitions.

•◆ **DEFINITION 3.4.1:** (Outer semicontinuous [26, Definition 5.9]) A set-valued mapping  $M : \mathbb{R}^m \rightrightarrows \mathbb{R}^n$  is outer semicontinuous at  $x \in \mathbb{R}^m$  if for every sequence of points  $x_i$  convergent to  $x$  and any convergent sequence of points  $y_i \in M(x_i)$ , one has  $y \in M(x)$ , where  $\lim_{i \rightarrow \infty} y_i = y$ . The mapping  $M$  is outer semicontinuous if it is outer semicontinuous at each  $x \in \mathbb{R}^m$ .

•◆ **DEFINITION 3.4.2:** (Local boundedness [26, Definition 5.14]) A set-valued mapping  $M : \mathbb{R}^m \rightrightarrows \mathbb{R}^n$  is locally bounded at  $x \in \mathbb{R}^m$  if there exists a neighborhood  $U_x$  of  $x$  such that  $M(U_x) \subset \mathbb{R}^n$  is bounded. The mapping  $M$  is locally bounded if it is locally bounded at each  $x \in \mathbb{R}^m$ .

❖ **ASSUMPTION 3:**

(Hybrid basic conditions).

- $\mathcal{C}$  and  $\mathcal{D}$  are closed subsets of  $\mathbb{R}^n$ ;
- $F : \mathbb{R}^n \rightrightarrows \mathbb{R}^n$  is outer semicontinuous and locally bounded relative to  $\mathcal{C}$ ,  $\mathcal{C} \subset \text{dom } F$ , and  $F(x)$  is convex for every  $x \in \mathcal{C}$ ;
- $G : \mathbb{R}^n \rightrightarrows \mathbb{R}^n$ , is outer semicontinuous and locally bounded relative to  $\mathcal{D}$ , and  $\mathcal{D} \subset \text{dom } G$ .

☀ **THEOREM 1.** (Basic conditions and well-posedness) [26, Theorem 6.30]. If a hybrid system  $\mathcal{H} = (\mathcal{C}, F, \mathcal{D}, G)$  satisfies Assumption 3 then it is well-posed.

Well-posedness is an important notion that is required for the applicability of a large number of results presented in [26]. We invite the reader to see the proof of well-posedness in [26].

## 3.5. Hybrid system stability

In this section, we are interested to characterize the stability of a certain compact set  $\mathcal{A}$ . To this end, let start by providing some definitions concerning stability of hybrid systems [26].

Firstly, some definitions used throughout this chapter are given.

❖ **DEFINITION 3.5.1:** (Distance to a closed set). For a given vector  $x \in \mathbb{R}^n$  and a closed set  $\mathcal{A} \subset \mathbb{R}^n$ , the distance of  $x$  to  $\mathcal{A}$  denoted  $|x|_{\mathcal{A}}$  is defined by  $|x|_{\mathcal{A}} := \inf_{y \in \mathcal{A}} |x - y|$ .

❖ **DEFINITION 3.5.2:** (Class  $\mathcal{K}_{\infty}$ ). A function  $\alpha : \mathbb{R}_{\geq 0} \rightarrow \mathbb{R}_{\geq 0}$ , is of class  $\mathcal{K}_{\infty}$  if  $\alpha$  is zero at zero, continuous, strictly increasing and unbounded.

❖ **DEFINITION 3.5.3:** (Uniform global asymptotic stability [26, Definition 3.6]) Consider a hybrid system  $\mathcal{H}$  on  $\mathbb{R}^n$ . A closed set  $\mathcal{A} \subset \mathbb{R}^n$  is

- Uniformly globally stable for system  $\mathcal{H}$ , if there exists a class  $\mathcal{K}_{\infty}$  function  $\alpha$ , such that every solution  $\phi$  to  $\mathcal{H}$  satisfies  $|\phi(t, j)|_{\mathcal{A}} \leq \alpha(|\phi(0, 0)|_{\mathcal{A}})$  for every  $(t, j) \in \text{dom } \phi$ .
- Uniformly globally attractive for  $\mathcal{H}$ , if every maximal solution to  $\mathcal{H}$  is complete and for every  $\varepsilon > 0$  and  $\mu > 0$  there exists  $T > 0$  such that, for any solution  $\phi$  to  $\mathcal{H}$  with  $|\phi(0, 0)|_{\mathcal{A}} \leq \mu$ ,  $(t, j) \in \text{dom } \phi$  and  $t + j \geq T$  implies  $|\phi(t, j)|_{\mathcal{A}} \leq \varepsilon$ .

- *Uniform globally asymptotically stable (UGAS) for  $\mathcal{H}$ , if it is uniformly globally stable and uniformly globally attractive.*

In the next, we consider Lyapunov functionals, which are a fundamental tool for stability analysis. We suppose that, all solutions are complete, (otherwise, the pre-stability need to be proven in such case).

◆ **DEFINITION 3.5.4:** (*Lyapunov function candidate*) A function  $V: \text{dom } V \rightarrow \mathbb{R}$  is said to be a Lyapunov function candidate for the hybrid system  $\mathcal{H} = (\mathcal{C}, F, \mathcal{D}, G)$  if the following conditions holds:

1.  $\bar{\mathcal{C}} \cup \mathcal{D} \cup G(\mathcal{D}) \subset \text{dom } V$ ;
2.  $V$  is continuously differentiable on an open set containing  $\bar{\mathcal{C}}$ .

In the next we provide a [26, Theorem 3.18], which gives the conditions on a Lyapunov function candidate that guarantees uniform global asymptotic stability:

☀ **THEOREM 2.** (*Sufficient Lyapunov conditions*) Let  $\mathcal{H} = (\mathcal{C}, F, \mathcal{D}, G)$  be a hybrid system and let  $\mathcal{A} \subset \mathbb{R}^n$  be closed set. If  $V$  is a Lyapunov function candidate for  $\mathcal{H}$  and there exist  $\alpha_1, \alpha_2 \in \mathcal{K}_\infty$ , and a continuous positive definite function  $\rho$  such that

$$\alpha_1(|x|_{\mathcal{A}}) \leq V(x) \leq \alpha_2(|x|_{\mathcal{A}}) \quad \forall x \in \bar{\mathcal{C}} \cup \mathcal{D} \cup G(\mathcal{D}) \quad (3.2a)$$

$$\langle \nabla V(x), f \rangle \leq -\rho(|x|_{\mathcal{A}}) \quad \forall x \in \mathcal{C}, f \in F(x) \quad (3.2b)$$

$$V(g) - V(x) \leq -\rho(|x|_{\mathcal{A}}) \quad \forall x \in \mathcal{D}, g \in G(x) \quad (3.2c)$$

then,  $\mathcal{A}$  is Uniformly Globally Asymptotically Stable (UGAS) for  $\mathcal{H}$ .

Let consider now the hybrid system parametrized by a small, positive parameter  $\varepsilon$ , of the form

$$\begin{cases} \dot{x} & \in F_\varepsilon(x), & x \in \mathcal{C}_\varepsilon \\ x^+ & \in G_\varepsilon(x), & x \in \mathcal{D}_\varepsilon \end{cases} \quad (3.3)$$

◆ **DEFINITION 3.5.5:** (*Semi-global practical asymptotic stability (SPAS) [27]*)

For the hybrid system (3.3), the compact set  $\mathcal{A} \subset \mathbb{R}^n$  is said to be semiglobally practically asymptotically stable as  $\varepsilon \rightarrow 0^+$ , if there exists  $\beta \in \mathcal{KL}^1$  and for each  $\Delta > 0$

<sup>1</sup>  $\beta \in \mathcal{KL}$  if  $\beta: \mathbb{R}_{\geq 0} \times \mathbb{R}_{\geq 0} \rightarrow \mathbb{R}_{\geq 0}$  is continuous,  $\beta(\cdot, r)$  is nondecreasing for each  $r \geq 0$ ,  $\beta(s, \cdot)$  is nonincreasing for each  $s$ , and  $\lim_{s \rightarrow 0^+} \beta(s, r) = \lim_{r \rightarrow \infty} \beta(s, r) = 0$ .

and  $\delta > 0$ , there exists  $\varepsilon^* > 0$  such that, for each  $\varepsilon \in (0, \varepsilon^*)$ , each solution  $x$  of (3.3) that satisfies  $|x(0, 0)|_{\mathcal{A}} \leq \Delta$  also satisfies

$$|x(t, j)|_{\mathcal{A}} \leq \beta(|x(0, 0)|_{\mathcal{A}}, t + j) + \delta \quad \forall (t, j) \in \text{dom } x.$$

The convergence toward a small neighborhood of  $\mathcal{A}$  in the definition of semiglobal, practical asymptotic stability is uniform over the set of initial conditions considered, whereas this attribute is not explicit in the definition of global asymptotic stability. However, under mild regularity assumptions on the data  $(C, F, D, G)$ , global asymptotic stability implies the existence of such that  $\beta \in \mathcal{KL}$  such that each solution  $x$  to (3.1) satisfies

$$|x(t, j)|_{\mathcal{A}} \leq \beta(|x(0, 0)|_{\mathcal{A}}, t + j) \quad \forall (t, j) \in \text{dom } x.$$

When  $\beta$  has the form  $\beta(s, r) = c_1 s \exp(-c_2 r)$  for some constants  $c_1, c_2 > 0$ , the compact set  $\mathcal{A}$  is globally exponentially stable. For more details, see [28, Theorem 6.5].

### 3.5.1. Singularly perturbed hybrid systems

Singular perturbations approaches are used to simplify a complex systems by separating the dynamics of the whole system into two dynamics (*slow* and *fast* dynamics) [29]. The *slow* dynamic represents the dynamic of the reduced model and it is dictated by a separation of time scales. Usually the fast dynamic is neglected. The *fast* dynamic is treated in the first step and represents the dynamic of *boundary layer system* evolving in the faster time scales. Moreover, the boundary layer model represents deviations from the predicted *slow* behavior.

Let's suppose that  $x = \overbrace{(x_1, x_2, \dots, \dots, x_n)}^{(X_1)} \in \mathbb{R}^n$ , with  $X_1 \in \mathbb{R}^{n_1 \times n_1}$ ,  $X_2 \in \mathbb{R}^{n_2 \times n_2}$  and  $n_1 + n_2 = n$ . Then the hybrid system can be written as [27]:

$$\begin{cases} \text{diag}(I_{n_1}, \varepsilon I_{n_2}) \dot{x} \in F(x), & x \in \mathcal{C}_1 \times \mathcal{C}_2 \\ x^+ \in G(x), & x \in \mathcal{D}_1 \times \mathcal{D}_2 \end{cases} \quad (3.4)$$

where  $\varepsilon > 0$  is a small positive scalar.  $I_{n_i}$  denotes the  $n_i \times n_i$  identity matrix.  $X_1$  contains the *slow* variables, whereas  $X_2$  contains the *fast* ones.

The singular perturbations system can be composed in three steps:

1. The first step is to consider the boundary layer system, which contains the fast variable evolution and neglects the dynamic of slow variable ( $\dot{X}_1 = 0$ ). In this

step, the considered model evolves in the faster time scales and represents deviations from the predicted slow behavior. In [29], an approximation of the evolution of the fast variable is given as

$$X_2(t) = X_{2_e}(t) + O(\varepsilon),$$

for  $t \in [t_1, T]$  where  $t_1 > t_0$ . This approximation establishes that during an initial interval  $[t_0, t_1]$ , the original variable  $X_2$  approaches  $X_{2_e}$ , and during  $[t_1, T]$ , remains close to  $X_{2_e}$ .

2. In this second step, the quasi-steady-state equilibrium manifold is considered.
3. The reduced system, generally the one that we want to control. In this step, we consider that the fast variables are in the steady state and we consider only the slow variables. Furthermore, the stability of this system can be proved.

We are interested in the stability of the next compact set for the reduced model.

$$\mathcal{A}_1 = \{X_1 = X_{1_e}\}$$

The following basic assumptions are considered.

#### A. Manifold:

The quasi-steady-state equilibrium manifold of classical singular perturbation theory appears in the case of hybrid approach as a set-valued mapping  $H : \mathbb{R}^{n_1} \rightrightarrows \mathbb{R}^{n_2}$ .

❖ **ASSUMPTION 4** (Regularity of "Manifold"):

*The set-valued mapping  $H : \mathbb{R}^{n_1} \rightrightarrows \mathbb{R}^{n_2}$  is outer semicontinuous and locally bounded, and for each  $X_1 \in \mathcal{C}_1$  then  $H(X_1)$  is nonempty subset of  $\mathcal{C}_2$ .*

#### B. Boundary layer system:

The family of boundary layer systems is given by:

$$\dot{x} \in \text{diag}(0, I_{n_2})F(x), \quad x \in (\mathcal{C}_1 \cap \rho\mathcal{B}) \times \mathcal{C}_2. \quad (3.5)$$

with  $\rho > 0$  makes the flow set compact.

The boundary layer system ignores jumps and the state  $X_1$  remains constant during the flows.

❖ **ASSUMPTION 5** (Stability of boundary layer):

*For each  $\rho > 0$ , the boundary layer system defined in (3.5), is such that the following compact set*

$$\mathcal{M}_\rho := \{(X_1, X_2) : X_1 \in \mathcal{C}_1 \cap \rho\mathcal{B}, X_2 \in \mathcal{H}(X_1)\}$$

*is globally asymptotically stable.*

### C. Reduced system:

The reduced system is given by

$$\begin{cases} \dot{X}_1 \in F_r(X_1), & x \in \mathcal{C}_1 \\ X_1^+ \in G_r(X_1), & x \in \mathcal{D}_1, \end{cases} \quad (3.6)$$

with

$$F_r(X_1) := \overline{\text{co}}\{v_1 \in \mathbb{R}^{n_1} : (v_1, v_2) \in F(X_1, X_2), X_2 \in \mathcal{H}(X_1), v_2 \in \mathbb{R}^{n_2}\} \quad (3.7)$$

$$G_r(X_1) := \overline{\text{co}}\{v_1 \in \mathbb{R}^{n_1} : (v_1, v_2) \in F(X_1, X_2), (X_2, v_2) \in \mathcal{C}_2 \times \mathcal{C}_2\} \quad (3.8)$$

✦ **ASSUMPTION 6** (Stability for the reduced system):

For the reduced system (3.6), the compact set  $\mathcal{A}_1 \in \mathbb{R}^{n_1}$  is globally asymptotically stable.

☀ **THEOREM 3.** Under Assumption 3 and Assumptions 4-6 for the hybrid system (3.4), the compact set  $\mathcal{A}_1 \times \mathcal{C}_2$  is semiglobally practically asymptotically stable as  $\varepsilon \rightarrow 0^+$ .

The reader is referred to [27] to see the proof of Theorem 3.

## 3.6. Conclusions

In this chapter, we have presented the hybrid dynamical system used in this dissertation. The principal definitions and properties used in this work are briefly provided.

# CHAPTER 4

## HYBRID CONTROL FOR DC-DC AND AC-DC CONVERTERS

---

### Sommaire

---

<b>4.1</b>	<b>Introduction</b>	<b>31</b>
<b>4.2</b>	<b>DC-DC Converters: Boost converter</b>	<b>32</b>
4.2.1	Problem formulation	33
4.2.2	Hybrid control for a boost converter	37
4.2.3	Hybrid adaptive control for a boost converter	43
4.2.4	Applications	53
4.2.5	Conclusions	60
<b>4.3</b>	<b>AC-DC Converters: Three-phase three-level NPC Converter</b>	<b>62</b>
4.3.1	The control objectives	64
4.3.2	Hybrid model and proposed control law	64
4.3.3	Applications	66
4.3.4	Conclusions	68
<b>4.4</b>	<b>Conclusions</b>	<b>68</b>

---

### 4.1. Introduction

This chapter deals with the design of control laws for a DC-DC and AC-DC converters. Since, these systems exhibit continuous dynamics (current and voltage) and discrete dynamics (switching signals), thus, a natural way for modeling them is to use the hybrid dynamical system described in Chapter 3. The control problem of these

classes of converters is characterized by the regulation of an operating point, which can be achieved by a combination of the different functioning modes defined by the switched signal. Therefore, we get a solution of the voltage and currents in the generalized sense of Fillipov.

First, we focus in Section 4.2, on the boost converter, which is a DC-DC converter. This section proposes a hybrid dynamical model formulation with the corresponding control law. Furthermore, an hybrid adaptive control law for the boost converter is proposed to deal with the unknown constant resistive load and to ensure that the voltage value is robust with respect to any reference. This adaptation is accomplished using a state observer and assuming that all states are accessible. Then, the full system stability can be established by using a singular perturbation analysis.

Secondly, in Section 4.3, we are interested in a Neutral Point Clamped (NPC) converter working as a rectifier. A hybrid dynamical control is proposed in order to regulate the output DC voltage and stability properties are guaranteed. The difficulty in this case is that the model of the NPC is a non-linear time-varying model.

## 4.2. DC-DC Converters: Boost converter

In this section, we are interested in the regulation problem of the boost converter with an unknown resistance load. The objective of the controller is to regulate the output voltage to a desired operating point with a fast response, low overshoot and low noise susceptibility. To this end, based on the work presented in [30], we propose to add to the hybrid scheme an adaptive control scheme in order to ensure a voltage regulation with the presence of unknown resistance load. This adaptation is accomplished using a state observer and assuming that all the states are measurable. Then, the full system stability can be studied by using a singular perturbation analysis.

As it is presented in Chapter 2, the boost converter can be modeled by a nonlinear model given in (2.3). The obtained model exhibits two kind of dynamics

- a continuous-time dynamics, i.e; the dynamic of inductor current,  $i_L(t)$ , and the dynamic of capacitor voltage,  $v_C(t)$ ,
- a discrete-time dynamic, i.e; the dynamic of the control input  $u$ .

Hence, it is not easy to handle rigorously the problem with standard mathematical tools since its dynamic is complex.

A first classical approach widely studied relies on the control design of averaged models.

As proposed in the introduction of this chapter, a natural way to handle this kind of system is to use the hybrid dynamical systems theory, more precisely the switching affine systems. Recently, the control community has concentrated some efforts to the



study of new hybrid control techniques [30], [31] such as the switched system, which can be considered as a subclass of hybrid systems.

Applications to DC-DC converters can be found for example in [32] where the problem is formulated in terms of control of switched systems whose modes are described by affine differential equations.

It is possible to show that the obtained switching rules can be interpreted as sliding mode control laws with sliding surfaces implicitly determined in terms of the state-space variables (current, voltage) and of the selected equilibrium operation [33]. Even if the implicit discontinuous nature of DC-DC converters is taken into account by an appropriate switched model, the limitation is due to the practical implementation of the control law whose properties are only ensured for an infinite switching frequency, while for practical reasons, the switching frequency must be constrained.

To deal with, this chapter states a control problem in the context of the control of hybrid dynamic systems [26] which seems to be an adequate way for handling the specificities of DC-DC converters while guaranteeing theoretically and practically, that the implemented control laws will satisfy all the specifications in terms of stability and performance. The interest of this approach is the possibility of identifying and managing some design parameters affecting important practical indicators such as: switching frequency, dissipated energy, overshoot... which are not easy to manage in general by using other methods like sliding mode control for example.

Here, the considered paradigm is the one developed in chapter 2 which associates to a continuous-time flow whose model is of a differential equation type, a discrete-time behavior capturing the switched characteristic imposed by the control law. Two subsets included in an extended space, built from the state and the control spaces, determine the regions where the continuous and discrete dynamics are active. The main tool for proving stability of a compact attractor defined in this extended space, proceeds by an appropriate extension of Lyapunov stability theory developed in the context of hybrid dynamic systems in [26] and [34]. Due to the affine structure of the modes, a quadratic Lyapunov function can be selected from a positive definite symmetric matrix satisfying a set of Lyapunov inequalities. A hybrid control law with its two associated flow and jump is deduced from this matrix and an upper bound of a LQ performance index for the controlled system can be computed. It is possible to deduce an optimal guaranteed cost control law leading to the tight upper bound, by solving a LMI optimization problem.

### 4.2.1. Problem formulation

The main considered assumptions are

#### ✦ ASSUMPTION 7:

Let consider

- the converter current is continuous and all the components are ideal,
- the current and voltage are measurable,
- the load  $R_0$  is unknown constant or/and slowly variable in the interval  $[R_0^m, R_0^M]$ .
- $x_2 = 0$  corresponds to the starting operation mode, and any starting strategy is used to bring our system to  $x_2 \neq 0$ .

The used components are modeled and assumed to be ideal components, meaning that, they do not dissipate power. Nevertheless, it is important to note that the real components present always some imperfections and the real components never have exactly their specified values. In this work, we consider only that the inductance  $L$  dissipate energy and they have a significant parasitic resistance denoted  $R_{LS}$ . However, we will not consider the imperfections of the others components.

Let start by rewritten this model by considering the unknown load  $R_0$ . To do this, let consider the following variable change

$$\beta := \frac{1}{R_0} \in [\beta^m, \beta^M]. \quad (4.1)$$

Then, considering the variable change given in equation (4.1), the model of the boost converter given in (2.3), can be rewritten as follows

$$(\Sigma) : \begin{cases} \dot{x}(t) = \overbrace{\begin{bmatrix} -\frac{R_{LS}}{L} & -\frac{1-u}{L} \\ \frac{1-u}{C_0} & -\frac{\beta}{C_0} \end{bmatrix}}^{A_u(\beta)} x(t) + \overbrace{\begin{bmatrix} \frac{V_{in}}{L} \\ 0 \end{bmatrix}}^a, \\ y(t) = \overbrace{\begin{bmatrix} 1 & 0 \\ 0 & 1 \end{bmatrix}}^C x(t), \end{cases} \quad (4.2)$$

where the available input  $u$  is the switching signal, assigning its value in:

$$u := \{0, 1\}. \quad (4.3)$$

Moreover, in dynamics (4.2),  $V_{in} \in \mathbb{R}$ , is a constant voltage source, the vector  $x(t) = [x_1(t) \ x_2(t)]^T = [i_L(t) \ v_C(t)]^T \in \mathbb{R}^2$  is the state and  $y(t) \in \mathbb{R}^p$  is the controlled output. We focus here on the design problem of a feedback control law for the switching signal  $u$ , in such a way to ensure suitable convergence properties of the plant state  $x$  to a value  $x_e$ , which is not necessarily an equilibrium for the continuous-time dynamics

in (4.2), but can be obtained as an equilibrium for the switching system with arbitrary switching and the estimation of the load  $\hat{\beta}$  to its real value,  $\beta$ .

Notice that, the all attainable equilibrium points for the boost converter are not difficult to find from (4.2) and are given as [32]

$$X_e = \{(x_{1e}, x_{2e}) : \frac{V_{in}}{R_{LS} + R_0} \leq x_{1e} \leq \frac{V_{in}}{R_{LS}}, x_{2e}^2 + R_{LS}R_0x_{1e}^2 - R_0V_{in}x_{1e} = 0\} \quad (4.4)$$

All equilibrium points given in the set 4.4, can be represented in Figure 4.1. Figure 4.2 shows the evolution of  $x_{2e}$  with respect to  $u_e$ . Notice that one can obtain larger value for  $x_{2e}$  compared to the input value  $V_{in}$  set to 100V in this example.

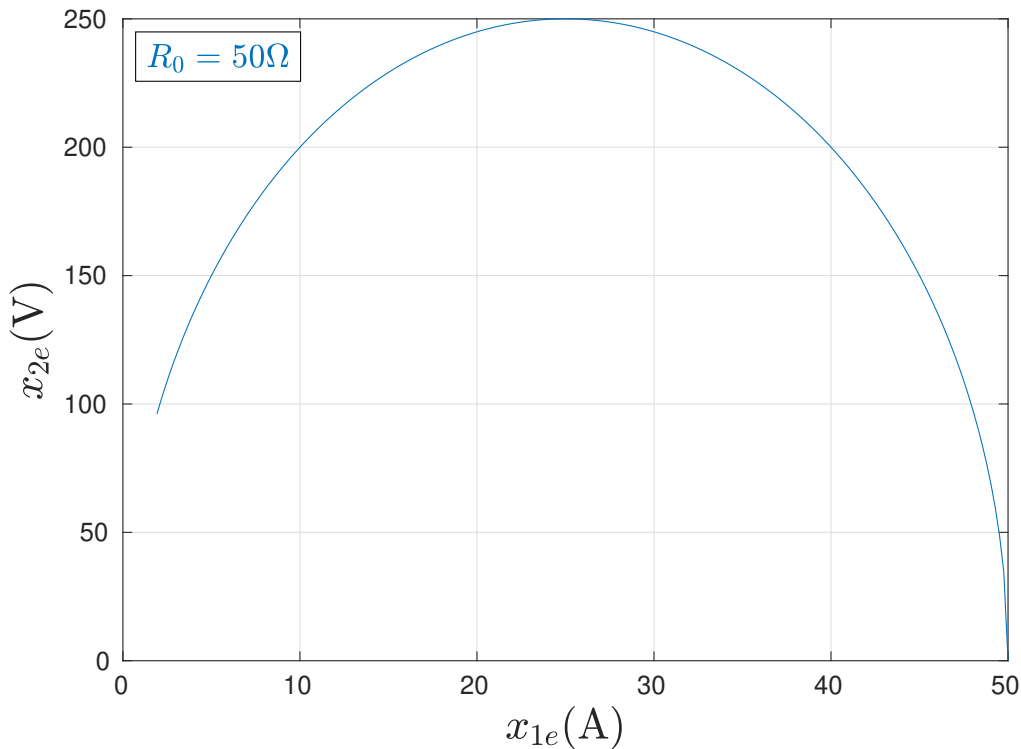


Figure 4.1: Attainable equilibrium points in sens of Fillipov.

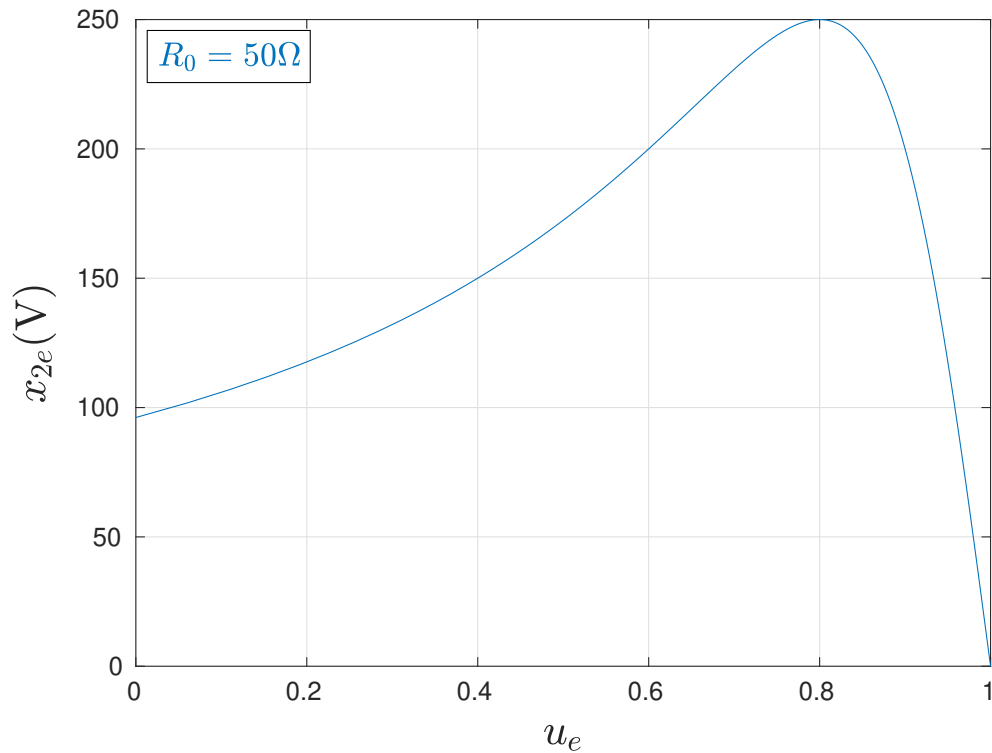


Figure 4.2: Hybrid adaptive control scheme.

★ **PROBLEM 1:**

The goal is to ensure the asymptotic stability of  $x_e$  for (4.2) and adaptation of the load for ensuring a reduced error in the voltage regulation.

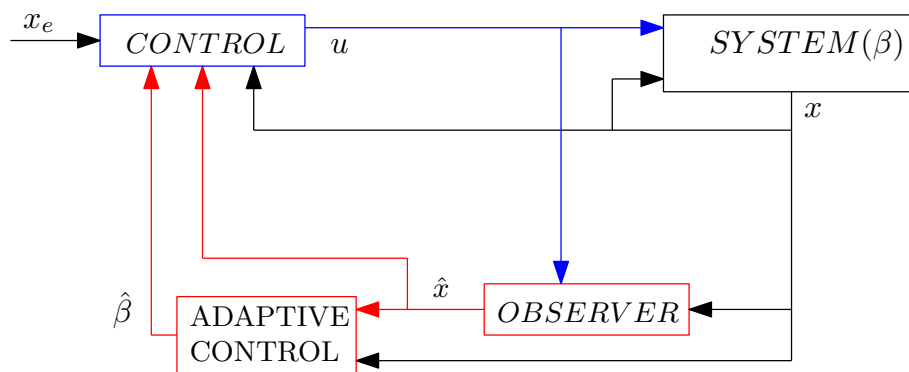


Figure 4.3: Hybrid adaptive control scheme.

► **PROPOSITION 1:**

To do this, let divide the problem in two parts:

- The first one is dedicated to the design a hybrid control for the boost converter 2.3 with a known parameter (see for instance [30]).
- The second part proposes an extension of the first part, by adding an adaptive control on the hybrid control scheme.

Let start with the first part of proposition 1, where, we detail the work done in [30] and we propose a hybrid formalism for the design problem associated with the determination of a switching signal  $u$  suitably stabilizing a point  $x_e$ .

### 4.2.2. Hybrid control for a boost converter

Here, we are focused on the design problem of a feedback law for the switching signal  $u$ , in such a way to ensure suitable convergence properties of the plant state  $x$  to a value  $x_e$ . A sufficient condition characterizing this equilibrium is then represented by the following standard assumption (see [32, 35]).

✦ **ASSUMPTION 8:**

There exists  $\lambda_e = [\lambda_{e_0}, \lambda_{e_1}]$  satisfying  $\sum_{l=0}^1 \lambda_{e_l} = 1$ , such that the following convex combination holds:

$$\sum_{l=0}^1 \lambda_{e_l} (A_l x_e + a) = 0. \quad (4.5)$$

📌 **REMARK 3.** It is emphasized that Assumption 8 is sufficient for the existence of a suitable switching signal ensuring forward invariance of the point  $x_e$  (namely inducing an equilibrium at  $x_e$ ) when understanding solutions in the generalized sense of Krasovskii or Filippov. Indeed, under (4.5), this switching signal is a periodic sequence of arbitrary small period  $T$ , spending a time equal to  $\lambda_{e_i} T$  in mode  $i$ . Conversely, if Assumption 8 does not hold, such a signal does not exist because any arbitrary switching signal can only generate an equivalent action on  $\dot{x}$  corresponding to a convex combination of the right hand sides obtained with each mode (namely, equation (4.5)).

In the next, we will assume the existence of the following set of matrices  $P$  and  $Q$  satisfying the next property.

★ **PROPERTY 1:**

Given matrices  $A_i, i \in [0, 1]$  in (2.3), there exists matrices  $P, Q \in \mathcal{S}^2$  satisfying

$$A_i^T P + P A_i + 2Q < 0, \quad (4.6)$$

for all  $i \in [0, 1]$ .

Note that Property 1 enforces the strong requirement that all matrices  $A_i$  be Hurwitz. Selection of matrices  $P$  and  $Q$  satisfying Property 1 will be discussed in Section A

where an optimization-based procedure will be suggested, also in light of the stability and optimality theorems presented below.

Let detail here the control law proposed by [30], where a formulation of the design problem as a hybrid dynamical system is proposed, following the formalism proposed in Chapter 2, wherein continuous-time behavior captures the evolution of  $f(\cdot)$  in (2.3), and the discrete-time behavior captures the jump of the control signal  $u$  from one mode to another. We represent the overall dynamics as:

$$\mathcal{H} : \begin{cases} \begin{bmatrix} \dot{x} \\ \dot{u} \end{bmatrix} = f(x, u), & (x, u) \in \mathcal{C} \\ \begin{bmatrix} x^+ \\ u^+ \end{bmatrix} \in G(x), & (x, u) \in \mathcal{D}, \end{cases} \quad (4.7)$$

with  $f$  is a single-valued mapping capturing the continuous evolution of the state and  $G$  is a set-valued mapping capturing the switching logic:

$$\begin{aligned} f(x, u) &:= \begin{bmatrix} A_u x + a \\ 0 \end{bmatrix} \\ G(x) &:= \begin{bmatrix} x \\ \operatorname{argmin}_{i \in \{0,1\}} (x - x_e)^T P (A_i x + a) \end{bmatrix} \end{aligned} \quad (4.8)$$

where the “flow” and “jump” sets  $\mathcal{C}$  and  $\mathcal{D}$  encompass, respectively, the regions in the (extended) space  $(x, u)$  where our switching strategy continues with the current mode  $u$  (set  $\mathcal{C}$ ) or is required to switch to a new mode (set  $\mathcal{D}$ ). If switching is allowed (namely, if  $(x, u) \in \mathcal{D}$ ) then  $u$  will switch according to  $G$  in (4.8). For the solution proposed in [30], the flow and jump sets are selected based on the desired equilibrium  $x_e$  introduced in Assumption 8 and on the parameters  $P$  and  $Q$  introduced in Property 1 as follows:

$$\mathcal{C} := \{(x, u) : \tilde{x}^T P (A_u x + a) \leq -\eta \tilde{x}^T Q \tilde{x}\} \quad (4.9)$$

$$\mathcal{D} := \{(x, u) : \tilde{x}^T P (A_u x + a) \geq -\eta \tilde{x}^T Q \tilde{x}\}, \quad (4.10)$$

where  $\tilde{x} = x - x_e$  and scalar  $\eta \in (0, 1)$  is a design parameter that will be shown to be useful for suitably achieving a trade-off between switching frequency and optimality level as characterized later in Theorem 5 and commented in Remark 7.

🔗 **REMARK 4.** Note that hybrid system (4.7)–(4.10) provides a solution strategy for the selection of the switching signal  $u$ . Indeed, sets (4.9) and (4.10) correspond to a specification about “when” a jump is or is not allowed, and map  $G$  in (4.8) specifies where a solution “may” jump (that is, what values of  $u$  are allowed after the jump). It is emphasized that both these elements of our solution may be sources of non-uniqueness of the solutions. Indeed, sets in (4.9) and (4.10) have overlapping boundaries so that multiple solutions (flowing or jumping) may arise from the same initial condition. Similarly, the “argmin” in the definition of  $G$  in (4.8) may be non-unique. Despite this non-uniqueness feature, the stability and optimality results proven below refer to all possible solutions and therefore it is not really important what solutions we select in a possible implementation of this control law (or in a MATLAB simulation) because stability and optimality properties hold for all of them.

The next lemma is a fundamental step to prove our main result in Theorem 4 below.

**\* LEMMA 1:**

Consider matrices  $P, Q \in \mathcal{S}^2$ , satisfying Property 1, a point  $x_e \in \mathbb{R}^2$  satisfying Assumption 8. Then, for each  $x \in \mathbb{R}^2$ ,

$$\min_{i \in [0,1]} \tilde{x}^T P (A_i x + a) \leq -\tilde{x}^T Q \tilde{x}. \quad (4.11)$$

*Proof.* First notice that the left hand side of (4.5) is linear in  $\lambda_n = [\lambda_0, \lambda_1]$ , and  $\lambda_e$  allows to the compact set  $\Lambda = \{\lambda_n = [\lambda_0, \lambda_1], \sum_{l=0}^1 \lambda_n = 1\}$ . Then, the following minimum is obtained at the extreme points:

$$\begin{aligned} & \min_{i \in [0,1]} \tilde{x}^T P (A_i x_e + a) \\ &= \min_{\lambda_n \in \Lambda} \tilde{x}^T P \left\{ \sum_{l=0}^1 \lambda_{n_l} A_l x_e + a \right\} \\ &\leq \tilde{x}^T P \left\{ \sum_{l=0}^1 \lambda_{e_l} A_l x_e + a \right\} = 0. \end{aligned} \quad (4.12)$$

Then, the proof easily follows from applying (4.6) and (4.12) as follows

$$\begin{aligned} & \min_{i \in [0,1]} \tilde{x}^T P (A_i x + a) \\ &\leq \min_{i \in [0,1]} \tilde{x}^T P A_i \tilde{x} + \min_{i \in [0,1]} (\tilde{x}^T P A_i x_e + \tilde{x}^T P a) \\ &\leq -\tilde{x}^T Q \tilde{x}. \end{aligned}$$

which concludes the proof. □

🔗 **REMARK 5.** We note here that, if  $\tilde{x} \neq 0$

$$-\tilde{x}^T Q \tilde{x} < -\eta \tilde{x}^T Q \tilde{x}.$$

because  $\eta < 1$ .

In the following, we comment here on its relevance in terms of the nature of the switching signals generated by the solution proposed in [30]. In particular, property (1) combined with (4.9) shows that unless  $\tilde{x} = \tilde{x}^+ = 0$  (which means that we are at the equilibrium  $x = x_e$ ), the solution always jumps to the interior of the flow set  $\mathcal{C}$ . Indeed,  $\tilde{x} \neq 0$  implies

$$-\tilde{x}^T Q \tilde{x} < -\eta \tilde{x}^T Q \tilde{x},$$

because  $\eta < 1$ . This fact, together with stability (ensuring boundedness of solutions) and the sector growth condition coming from the linearity of the flow dynamics (2.3), implies that there is a uniform lower bound on the dwell time between each pair of consecutive resets before solutions approach  $x = x_e$ . Clearly this lower bound shrinks to zero as solutions approach  $x = x_e$  because only arbitrarily fast switching can lead to  $x_e$  and equilibrium, in general.

In [30], following up to standard stability theory for hybrid systems given in Chapter 3, they have established suitable stability properties of the point  $x_e$  in terms of uniform global attractivity of a bounded (and closed) set in the higher-dimensional space spanned by  $(x, u)$ . In particular, they have established properties of the following compact attractor:

$$\mathcal{A} := \{(x, u) : x = x_e, u \in \{0, 1\}\}, \quad (4.13)$$

encompassing the fact that we are interested in uniform stability and convergence to a set where  $x = x_e$  and  $u$  assumed some unspecified value or pattern within the desired limit set of solutions.

☀ **THEOREM 4.** *Consider a point  $x_e$  satisfying Assumption 8 and matrices  $P, Q \in \mathcal{S}^2$ , satisfying Property 1. Then attractor (4.13) is uniformly globally asymptotically stable (UGAS) for hybrid system (4.7)–(4.10). Moreover, UGAS is robust because the attractor (4.13) is compact.*

*Proof.* Let take the Lyapunov function candidate  $V(\tilde{x}) = \frac{1}{2} \tilde{x}^T P \tilde{x}$ , where  $\tilde{x} = x - x_e$ . In the flow set,  $\mathcal{C}$ , using its definition in (4.9), we get

$$\langle \nabla V(\tilde{x}), f(\tilde{x}, u) \rangle = \tilde{x}^T P (A_u(\tilde{x} + x_e) + a) \leq -\eta \tilde{x}^T Q \tilde{x}. \quad (4.14)$$

In the jump set,  $\mathcal{D}$ , we get for all  $g \in G(x)$ , denoting  $\tilde{x}^+ = g - x_e$

$$V(\tilde{x}^+) - V(\tilde{x}) = \frac{1}{2} \{ \tilde{x}^T P \tilde{x} - \tilde{x}^T P \tilde{x} \} = 0. \quad (4.15)$$

Uniform global asymptotic stability is then shown applying [34, Theorem 1]. In particular, since the distance of  $x$  to the attractor (4.13) is defined by  $|x|_{\mathcal{A}} = |\tilde{x}|$ , we have that [34, eq. (6)] holds from the structure of  $V$  and from (4.14) and (4.15). To show



practical persistent flow, we first need to build a restricted hybrid system  $\mathcal{H}_{\delta,\Delta}$  by intersecting  $\mathcal{C}$  and  $\mathcal{D}$  with set

$$S_{\delta,\Delta} = \{\tilde{x} : |\tilde{x}| \geq \delta \quad \text{and} \quad |\tilde{x}| \leq \Delta\} \quad (4.16)$$

(see [34] for details). Then, notice that after each jump, from the definition of  $G$  in (4.8) and from inequality (4.11) (in Lemma 1), we have:

$$\tilde{x}^T (A_{u+x} + a) \leq -\tilde{x}^T Q \tilde{x} < -\eta \tilde{x}^T Q \tilde{x}, \quad (4.17)$$

where we used the fact that  $\eta < 1$  and that  $0 \notin S_{\delta,\Delta}$ . Therefore, if any solution to  $\mathcal{H}_{\delta,\Delta}$  performs a jump, it either jumps outside  $S_{\delta,\Delta}$  (and it terminates prematurely) or, from (4.10), it jumps to the interior of the flow set  $\mathcal{C} \cap S_{\delta,\Delta}$ . Indeed, from (4.16) we have that  $\tilde{x}$  is bounded away from zero in  $S_{\delta,\Delta}$ , so that, the right inequality in (4.17) is strict from positive definiteness of  $Q$ . Then all non terminating solutions must flow for some time and since  $\mathcal{C} \cap S_{\delta,\Delta}$  is bounded, there is a uniform dwell-time  $\rho(\delta, \Delta)$  in between each pair of consecutive jumps. This dwell-time  $\rho(\delta, \Delta)$  clearly implies [34, equ. (4)] with the class  $\mathcal{K}_\infty$  function  $\gamma(j) = \rho(\delta, \Delta)j$  and  $N = 1$ . Then, all the assumptions of [34, Theorem 1] hold and UGAS of  $\mathcal{A}$  is concluded.  $\square$

Theorem (4) establishes UGAS of the attractor, which results in desirable uniform stability and convergence properties. However, we are interested in further providing a suitable performance guarantee for our solution, which follows the same paradigm as that one in [32]. This performance guarantee may, for example, refers to desirable levels of dissipated energy, current peak, response time among others. Let comment in the next paragraph the choice of the matrices  $P$  and  $Q$ .

#### A. Optimality and parameters tuning

We first recall that solutions are parametrized by ordinary time  $t$  (measuring amount of flow) and discrete-time  $j$  (measuring the number of switches) so that the domain of a solution  $\xi$  (see Chapter 3) corresponds to a finite or infinite union of intervals of the following form:

$$\text{dom } \xi = \bigcup_{j \in \text{dom}_j \xi} I^j \times \{j\}, \quad (4.18)$$

with  $I^j = [t_j, t_{j+1}]$  being a bounded time interval having the so-called ‘‘jump times’’  $t_k$  as extremes, or possibly being a last unbounded interval open to the right and of the form  $I^j = [t_j, +\infty)$ . In (4.18), we use the notation  $\text{dom}_j \xi := \{j \in \mathbb{Z} : (t, j) \in \text{dom } \xi, \text{ for some } t \in \mathbb{R}\}$ , namely  $\text{dom}_j \xi$  includes all  $j \in \mathbb{Z}$  such that  $I^j$  is non-empty. Within this context, we represent an LQ performance metric focusing on flowing characteristics of the plant state, using the following expression:

$$J(\xi) := \sum_{k \in \text{dom}_j \xi} \int_{t_k}^{t_{k+1}} |\tilde{y}(\tau, k)|^2 d\tau, \quad (4.19)$$

where  $\xi = (x, u) : \text{dom } \xi \rightarrow \mathbb{R}^2 \times [0, 1]$  is a solution to hybrid system (4.7)–(4.10),  $\tilde{y}(t, j) = C_{u(t,j)} \tilde{x}(t, j)$  for all  $(t, j) \in \text{dom } \xi$ . With the hybrid switching solution presented in [30], we may then give the following guarantee on the performance cost (4.19).

☀ **THEOREM 5.** *Consider hybrid system (4.7)–(4.10) satisfying Assumption 8 and Property 1. If*

$$C^T C \leq Q, \quad (4.20)$$

then the following bound holds along any solution  $\xi = (x, u)$  of (4.7)–(4.10):

$$J(\xi) \leq \frac{1}{2\eta} \tilde{x}(0, 0)^T P \tilde{x}(0, 0) = \frac{1}{2\eta} \|\tilde{x}(0, 0)\|_P^2, \quad (4.21)$$

where  $\tilde{x}(t, j) = x(t, j) - x_e$ , for all  $(t, j) \in \text{dom}(\xi)$ .

*Proof.* Consider any solution  $\xi = (x, u)$  to  $\mathcal{H}$ . For each  $(t, j) \in \text{dom } \xi$ , denoting  $t = t_{j+1}$  to simplify notation, we have from (4.14)

$$\begin{aligned} V(\tilde{x}(t, j)) - V(\tilde{x}(0, 0)) &= \sum_{k=0}^j V(\tilde{x}(t_{k+1}, k)) - V(\tilde{x}(t_k, k)) \\ &= \sum_{k=0}^j \int_{t_k}^{t_{k+1}} \langle \nabla V(\tilde{x}(\tau, k)), f(x(\tau, k), u(\tau, k)) \rangle d\tau \\ &\leq \sum_{k=0}^j \int_{t_k}^{t_{k+1}} -\eta \|\tilde{x}(\tau, k)\|_Q^2 d\tau \leq -\eta \sum_{k=0}^j \int_{t_k}^{t_{k+1}} \|\tilde{x}(\tau, k)\|_{C^T C}^2 d\tau, \end{aligned} \quad (4.22)$$

where the last inequality comes from (4.20). Considering  $\tilde{z}(\tau, k) = C\tilde{x}(\tau, k)$ , taking the limit as  $t + j \rightarrow +\infty$  and using the fact that UGAS established in Theorem 4 implies  $\lim_{t+j \rightarrow +\infty} V(\tilde{x}(t, j)) = 0$ , we get from (4.22),  $\eta J(\xi) \leq V(\tilde{x}(0, 0)) = \frac{1}{2} \|\tilde{x}(0, 0)\|_P^2$ , as to be proven.  $\square$

🔗 **REMARK 6.** It should be emphasized that once matrices  $P$  and  $Q \in \mathcal{S}^2$  have been fixed compliantly with requirement (4.20), the guaranteed performance level for our scheme (in terms of size of the upper bound for index  $J$  in (4.19) along solutions) is proportional to the inverse of  $\eta \in (0, 1)$  (see (4.21)). To this end, large values of  $\eta$  (as close as possible to 1) are expected to lead to improved LQ performance along solutions.

On the other hand, one may appreciate by looking at the flow and jump sets in (4.9)–(4.10), that smaller values of  $\eta$  correspond to strictly smaller jump sets (and larger flow sets), which reveals that solutions are expected to flow longer before switches of control input  $u$  are experienced. Therefore we anticipate that solutions with smaller values of  $\eta$  exhibit a smaller switching frequency. In other words, one may play with parameter  $\eta$  to suitably adjust the switching frequency along solutions. This operation clearly affects the level of guaranteed optimality, according to (4.21).

The problem addressed next is the computation of parameters  $P$ ,  $Q$ , following some kind of optimization with the goal of reducing as much as possible the right hand side in bound (4.21). To this end, we make the following natural selection of matrices  $Q$ :

$$Q = C^T C + \varepsilon I, \quad (4.23)$$

where  $\varepsilon > 0$  is a (typically small) positive constant, which may be selected equal to zero if  $C^T C > 0$ . Then it is clear that selection (4.23) ensures  $Q > 0$ , as required, in addition to ensuring bound (4.20).

Once parameters  $Q$  are selected, under the assumption that  $A_i$  are Hurwitz matrices for all  $i \in [0, 1]$ , the following convex optimization problem:

$$\begin{aligned} \min_{P=P^T>0} \quad & \text{Trace} P, \\ \text{Such that} \quad & A_i^T P + P A_i^T \leq -2Q, \quad \forall i \in [0, 1], \end{aligned} \quad (4.24)$$

which provides the common matrix  $P$  satisfying Property 1.

**REMARK 7.** Note that, parameter  $\eta$  can adjust the switching frequency. Indeed, by decreasing  $\eta$ , we reduce the switching frequency and on the contrary, by increasing  $\eta$ , we raise the switching frequency. For practical reasons, the switching frequency must be low enough. Nevertheless, according to [30], this tuned parameter can manage some LQ performances.

Now that the hybrid control is proposed for the boost converter, the next section deals with the second part of proposition 1, meaning, extend the previous work and adding a adaptive control to deal with the unknown resistance  $R_0$ .

### 4.2.3. Hybrid adaptive control for a boost converter

The idea of this sub-section is to adapt the control law proposed in the previous sub-section to deal with the unknown resistance  $R_0$ . Firstly, let begin with the proposed adaptive law and then stability properties will be proven. Furthermore, assumption 8 and property 1 are adapted to take into account to the unknown  $R_0$  ( $\beta$  given in equation 4.1) and are given as;

**ASSUMPTION 9:**

There exists  $\lambda_e = [\lambda_{e_0}, \lambda_{e_1}]$  satisfying  $\lambda_{e_0} + \lambda_{e_1} = 1$ , such that the following convex combination holds:

$$\sum_{l=0}^1 \lambda_{e_l} (A_l(\beta)x_e + a) = 0 \quad \forall \beta \in [\beta^m, \beta^M]. \quad (4.25)$$

❖ **ASSUMPTION 10:**

Let consider that, the parameter  $\beta$  can be embedded into a polytope described as:

$$\Omega := \sum_{m=0}^1 \lambda_{\beta_m} \beta_m, \quad \text{for all } 0 \leq \lambda_{\beta_m} \leq 1, \quad \sum_{m=0}^1 \lambda_{\beta_m} = 1,$$

where the vertices of the polytope are given by  $\beta_m \in \{\beta^m, \beta^M\}$ .

★ **PROPERTY 2:**

Consider Assumption 10, then given matrices  $A_i(\beta)$ ,  $i \in \{0, 1\}$  in (4.2) with  $\beta \in [\beta^m, \beta^M]$ , there exists matrices  $P, Q \in \mathcal{S}^2$  satisfying

$$A_i^T(\beta_m)P + PA_i(\beta_m) + 2Q < 0 \quad (4.26)$$

for all  $i, m \in \{0, 1\}$ , where  $\beta_m \in \{\beta^m, \beta^M\}$  are the vertices of the polytope given in Assumption 10.

Note that Property 2 assumes that all matrices  $A_i^T(\beta_m)$  are Hurwitz. Selection of matrices  $P$  and  $Q$  satisfying Property 2 are discussed as for property 1 and resumed in sub-section A.

### A. Adaptation law

The adaptive law is composed by an observer to estimate the value of the state  $x_2$  ( $\hat{x}_2$ ), then gives an estimate  $\hat{\beta}$ , for the load  $\beta$ , since the variable  $\beta$  appears in the dynamic of the state  $x_2$ . The hybrid dynamical scheme considers the continuous-time dynamics,  $x_1, x_2, \hat{x}_2, \hat{\beta}$ , and the discrete-time dynamic,  $u$ . Hence, the goal of the proposed hybrid adaptive control is to regulate the state  $x_2$  around a reference value and find an estimate of  $\beta$  (see Fig. 4.3). The proposed control is detailed, and the stability properties are studied in the following.

The proposed adaptation law is composed of a state observer for the voltage  $x_2$ , and an adaptation law for parameter  $\beta$ , which are given as follows:

$$\dot{\hat{x}}_2 = \frac{1}{C_0}((1-u)x_1 - \hat{\beta}x_2) + \alpha(x_2 - \hat{x}_2) \quad (4.27)$$

$$\dot{\hat{\beta}} = g(x_2, \hat{x}_2), \quad (4.28)$$

where  $g(x_2, \hat{x}_2)$  is the adaptation law to be designed,  $\hat{x}_2$  is the estimated state of  $x_2$ ,  $\hat{\beta}$  is the estimated value of  $\beta$  and  $\alpha$  is a positive constant parameter, which is associated with the convergence speed of the observer.

### A.1. Error equation

In order to achieve a mathematical expression for  $g(x_2, \hat{x}_2)$ , let define the following error variables, considering  $\dot{\hat{\beta}} = 0$ ,

$$\check{x}_2 := x_2 - \hat{x}_2, \quad \tilde{\beta} := \beta - \hat{\beta}, \quad \dot{\tilde{\beta}} = -\dot{\hat{\beta}} \quad (4.29)$$

From (4.2) and (4.27), we derive the error equation of  $x_2$

$$\dot{\check{x}}_2 = -\frac{\tilde{\beta}}{C_0}x_2 - \alpha\check{x}_2. \quad (4.30)$$

Now, let introduce the candidate Lyapunov function

$$W(\check{x}_2, \tilde{\beta}) = \frac{1}{2} \left( \check{x}_2^2 + \frac{\tilde{\beta}^2}{\gamma} \right), \quad (4.31)$$

where  $\gamma$  is constant and positive and the derivative of  $W(\check{x}_2, \tilde{\beta})$  along the trajectories of (4.27) and (4.28) is given as:


$$\dot{W}(\check{x}_2, \tilde{\beta}) = -\alpha\check{x}_2^2 - \frac{x_2\check{x}_2}{C_0}\tilde{\beta} + \frac{\tilde{\beta}\dot{\tilde{\beta}}}{\gamma} = -\alpha\check{x}_2^2 + \tilde{\beta} \left( -\frac{x_2\check{x}_2}{C_0} + \frac{\dot{\tilde{\beta}}}{\gamma} \right).$$

The adaptation law is now defined by canceling the terms in parentheses, i.e.

$$\dot{\tilde{\beta}} = \frac{\gamma x_2 \check{x}_2}{C_0}, \quad (4.32)$$

and from equation (4.29)

$$\dot{\hat{\beta}} = -\frac{\gamma x_2 \check{x}_2}{C_0}. \quad (4.33)$$

 **REMARK 8.** Note that  $\gamma$  defines the adaptation speed, and consequently, if  $\gamma$  is larger, then the adaptation speed comes larger.

Stability properties of (4.30), (4.32) are then stated in the following lemma:

**\* LEMMA 2:**

Consider the system (4.2), and assume that its solutions are bounded. The extended observer (4.30)–(4.32) has the following properties:

- i) The estimated states  $\hat{x}_2, \hat{\beta}$  are bounded.
- ii)  $\lim_{t \rightarrow \infty} \hat{x}_2(t) = x_2(t)$ .
- iii)  $\lim_{t \rightarrow \infty} \hat{\beta}(t) = \beta$ , if and only if  $x_2(t) \neq 0, \forall t \geq 0$ .

*Proof.* The observer and the adaptive law error equations are fully defined from (4.30) and (4.32), and stability properties of these equations follow from the Lyapunov function  $W$  defined above. Note that with the choice (4.32)

$$\dot{W}(\check{x}_2, \tilde{\beta}) = -\alpha \check{x}_2^2$$

and from standard Lyapunov arguments, it follows that the error variable  $\check{x}_2$  and  $\tilde{\beta}$  are bounded. In addition by LaSalle invariant principle and from Assumption (7), that specifies  $x_2 \neq 0$ , we easily conclude that  $\lim_{t \rightarrow \infty} \check{x}_2(t) \rightarrow 0$ , which implies from (4.32) that  $\lim_{t \rightarrow \infty} \dot{\tilde{\beta}}(t) \rightarrow 0$ . Likewise from (4.30), and concluding from  $\lim_{t \rightarrow \infty} \check{x}_2(t) \rightarrow 0$  that  $\lim_{t \rightarrow \infty} \dot{\check{x}}_2(t) \rightarrow 0$ , we get  $\lim_{t \rightarrow \infty} \tilde{\beta}(t) \rightarrow 0$ .  $\square$

Based on assumption 7, an adaptive law is proposed, and the convergence of the error states  $(\check{x}_2, \tilde{\beta})$  are provided using the standard Lyapunov arguments and LaSalle invariant principle. Furthermore, a complete hybrid scheme, that encompasses the adaptive law is presented below.

## B. Hybrid model and proposed control law

In this section, we design an hybrid dynamical system, following the paradigm presented in Chapter 2, wherein continuous-time behavior resembles the evolution of  $x$ , given in (4.2) and the evolution of  $\hat{x}_2$  and  $\hat{\beta}$  presented in (4.27) and (4.33), respectively. Moreover, the discrete-time behavior captures the jump of the switch boost converter signal,  $u$ , and the jump of a discrete signal,  $q \in \{1, 2\}$ , which detects if the parameter  $\beta$  needs to be adapted.  $q = 1$  allows the  $\beta$  adaptation and  $q = 2$  interdicts this possibility.

We characterize the overall closed-loop dynamics

$$\mathcal{H} : \left\{ \begin{array}{l} \begin{bmatrix} \dot{x} \\ \dot{u} \\ \dot{\hat{x}}_2 \\ \dot{\hat{\beta}} \\ \dot{q} \end{bmatrix} = f(x, u, \hat{x}_2, \hat{\beta}), \quad \xi \in \mathcal{C} \\ \begin{bmatrix} x^+ \\ u^+ \\ \hat{x}_2^+ \\ \hat{\beta}^+ \\ q^+ \end{bmatrix} \in G(x, \hat{x}_2, \hat{\beta}, q), \quad \xi \in \mathcal{D}, \end{array} \right. \quad (4.34)$$

where  $\xi = [x \ u \ \hat{x}_2 \ \hat{\beta} \ q]$  and  $G$  is a (set-valued) map representing the switching logic:

$$f(x, u, \hat{x}_2, \hat{\beta}) := \begin{bmatrix} A_u(\beta)x + a \\ 0 \\ \frac{1}{C_0}(ux_1 - \hat{\beta}x_2) + \alpha(x_2 - \hat{x}_2) \\ -\frac{\gamma x_2(x_2 - \hat{x}_2)}{C_0} \\ 0 \end{bmatrix} \quad (4.35)$$

$$G(x, \hat{x}_2, \hat{\beta}, q) := \begin{bmatrix} x \\ \operatorname{argmin}_{i \in \mathbb{K}} \tilde{x}^T P(A_i(\hat{\beta})x + a) \\ \hat{x}_2 \\ \hat{\beta} \\ 3 - q \end{bmatrix} \quad (4.36)$$

and where  $\tilde{x} = [\tilde{x}_1 \ \tilde{x}_2]$  is defined from the desired values  $x_e = [i_e \ v_e]^T = [x_{e1} \ x_{e2}]^T$  as

follows

$$\begin{cases} \tilde{x}_1 = x_1 - x_{e1} \\ \tilde{x}_2 = (x_2 - x_{e2}) + (x_2 - \hat{x}_2). \end{cases} \quad (4.37)$$

Inspired by [30], we select the flow and jump sets as follows

$$\mathcal{C}_1 := \{(x, \hat{x}_2, q) : \{q = 1\} \text{ and } |x_2 - \hat{x}_2| \geq \varepsilon\} \quad (4.38)$$

$$\mathcal{D}_1 := \{(x, \hat{x}_2, q) : \{q = 1\} \text{ and } |x_2 - \hat{x}_2| \leq \varepsilon\}, \quad (4.39)$$

$$\mathcal{C}_2 := \{\xi : \{q = 2\} \text{ and } |x_2 - \hat{x}_2| \leq \varepsilon \text{ and } \tilde{x}^T P(A_u(\hat{\beta})x + a) \leq -\eta \tilde{x}^T Q_u \tilde{x}\}, \quad (4.40)$$

$$\mathcal{D}_2 := \{\xi : \{q = 2\} \text{ and } |x_2 - \hat{x}_2| \geq \varepsilon \text{ or } \tilde{x}^T P(A_u(\hat{\beta})x + a) \geq -\eta \tilde{x}^T Q_u \tilde{x}\}, \quad (4.41)$$

where  $\mathcal{D} := \mathcal{D}_1 \cup \mathcal{D}_2$  and  $\mathcal{C} := \mathcal{C}_1 \cap \mathcal{C}_2$ ,  $\eta \in (0, 1)$  and  $\varepsilon > 0$  is small enough. The so-called “flow” and “jump” sets  $\mathcal{C}$  and  $\mathcal{D}$  encompass, respectively, the regions in the (extended) space  $(x, u, \hat{x}_2, \hat{\beta}, q)$  where our switching strategy continues with the current mode  $u$  (set  $\mathcal{C}$ ) or is required to switch to a new mode (set  $\mathcal{D}$ ). If switching is allowed (namely, if  $(x, u) \in \mathcal{D}$ ) then  $u$  will switch according to  $G$  in (4.36). For the solution proposed here, we select the flow and jump sets based on the desired equilibrium  $x_e$  introduced in Assumption 9 and on the parameters  $P$  and  $Q$ . The selection of  $\mathcal{C}$  and  $\mathcal{D}$  can be summarized as in Figure 4.4

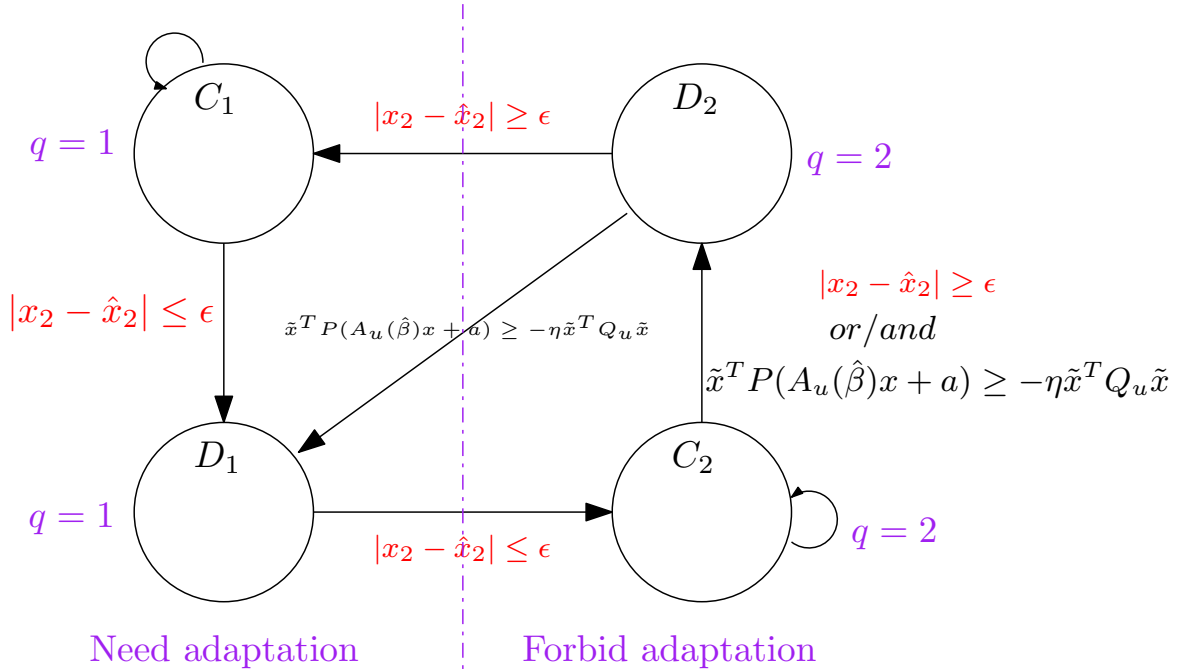


Figure 4.4: Schematic representation of the flow and jump sets.

We propose therefore Theorem 1, which ensures that the hybrid closed loop system is well-posed.



► **PROPOSITION 2:**

The hybrid dynamical system (4.34)–(4.41) satisfies the basic hybrid conditions presented in Assumption 3, then it is well-posed.

Now, we invokes the lemma [30, Lemma 1], which is a fundamental step to prove the stability properties and it is presented in the above section.

\* **LEMMA 3:**

Consider matrices  $P, Q \in \mathcal{S}^2$  satisfying Property 2, a point  $x_e \in \mathbb{R}^2$  satisfying Assumption 9. Then for each  $x \in \mathbb{R}^2$ ,

$$\min_{i \in [0,1]} \tilde{x}^T P(A_i(\beta)x + a) \leq \min_{i \in [0,1]} -\tilde{x}^T Q \tilde{x} \quad (4.42)$$

▢ **REMARK 9.** We note here that, if  $\tilde{x} \neq 0$

$$-\tilde{x}^T Q \tilde{x} < -\eta \tilde{x}^T Q \tilde{x}.$$

because  $\eta < 1$ .

We comment here the behavior of any solution to hybrid system (4.34)–(4.41) (see Figure 4.4). Note that if any solution is in  $\mathcal{C}_1$  or  $\mathcal{D}_1$ , that means  $q = 1$ , the adaptation of the parameter  $\beta$  is possible and, the contrary case is, if any solution is in  $\mathcal{C}_2$  or  $\mathcal{D}_2$ , that means  $q = 2$ . First, consider that any solution is in  $\mathcal{C}_1$ , then the observer error  $\check{x}_2$  given in 4.29 is larger than any small and positive  $\varepsilon$  and the parameter  $\beta$  is adapting. When the adaptation error of  $\beta$  is arbitrary small, that means  $\check{x}_2 \leq \varepsilon$ , then, the solution will be in  $\mathcal{D}_1$  and the solution jumps. After the jump, we have  $q = 2$  and the solution is in  $\mathcal{C}_2$  until that one of theses cases happens:

- $|x_2 - \hat{x}_2| \geq \varepsilon$ , then solution is in  $\mathcal{D}_2$  and jumps to  $\mathcal{C}_1$ , flowing here until  $\check{x}_2 \leq \varepsilon$ .
- $\tilde{x}^T P(A_u(\hat{\beta})x + a) \geq -\eta \tilde{x}^T Q_u \tilde{x}$  and  $|x_2 - \hat{x}_2| \leq \varepsilon$ , then solution is in  $\mathcal{D}_2$ , it jumps to  $\mathcal{D}_1$  and following the result of Lemma 4 the solution jumps again to  $\mathcal{C}_2$ , flowing here for a time (as proven bellow).

▢ **REMARK 10.** Note that when  $|x_2 - \hat{x}_2| \geq \varepsilon$ , any solution to  $\mathcal{H}$  flows in  $\mathcal{C}_1$  with  $u$  constant. Then the state  $x$  will flow according (4.2) to

$$i_{L,c} = \frac{V_{in}}{R_{LS} + (1-u)^2 R_0} \quad (4.43)$$

$$v_{C,c} = (1-u)R_0 i_{L,c}. \quad (4.44)$$

If  $u = 1$ ,  $x_2$  converges to  $v_{C,c} = 0$ , however from (4.2), we have  $x_2(t) = x_2(0)e^{-\frac{1}{R_0 C_0} t}$ , then  $x_2 \neq 0, \forall t \geq 0$ .

Following up to standard stability theory for hybrid systems [26], we will establish suitable stability properties of the point  $x_e$  in terms of uniform global attractivity of a bounded (and closed) set in the higher-dimensional space spanned by  $(x, u, \hat{x}_2, \hat{\beta}, q)$ . In particular, we will establish stability properties of the following compact attractor:

$$\mathcal{A} := \{\xi : x = x_e, u \in \{0, 1\}, \hat{x}_2 = x_2, \hat{\beta} = \beta, q \in \{1, 2\}\}. \quad (4.45)$$

☀ **THEOREM 6.** *Consider Assumption 7,9, 10 and matrices  $P, Q \in \mathcal{S}^2$  satisfying Property 2 and  $\gamma > 0$ . Then attractor (4.45) is Semiglobally Practically asymptotically stable (SPAS) for hybrid system (4.34)–(4.41).*

*Proof.* The next section is dedicated to the proof of our main result. For this, we apply singular perturbation analysis presented in section 3.5.1, due to fast dynamics in hybrid control given in [27] assuming that there are slow time-continuous variables,  $\xi_1 := (x, u, q)$ , and fast time-continuous variables,  $\xi_2 := (\hat{x}_2, \hat{\beta})$ , then we apply singular perturbation analysis to establish the stability properties. For this, we will rewrite the complete system in singular perturbation form.  $\square$

### B.1. Singular perturbation form

In order to put the system above in the standard singular perturbation form, let define the parameters  $\nu := \frac{1}{\alpha}$ ,  $\bar{\alpha} := \frac{1}{\alpha C_0}$  and  $\bar{\gamma} := \frac{\gamma}{\alpha C_0}$ .

With these considerations, let rewrite the hybrid scheme 4.34– 4.36 as follows:

$$\mathcal{H}_p : \left\{ \begin{array}{l} \begin{array}{l} \dot{x} \\ \dot{u} \\ \nu \dot{\hat{x}}_2 \\ \nu \dot{\hat{\beta}} \\ \dot{q} \end{array} \\ \begin{array}{l} x^+ \\ u^+ \\ \hat{x}_2^+ \\ \hat{\beta}^+ \\ q^+ \end{array} \end{array} \right. := \left[ \begin{array}{l} A_u(\beta)x + a \\ 0 \\ \bar{\alpha}(ux_1 - \hat{\beta}x_2) + (x_2 - \hat{x}_2) \\ -\bar{\gamma}x_2(x_2 - \hat{x}_2) \\ 0 \\ x \\ \underset{i \in \mathbb{K}}{\operatorname{argmin}} \tilde{x}^T P (A_i(\hat{\beta})x + a) \\ \hat{x}_2 \\ \hat{\beta} \\ 3 - q \end{array} \right] \begin{array}{l} \xi \in \mathcal{C} \\ \xi \in \mathcal{D}. \end{array} \quad (4.46)$$

Note that the fast variables directly impact the stability of the slow variables. However, the jumps do not affect the fast variables, because they do not present any jump. Indeed, when the resistance load need to be adapted ( $q=1$ ), the control state remains constant.

In order to perform a singular perturbation analysis details in 3.5.1, we need to check the assumptions given in section 3.5.1.

### B.1.1. Regularity of "manifold"

The "manifold", which corresponds to the quasi-steady-state equilibrium manifold of classical singular perturbation theory [36], that means when  $\nu \rightarrow 0^+$  is

$$\begin{aligned} x_2 - \hat{x}_2 &= 0 \\ \beta - \hat{\beta} &= 0. \end{aligned} \tag{4.47}$$

Note that  $\beta - \hat{\beta} = 0$  comes from (4.30). As (4.47) is continuous, we can ensure that the manifold is empty outside of  $\mathcal{C}$ , leading to the following set-valued:

$$\mathcal{M}(x_2) := \begin{cases} \begin{cases} x_2 \\ \beta \end{cases} & x_2 \in \mathcal{C} \\ 0 & x_2 \notin \mathcal{C}. \end{cases}$$

Notice that  $\mathcal{M}$  is outer semi-continuous, locally bounded and nonempty.

### B.1.2. Stability for reduced system

The reduced system is the system (4.34)–(4.36) in the manifold  $\mathcal{M}$ , which is

$$\begin{aligned} \begin{bmatrix} \dot{x} \\ \dot{u} \\ \dot{q} \end{bmatrix} &:= \begin{bmatrix} A_u(\beta)x + a \\ 0 \\ 0 \end{bmatrix} & \xi_r \in \mathcal{C}(\mathcal{M}) \\ \begin{bmatrix} x^+ \\ u^+ \\ q^+ \end{bmatrix} &:= \begin{bmatrix} x \\ \underset{i \in \mathbb{K}}{\operatorname{argmin}} \tilde{x}^T P(A_i(\hat{\beta})x + a) \\ 3 - q \end{bmatrix} & \xi_r \in \mathcal{D}(\mathcal{M}). \end{aligned} \tag{4.48}$$

where  $\xi_r = (x, u, q)$ . Note there is no jump in  $\mathcal{M}$ , therefore the reduced system ignores  $\hat{x}_2$  and  $\hat{\beta}$  when determining jumps. Moreover, remark that  $q$  nor presents any effect in the reduced system dynamic and neither generates any extra jump.

### B.1.3. Stability of the boundary layer

The boundary layer, for each  $r > 0$ , is given by

$$\mathcal{H}_{bl} := \begin{cases} \dot{\xi}_1 = 0 \\ \dot{\hat{x}}_2 = \bar{\alpha}(ux_1 - \hat{\beta}x_2) + (x_2 - \hat{x}_2) \\ \dot{\hat{\beta}} = -\bar{\gamma}x_2(x_2 - \hat{x}_2) \end{cases} \quad \zeta \in \mathcal{C} \cap r\mathbb{B}$$

being  $r\mathbb{B}$  a closed ball of radius  $r$ . Note that the boundary layer system ignores the jumps, and during, flows  $\xi_1$  remains constant.

In order to evaluate the stability of the boundary layer, let consider the error equations of  $\mathcal{H}_{bl}$  and re-scale time  $t$  to  $\tau = (t - t_0)/\nu$ , getting

$$\begin{aligned} \frac{d}{d\tau}\check{x}_2 &= -\bar{\alpha}x_{2bl}\tilde{\beta} - \check{x}_2 \\ \frac{d}{d\tau}\tilde{\beta} &= \bar{\gamma}x_{2bl}\check{x}_2. \end{aligned}$$

which can be rewritten as:

$$\frac{d}{d\tau}z = Jz$$

with

$$J = \begin{pmatrix} -1 & -\bar{\alpha}x_{2bl} \\ \bar{\gamma}x_{2bl} & 0 \end{pmatrix}.$$

Without lost of generality and from Assumption 7,  $x_{2bl} \in \{\mathbb{R} \setminus \{0\}\}$ . Therefore, we can define the next property:

**★ PROPERTY 3:**

*The real part of the eigenvalues of  $J$ , for  $x_{2bl} \in \{\mathbb{R} \setminus \{0\}\}$  are all strictly negative, i.e.*

$$\begin{aligned} \lambda_1 &= \Re \left\{ \frac{-1 + \sqrt{1 - 4\bar{\alpha}^2\gamma x_{2bl}^2}}{2} \right\} < 0 \\ \lambda_2 &= \Re \left\{ \frac{-1 - \sqrt{1 - 4\bar{\alpha}^2\gamma x_{2bl}^2}}{2} \right\} < 0 \end{aligned}$$

*Proof.* From the analysis given in B.1 and Proposition 2, we prove SPAS of attractor (4.45) by applying [27, Theorem 1].  $\square$

**REMARK 11.** In order to ensure a singular perturbation form, we need to ensure that the observer time response must be larger than the time response of  $x$ , i.e.,  $|\lambda_s| \ll \alpha$ , where  $\lambda_s$  is the minimum eigenvalue of the slow subsystem.

**REMARK 12.** Note that the real part of the eigenvalues are strictly negative for all  $\gamma > 0$ . However, we deduce that

- the response of the fast variables  $\xi_2$  is non-oscillating for all

$$0 < \gamma \leq \frac{\bar{\alpha}^2}{4x_{2bl}^2}.$$

- likewise, we get oscillations in the transient response of the fast subsystem for

$$\gamma > \frac{\bar{\alpha}^2}{4x_{2bl}^2}.$$

#### 4.2.4. Applications

In this section, we validate our hybrid approach for the boost converter (2.3) in simulation. These simulations are performed in MATLAB/Simulink by exploiting the HyEQ Toolbox [37].

Consider  $V_{in} = 100V$ ,  $R = 2\Omega$ ,  $L = 500\mu H$ ,  $C_0 = 470\mu F$ ,

$$R_0 = 50\Omega \in [25, 75]\Omega \Rightarrow \beta = 0.02 \in [0.0133, 004], \quad (4.49)$$

which corresponds to 50% of variation with respect to the nominal value of  $R_0$  and a sampling time  $T_s = 10^{-6}s$ .

The switched system state space model (2.3) is defined by the following matrices:

$$A_1 = \begin{bmatrix} -\frac{R}{L} & 0 \\ 0 & -\frac{1}{R_0 C_0} \end{bmatrix}, \quad A_2 = \begin{bmatrix} -\frac{R}{L} & -\frac{1}{L} \\ \frac{1}{C_0} & -\frac{1}{R_0 C_0} \end{bmatrix},$$

$$B_1 = B_2 = \begin{bmatrix} \frac{1}{L} \\ 0 \end{bmatrix}.$$

For our simulations, the chosen equilibrium is

$$x_e = [i_e(\beta) \quad 120]^T. \quad (4.50)$$

Following the specification given at the end of Section 4.3.2 and considering the variation of  $\beta$  (4.49), the quadratic cost function is defined as

$$J = \min_u \sum_{k \in \text{dom}_j(\xi)} \int_{t_k}^{t_{k+1}} \frac{\rho}{R_0} (v_c(\tau, k) - v_e)^2 + R(i_L(\tau, k) - i_e(\beta))^2 d\tau \quad (4.51)$$

with  $\rho = 1000$  to suitably penalize the voltage error.

Multiplying the cost by  $(\rho R)^{-1}$ , one clearly sees that this corresponds to selecting  $C = [0 \ (RR_0)^{-\frac{1}{2}}]$  and  $\varepsilon = \rho^{-1}$  in (4.23), which gives  $Q = \begin{bmatrix} R & 0 \\ 0 & \rho/R_0 \end{bmatrix}$ .

With this value of  $Q$ , in order to satisfy Property 2, we choose

$$P = \begin{bmatrix} 23.14 & 1.08 \\ 1.08 & 37.04 \end{bmatrix} \cdot 10^{-2}.$$

Moreover, we take  $\eta = 0.1$  which corresponds to a sub-optimal value that guarantees a trade-off between performance level and switching frequency, as shown in [30].

Let start by a known resistance  $R_0$ . Figure. 4.5 reports voltage and current evolutions for different selections of  $\eta$  and for the choice  $\lambda_e = [0.22 \ 0.78]$  that satisfies Assumption 8. Just as before, Theorems 4 and 5 guarantee asymptotic stability and optimality for the scheme. Once again, as  $\eta$  gets larger, the transient becomes closer to the one obtained when the switched control proposed in [32]. In all cases, the transient duration is less than  $30ms$  with a maximum current peak near  $3.25A$  of magnitude. The switching frequency in a time slot of the transient is reported in Figure. 4.6 for different values of  $\eta$ , we see the expected trend (from Remark 7) of the switching frequency, as a function of  $\eta$ .

A more informative picture can be grasped by Figure. 4.7 where, it is shown that selecting small values of  $\eta$  allows us to suitably adjust the switching frequency while giving up a little on the performance guarantee (even though Figure. 4.5 shows that the performance is not much deteriorated when  $\eta$  is very small, thus showing some level of conservativeness of our bound). Note that, the value of  $\eta$  for which we obtain essentially the same behavior as the scheme in [32] is much larger than 0.5 and grows up to somewhere around 0.95.

Let simulate with the unknown resistance  $R_0$ . Likewise, we select the convergence speed of the observer state,  $\alpha$ , according to Remark 11 and, having  $|\lambda_s| = 4000$  for the slow sub-system minimum eigenvalue. Then, we need to satisfy  $4000 \ll \alpha$ ; for this issue, we chose  $\alpha = 40000$ .

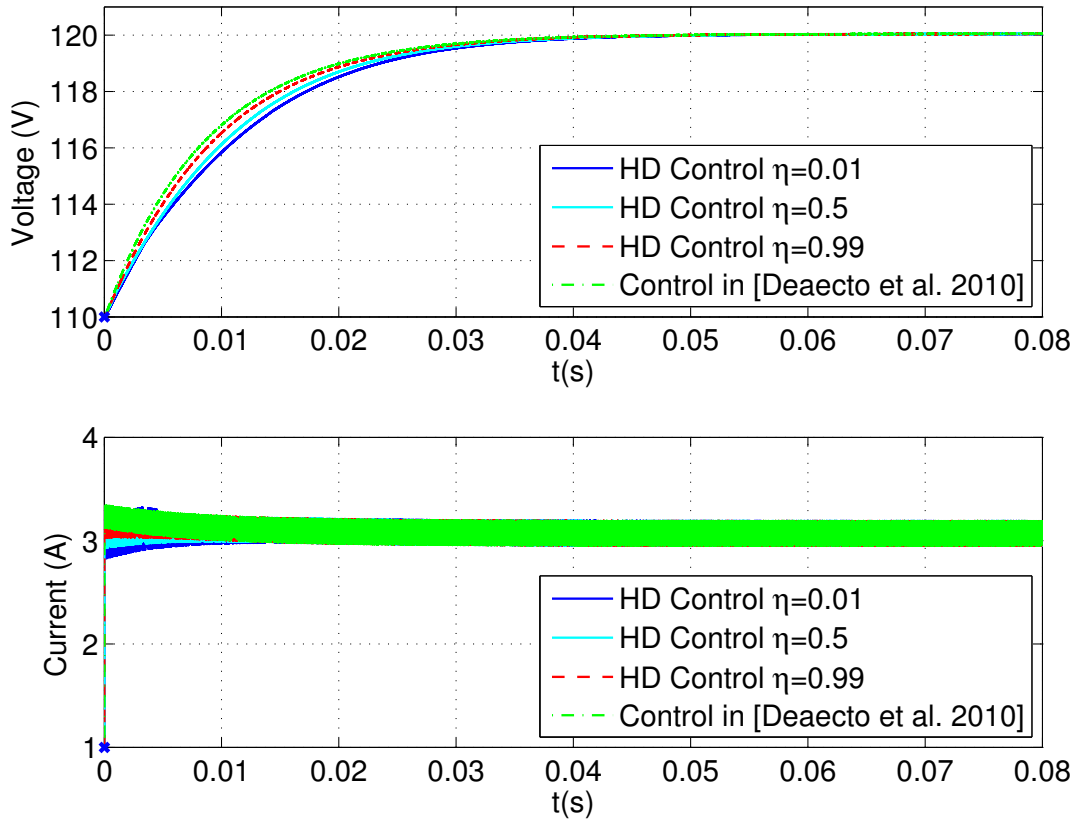


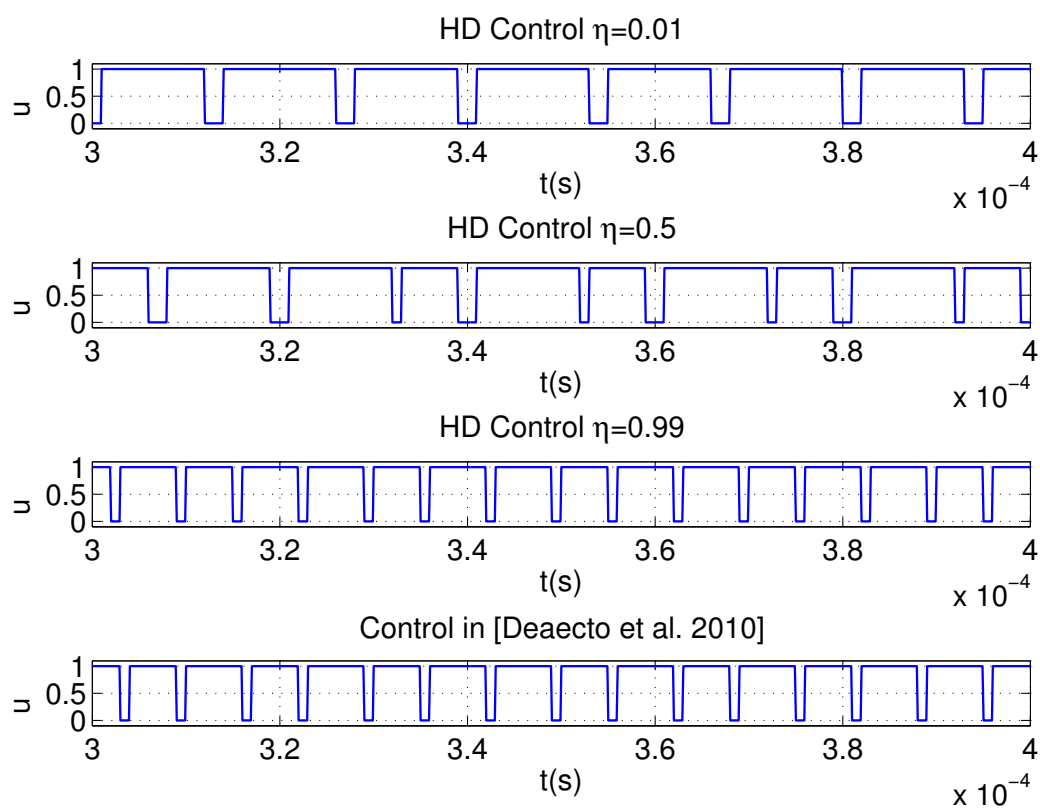
Figure 4.5: Voltage and current evolution of the boost converter.

The next step is to select the adaptation speed,  $\gamma$ , according to Remark 12. At the first instance, we choose  $\gamma$  such that, there is no oscillation during the steady-state ( $x_{2bl} = x_{e2} = 120$ ), i.e.,  $0 < \gamma \leq \frac{\bar{\alpha}^2}{4x_{2bl}^2} = 61 \cdot 10^{-4}$ . Then, we take  $\gamma = 5 \cdot 10^{-4}$  in Figure. 4.8, and  $\gamma = 50 \cdot 10^{-4}$  in Figure. 4.9. Finally, we take  $\varepsilon = 10^{-3}$ . Note that in these simulations, the load changes twice, in the transient time at  $t = 0.001s$  and in the steady state at  $t = 0.03s$ .

Figure 4.8-a) and 4.9-a) show the convergence of  $x_2$  to the equilibrium (4.3.3) for any change of  $\beta$ , which is achieved with  $\lambda_e = [0.17 \ 0.83]^T$  satisfying Assumption 9. Note that during the adaptation of  $\beta$ , that means, when  $|\check{x}_2| \geq \varepsilon$ , at  $t = 0.001s$  and  $t = 0.03s$  the states flow with  $u$  constant converging to  $i_{L,c}$ ,  $v_{C,c}$ , given in (4.43)–(4.44). When  $|\check{x}_2| \leq \varepsilon$  the states evolve switching the discrete variable  $u$ . This evolution can be seen in the zoom of  $u$  in Fig. 4.8-d) and 4.9-d) for different adaptation speed,  $\gamma$ . Note that if  $\gamma$  is larger the adaptation faster is, according Remark 8.

We can also see during the load changes that, the error  $\check{x}_2$  increases, but it converges to zero, due to the fact that  $\hat{\beta}$  is adapted to its real value  $\beta$ , as is established in Lemma 2. Then, we can conclude from Theorem 7 that our attractor (4.60) is SPAS.

Now, we show some simulations for the case when the adaptation presents some

Figure 4.6: Zoom of  $u$  in the boost converter.



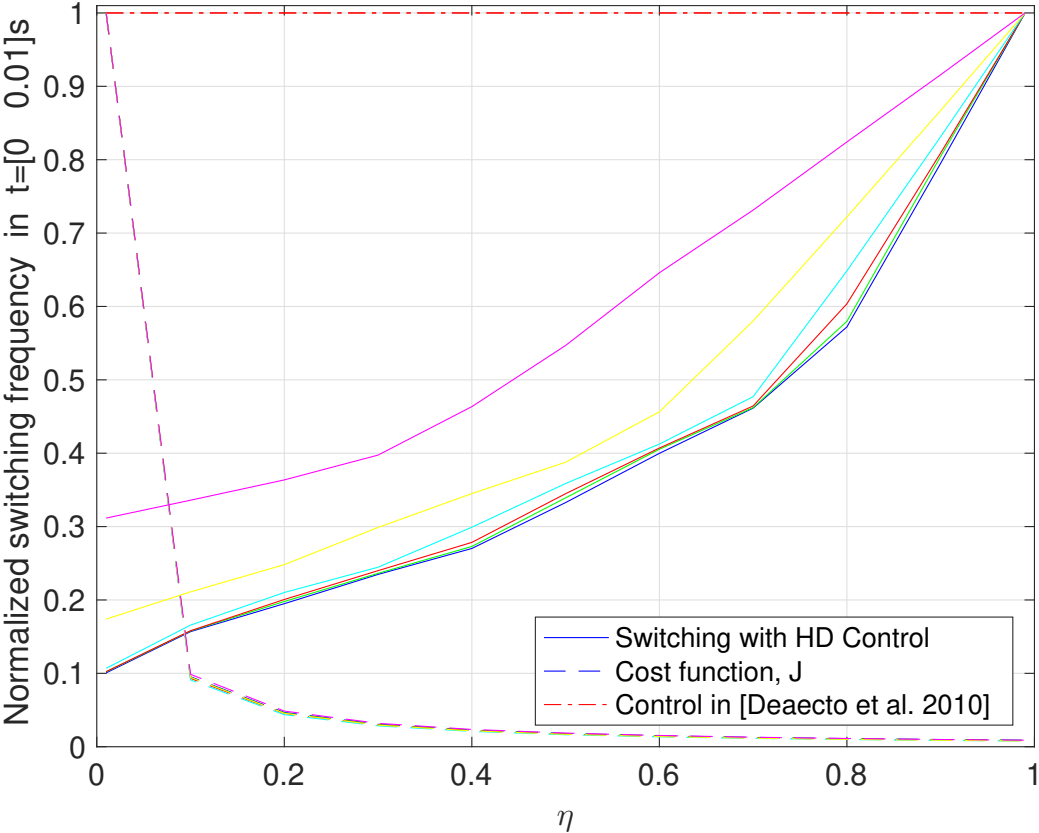


Figure 4.7: Evolution of the normalized switching frequency w.r.t.  $\eta$  for different initial conditions in the boost converter.

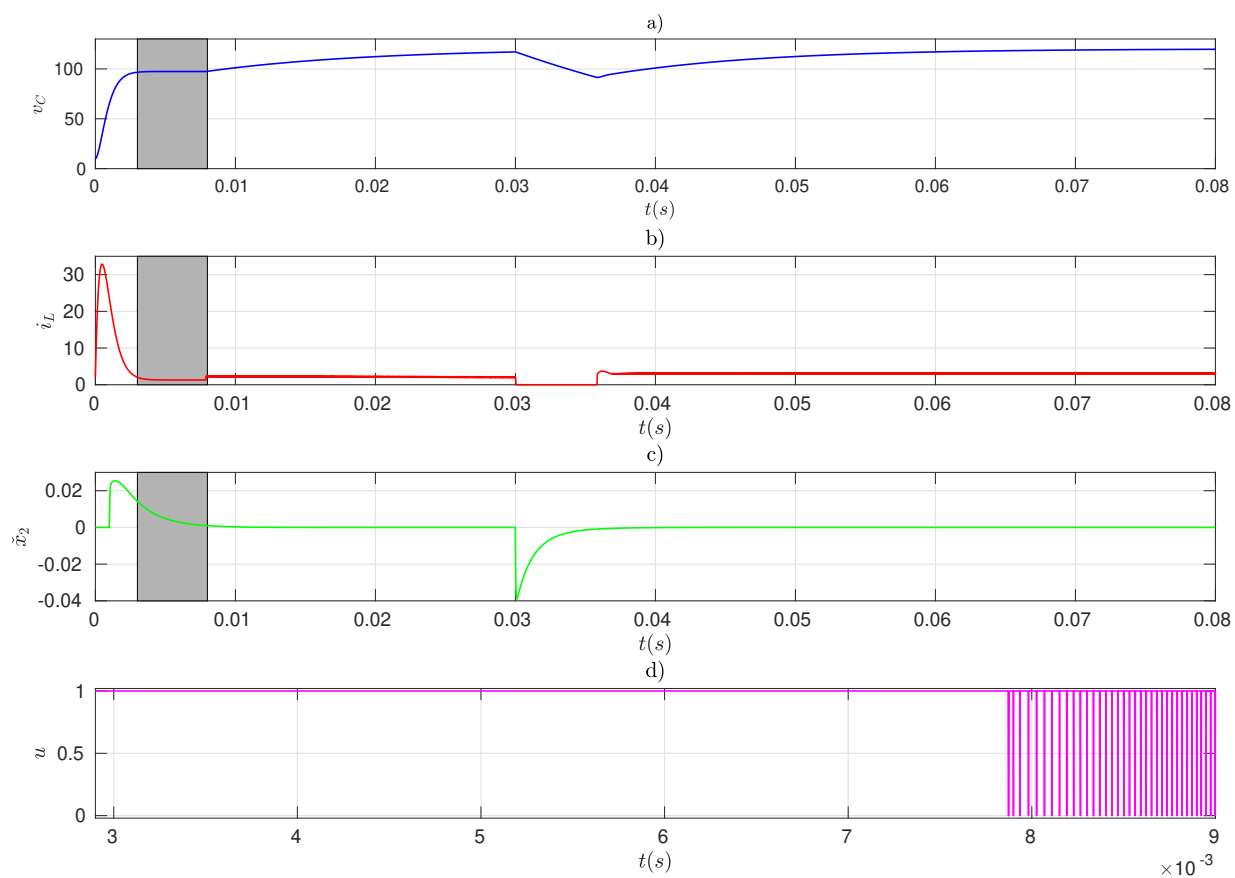


Figure 4.8: Evolutions for  $\gamma = 5 \cdot 10^{-4}$  of the voltage and current in a) and b) resp.,  $\check{x}_2$  in c) and, zoom of  $u$  in d).

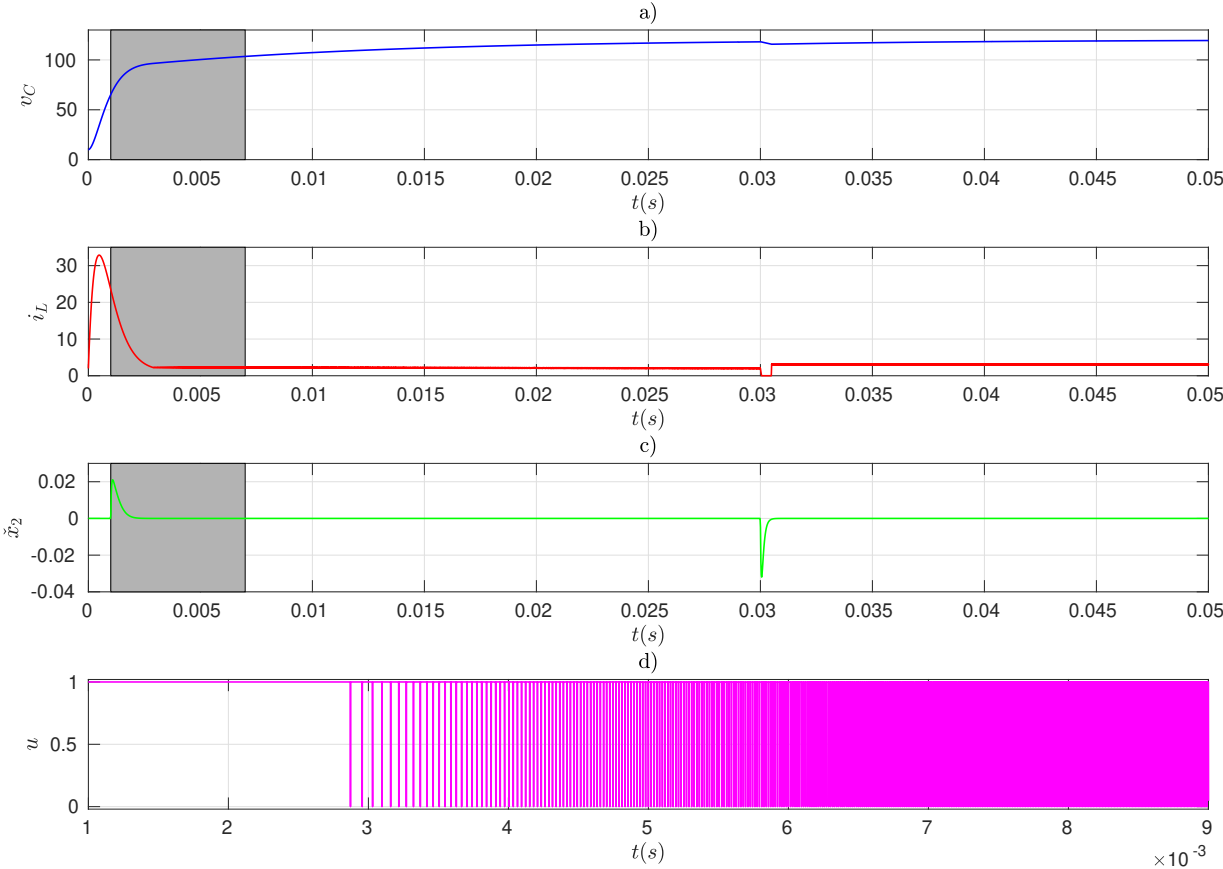


Figure 4.9: Evolutions for  $\gamma = 50 \cdot 10^{-4}$  of the voltage and current in a) and b) resp.,  $\check{x}_2$  in c) and, zoom of  $u$  in d)

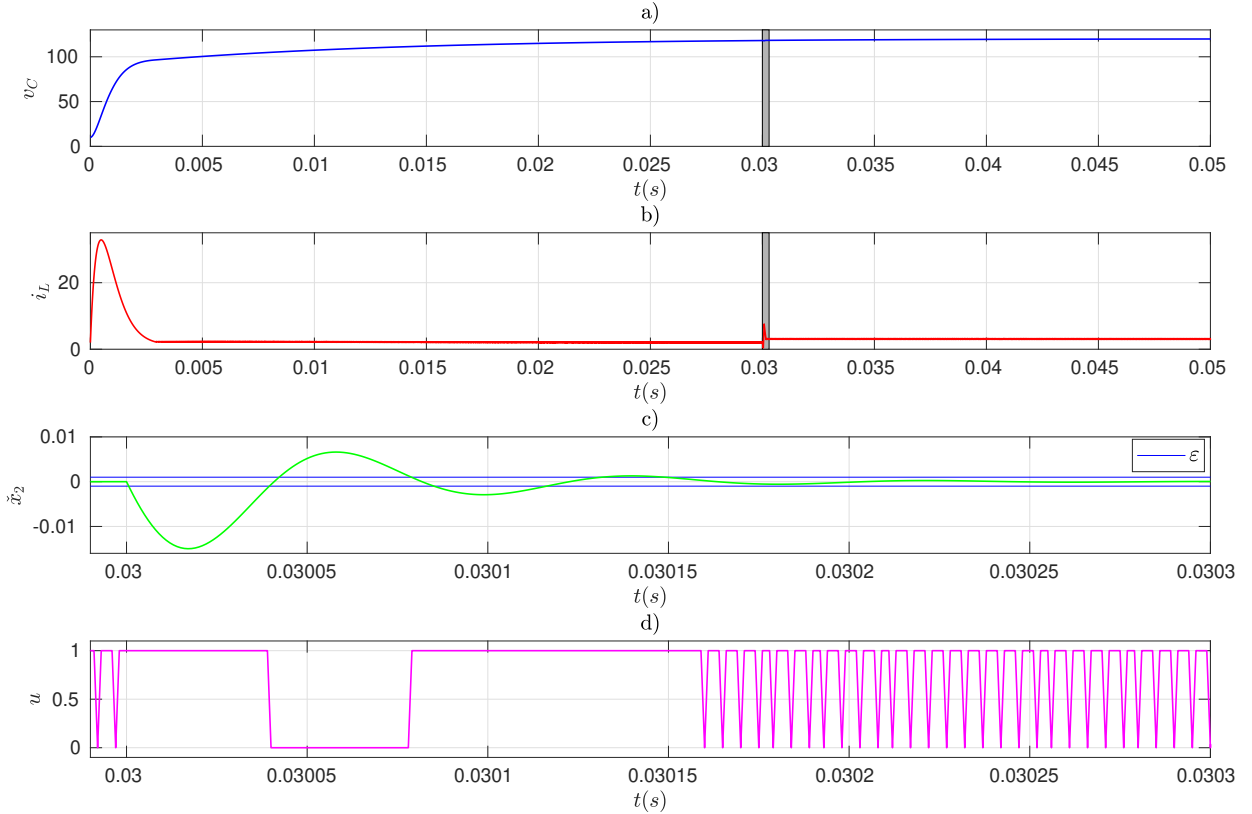


Figure 4.10: Evolutions for  $\gamma = 0.1$  of the voltage and current in a) and b) resp., and zoom of  $\check{x}_2$  and  $u$  in c) and d) resp.

oscillations in the steady-state, i.e.  $\gamma > \frac{\alpha^2 C_0^2}{4x_2^2 b l} = 61 \cdot 10^{-4}$ , according to Remark 12. We select  $\gamma = 0.1$  in Figure. 4.10 and  $\gamma = 1$  in Figure. 4.11. Note that  $\check{x}_2$  converges to zero after some oscillations in Figure. 4.10-c) and in Figure. 4.11-c), maintaining  $x_2$  robust w.r.t. its equilibrium value. We can also see that the observer convergence is faster, as  $\gamma$  larger is.

### 4.2.5. Conclusions

A hybrid adaptive control for unknown constant or/and slowly variable load is presented for a boost converter. The method focuses on a hybrid dynamical theory, that considers the real nature of the signals, that means, the continuous-time and the discrete-time signals. On this paradigm, an adaptive control is proposed which guarantees the robustness of the voltage in a reference value. This adaptive control is fed by a state observer designed by assuming that the state variables are measured. SPAS of the full system is proven by using a standard singular perturbation analysis.

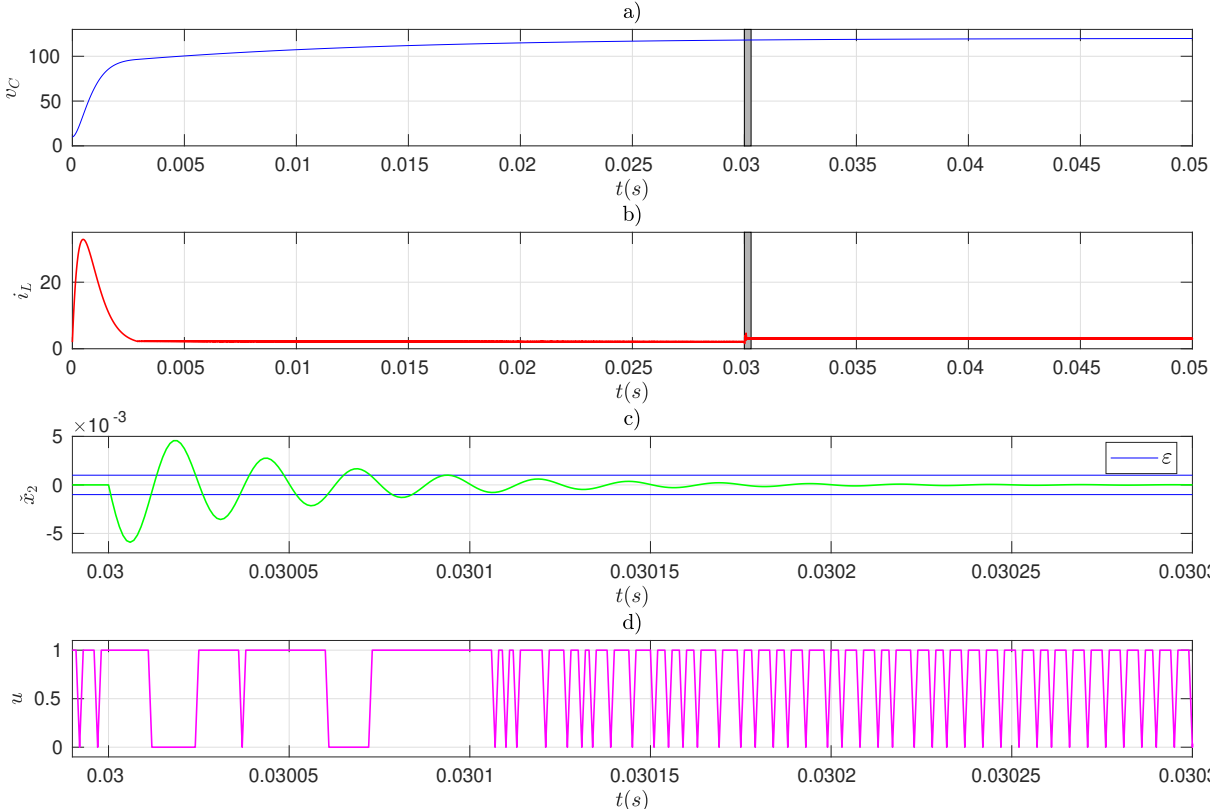


Figure 4.11: Evolutions for  $\gamma = 1$  of the voltage and current in a) and b) resp., and zoom of  $\check{x}_2$  and  $u$  in c) and d) resp.

### 4.3. AC-DC Converters: Three-phase three-level NPC Converter

The main control objective of this device is to generate a desired sinusoidal input currents, that provides a DC link voltage keeping it constant at the desired reference value, while maintaining the neutral point voltage close to zero. In order to achieve these control objectives, some control strategies have been developed in the literature. A first classical approach widely studied relies on the control design of averaged models [38][39]. The most employed averaged controller for the NPC rectifier is called Direct Power Control (DPC) method. This approach generally uses several PI controllers, one for the instantaneous powers, the second one to keep the neutral point voltage close to zero and the third one to regulate the dc-link voltage to a desired value [23][40].

Recently, some control strategies have been proposed to control the switches without considering an averaged model, which led to discontinuous control laws. Among them, we can cite predictive control algorithms (for inverters in [41] and converters in [42]), sliding mode controllers (for inverters in [43],[44] and converters in [45],[46]) and hybrid controllers (for inverters in [47] and converters in [30]). For the case of the NPC, to the best of our knowledge, only a few papers have considered explicitly the discrete nature of the switches. In [48],[49], a predictive control algorithm is used to predict the capacitor voltages for the next sampling time. In [50], a sliding mode control design is considered and the sliding surfaces use directly the error between the state variables and their references.

In this work, we propose to model the NPC as a hybrid model by considering, the voltage and current signals as continuous dynamics, as well as, the switching control signals as discrete dynamics. However, compared to the others topics studied in this thesis, the main challenge is to consider the nonlinear time-varying nature of the system. Following the Hybrid Dynamical System (HDS) theory [26], we propose a control guaranteeing Uniform Global Asymptotic Stability (UGAS) of the operating point.

The NPC converter can be modeled by a nonlinear time varying model given in (2.19) and is remembered in the following

$$\begin{cases} \dot{x}(t) = A_u(t)x(t) + a \\ y(t) = Cx(t), \end{cases} \quad (4.52)$$

The next assumption is necessary to guarantee the existence of a switching signal that ensures forward invariance of the equilibrium point,  $x_e$ , in the generalized sense of Filippov, considering  $u \in \{u^{(1)}, \dots, u^{(25)}\}$  and equation (2.21), and  $A_u(t)$ ,  $a$  and  $C$  given in Equation (2.19).

❖ **ASSUMPTION 11:**

There exist 25 functions of time  $\lambda_{1eq}(t), \lambda_{2eq}(t), \dots, \lambda_{25eq}(t)$  satisfying  $\sum_{l=1}^{25} \lambda_{leq}(t) = 1$  for all  $t > 0$ , such that the following convex combination holds for every  $t$ :

$$\sum_{l=1}^{25} \lambda_{leq}(t) (A_{u^{(l)}}(t)x_e + a) = 0, \quad (4.53)$$

with

$$A_{u^{(l)}}(t) = \begin{bmatrix} M_1 & M_2 & M_3 & M_4 \end{bmatrix} \left( \begin{bmatrix} \Gamma & 0 \\ 0 & \Gamma \end{bmatrix} u^{(l)} \right) \otimes 1_4 + M_0$$

where  $u^{(l)} \in U$  and  $x_e$  is the desired value of the regulation, meaning that the equilibrium point is reached in sense of Filippov. The matrices  $M_0, M_1, M_2, M_3$  and  $M_4$  are given in equation (2.22).

In order to establish the stability properties of the equilibrium point  $x_e$ , we introduce the following property.

★ **PROPERTY 4:**

For matrices  $\tilde{A}_u(j)$  defined in (2.22), there exist common matrices  $P, Q \in \mathcal{S}^4$  satisfying

$$\tilde{A}_{u^{(i)}}(j)^T P + P \tilde{A}_{u^{(i)}}(j) + 2Q < 0, \quad (4.54)$$

for all  $j \in \{1, \dots, 4\}$  and  $u^{(i)} \in U$  with  $i \in \{1, \dots, 25\}$ . Therefore, matrices  $\tilde{A}_{u^{(i)}}(j)$  are Hurwitz.

*Proof.* The statement can be easily proven choosing

$$P = \begin{bmatrix} L & 0 & 0 & 0 \\ 0 & L & 0 & 0 \\ 0 & 0 & CV_s^2 & 0 \\ 0 & 0 & 0 & CV_s^2 \end{bmatrix},$$

$$Q = \begin{bmatrix} -R_{LS} & 0 & 0 & 0 \\ 0 & -R_{LS} & 0 & 0 \\ 0 & 0 & -(\frac{1}{R} + \frac{1}{2R_p})V_s^2 & 0 \\ 0 & 0 & 0 & -\frac{g}{2R_p} \end{bmatrix},$$

which are found from the system structure and energy-like arguments, meaning that the energy of the system is dissipated only through the resistances. □

### 4.3.1. The control objectives

The objectives of the control problem are summarized as follows:

1. The instantaneous active power  $p$  and the instantaneous reactive power  $q$  should track their references denoted  $p^*$  and  $q^*$ , respectively,

$$p \rightarrow p^*$$

$$q \rightarrow q^*.$$

2. The sum of the converter capacitors voltages  $v_{dc}$  should be regulated towards its reference denoted  $v_{dc}^*$ ,

$$v_{dc} \rightarrow v_{dc}^*.$$

3. The difference of the converter capacitors voltages  $v_d$  should be as small as possible,

$$v_d \rightarrow 0.$$

The desired equilibrium point can then be represented as  $x_e = [x_{e1} \ x_{e2} \ x_{e3} \ x_{e4}]^T = [p^* \ q^* \ v_{dc}^* \ 0]^T$ .

In order to achieve these objectives, while taking into account the characteristics of the system, we propose a control algorithm described in the next section.

### 4.3.2. Hybrid model and proposed control law

Continuous-time and discrete-time dynamics are present in the considered system and the HDS theory developed in [26] is a potential way to take both dynamics into consideration. The continuous evolution (or flows) represents the evolution of the instantaneous active and reactive power states and the voltages  $v_{dc}$  and  $v_d$ . Likewise, the discrete evolution (or jumps) represents switching control inputs  $u \in \{u^{(1)}, \dots, u^{(25)}\}$ .

Then, the closed loop system can be easily described as a hybrid system of the form  $\mathcal{H} = (\mathcal{C}, f, \mathcal{D}, G)$ :

$$\mathcal{H} : \begin{cases} \begin{bmatrix} \dot{x} \\ \dot{u} \end{bmatrix} = f(t, x, u), & (x, u) \in \mathcal{C}, \\ \begin{bmatrix} x^+ \\ u^+ \end{bmatrix} \in G(t, x, u), & (x, u) \in \mathcal{D}, \end{cases} \quad (4.55)$$



$$\begin{aligned}
 f(t, x, u) &:= \begin{bmatrix} A_u(t)x + a \\ 0 \end{bmatrix}, \\
 G(t, x, u) &:= \begin{bmatrix} x \\ \operatorname{argmin}_{i \in \mathbb{K}} \tilde{x}^T P(A_{u^{(i)}}(t)x + a) \end{bmatrix}
 \end{aligned} \tag{4.56}$$

with  $i \in \{1, 2, \dots, 25\}$  and  $\tilde{x} = x - x_e$  the error between  $x$  and the equilibrium  $x_e$ .

The flow and jump sets are given as:

$$\mathcal{C} := \{(x, u) : \tilde{x}^T P(A_u(t)x + a) \leq -\eta \tilde{x}^T Q \tilde{x}\}, \tag{4.57}$$

$$\mathcal{D} := \{(x, u) : \tilde{x}^T P(A_u(t)x + a) \geq -\eta \tilde{x}^T Q \tilde{x}\}, \tag{4.58}$$

where  $\eta \in (0, 1)$  is a design parameter.

The basic idea used in model (4.55)-(4.58) is as in Section 4.2.2 and is given as follows: assume there exists a common Lyapunov function,  $V(\tilde{x}) = \tilde{x}^T P \tilde{x}$ , for all modes of the system, then

- if the Lyapunov function is sufficiently decreasing for a given control input, then this value of control is maintained.
- If the derivative of the Lyapunov function is not sufficiently negative, the control input is changed in order to improve the decreasing of  $V(\tilde{x})$ .

► **PROPOSITION 3:**

The hybrid system (4.55) – (4.58) satisfies the basic hybrid conditions given in assumption 3. Then, we can conclude that the hybrid system (4.55) – (4.58) is well-posed.

The next Lemma guarantees the control mechanism described before, ensuring that the Lyapunov function is decreasing enough after each jump.

\* **LEMMA 4:**

Consider matrices  $P, Q \in \mathcal{S}^4$  satisfying Property 4, a point  $x_e \in \mathbb{R}^4$  satisfying Assumption 11, then, for each  $x \in \mathbb{R}^4$ ,

$$\min_{i \in \mathcal{K}} \tilde{x}^T P(A_{u^{(i)}}(t)x + a) \leq -\tilde{x}^T Q \tilde{x}, \tag{4.59}$$

with  $\tilde{x} = x - x_e$ .

🔗 **REMARK 13.** We note here that, if  $\tilde{x} \neq 0$

$$-\tilde{x}^T Q \tilde{x} < -\eta \tilde{x}^T Q \tilde{x}.$$

because  $\eta < 1$ .

Following the hybrid system theory, we will establish stability properties of the given compact set

$$\mathcal{A} := \{(x, u) : x = x_e, u \in U\}. \quad (4.60)$$

☀ **THEOREM 7.** *Consider Assumption 11 and matrices  $P, Q \in \mathcal{S}^4$  satisfying Property 4. Then, the set (4.60) is UGAS for hybrid system (4.55)–(4.58) for each  $x_e$  satisfying Assumption 11.*

### 4.3.3. Applications

In this section, some simulations are performed on the proposed closed loop system by using MATLAB/Simulink and by exploiting the HyEQ Toolbox [37] to verify the properties of the closed loop (4.55)–(4.58).

The parameters of the NPC are given in Table 4.1. The simulations are made for different values of sampling time  $T_s$  (where the switching frequency is  $f_s = \frac{1}{T_s}$ ). Moreover, we choose  $\eta = 0.1$  following up the trade-off between switching frequency and performance mentioned in Remark 7.

Table 4.1: Simulation parameters

Parameter	Convention	Value/(Units)
Estimated series resistance	$R_{LS}$	0.4 ( $\Omega$ )
load resistance	$R$	30 ( $\Omega$ )
Estimated parasitic resistance	$R_p$	20 ( $K\Omega$ )
Inductor	$L$	15 ( $mH$ )
Output capacitor	$C$	1500 ( $\mu F$ )
Total dc-link voltage reference	$V_{dc}^*$	150 ( $V$ )
Amplitude of the grid voltages	$V_{s\alpha}$	$62\sqrt{2}$ ( $V$ )
Grid frequency	$f$	50 ( $Hz$ )

The chosen matrix  $Q$  can achieve some LQ performance level, for example, reduce

the levels of dissipated energy, following [30, Theorem 2]:

$$Q = \begin{bmatrix} 1 & 0 & 0 & 0 \\ 0 & 1 & 0 & 0 \\ 0 & 0 & 0.5 & 0 \\ 0 & 0 & 0 & 0.1 \end{bmatrix}.$$

Further, a common matrix  $P$  can be obtained such that Property 4 is satisfied:

$$P = \begin{bmatrix} 7.91 & 0 & 0 & 0 \\ 0 & 7.91 & 0 & 0 \\ 0 & 0 & 2773.78 & 0 \\ 0 & 0 & 0 & 3040.37 \end{bmatrix} \cdot 10^{-2}.$$

The desired equilibrium point is given as follows:

$$x_e = \begin{bmatrix} x_{1e} & 0 & V_{dc}^* & 0 \end{bmatrix}^T,$$

where  $x_{1e}$  is obtained from the equilibrium of model (4.52)

$$x_{1e} = \frac{2V_s^2 - V_s^2 \sqrt{4 - \frac{8R_{LS}}{V_s^2} \left( \frac{2R_p + R}{R^* R_p} \right) V_{dc}^{*2}}}{4R_{LS}},$$

which is,  $x_e = [782.4 \ 0 \ 150 \ 0]^T$ .

Figure 4.12 shows the evolution of states for different values of sampling time  $T_s = \{10^{-4}, 10^{-5}, 10^{-6}\}s$ . Note that, for these different values of  $T_s$ , the instantaneous active and reactive power,  $p$  and  $q$ , and the voltages  $v_{dc}$  and  $v_d$  converge respectively towards their desired references with a response time of to 0.02s. Furthermore, we can notice that the instantaneous active and reactive powers signals admit a high-frequency ripple phenomenon due to switching control. Note also that, when the switching frequency is increased, then the ripple amplitude is reduced. Similar arguments are found for the phase currents, as shown in Figure 4.13, showing the trade-off between switching frequency and performance (if  $T_s$  increases, then the ripple signal increases). Finally, these simulations illustrate Theorem 7 statement.

Furthermore, the evolution of the Lyapunov function is depicted in Fig. 4.14, we can remark that when  $T_s$  is small then the steady state error of  $V$  is reduced. Likewise, when  $T_s$  is large, the Lyapunov function increases because we forbid the switches along period  $T_s$ .

Consequently, we can conclude from the simulations that:

- the desired equilibrium point is reached in the generalized sense of Filippov as expected in Assumption. 11. It means that the desired equilibrium is generally obtained for a not constant control, meaning that the control switches between several values at an infinite switching frequency. As expected, a Zeno behavior appears.
- In practical applications, as well as in simulation purposes, it is necessary to include a maximal switching frequency to avoid a Zeno behavior at the steady-state. However, a significant impact on the quality of the convergence towards the desired equilibrium is expected as shown in Fig. 4.12 and Fig. 4.13.
- If the switching frequency is reduced, then the difference between the balance and the state increases, and the ripple also increases. Hence, it appears that a right trade off between the number of switches and error should be found. This phenomenon has not only been studied in the context of hybrid framework (see report [51]), but also in the problem of the discretization of the sliding mode control [52].

#### 4.3.4. Conclusions

We have considered a nonlinear time varying model of a three-phase three-level NPC converter. Furthermore, to ease the design of an efficient control law, a polytopic model is developed. Then a hybrid control scheme is proposed, ensuring that a desired attractor is UGAS for this hybrid closed loop system. Finally, the main result is validated in simulation.

### 4.4. Conclusions

This chapter is devoted to the regulation problem for two different cases. Firstly, an Hybrid adaptive control is proposed for the boost converter. The idea of the control is to manage the switches in order to perform stability properties and an adaptive control is used to deal with the unknown resistive load. The stability of the system is provided using the hybrid theory.

Secondly, a hybrid control law is proposed for a three-level three-phase NPC converter. Basically, a polytopic representation of the entire system is proposed to deal with the time varying of model of NPC. This control law makes the system switches infinitely (Zeno phenomena). From practical point of view, the Zeno behaviors are not suitable. In order to deal with this problem, in Chapter 6, a practical stability is ensured by imposing a dwell-time between consecutive switches.

4.4. CONCLUSIONS

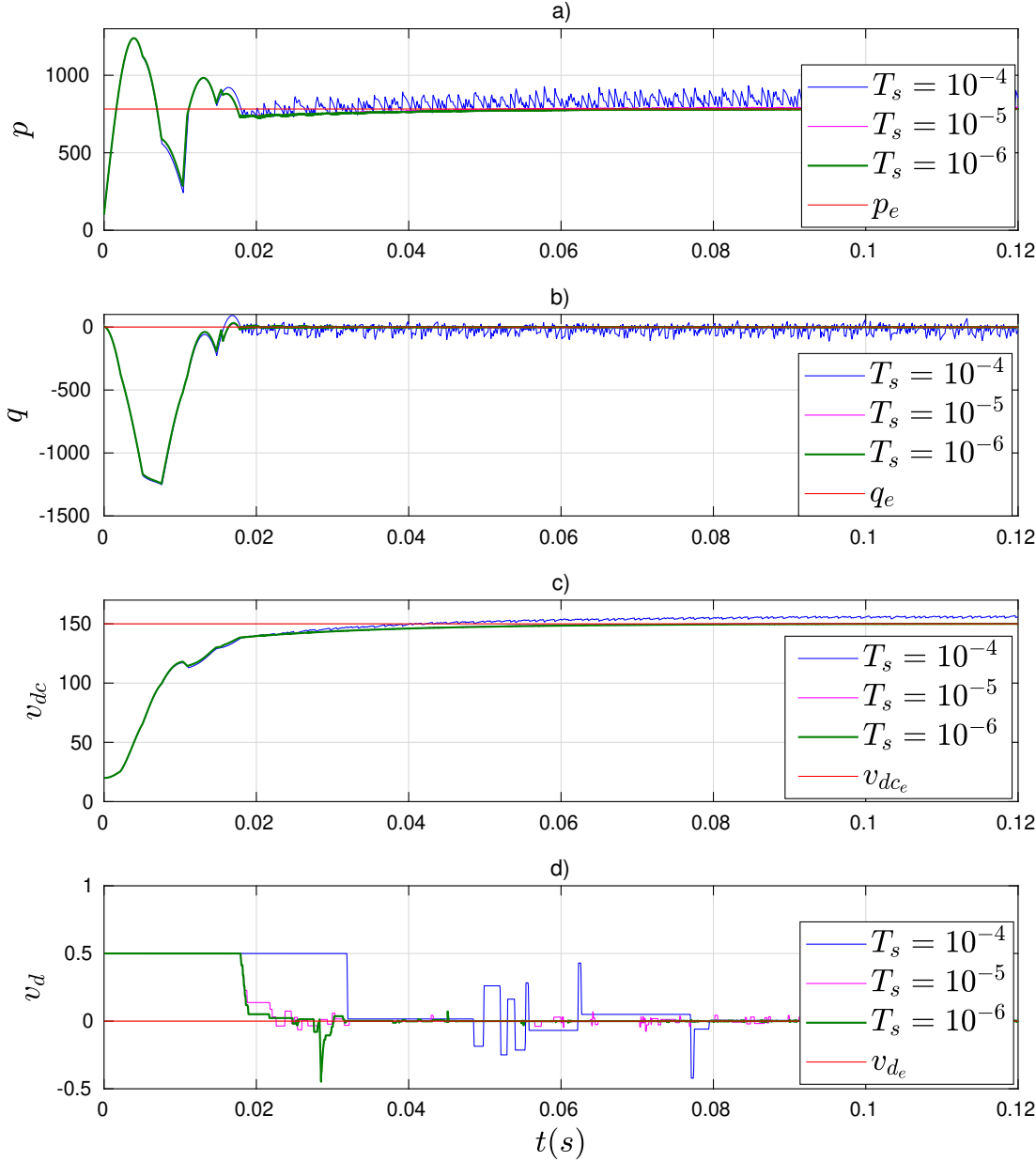


Figure 4.12: Evolution of the states for different values of sampling time  $T_s$ .

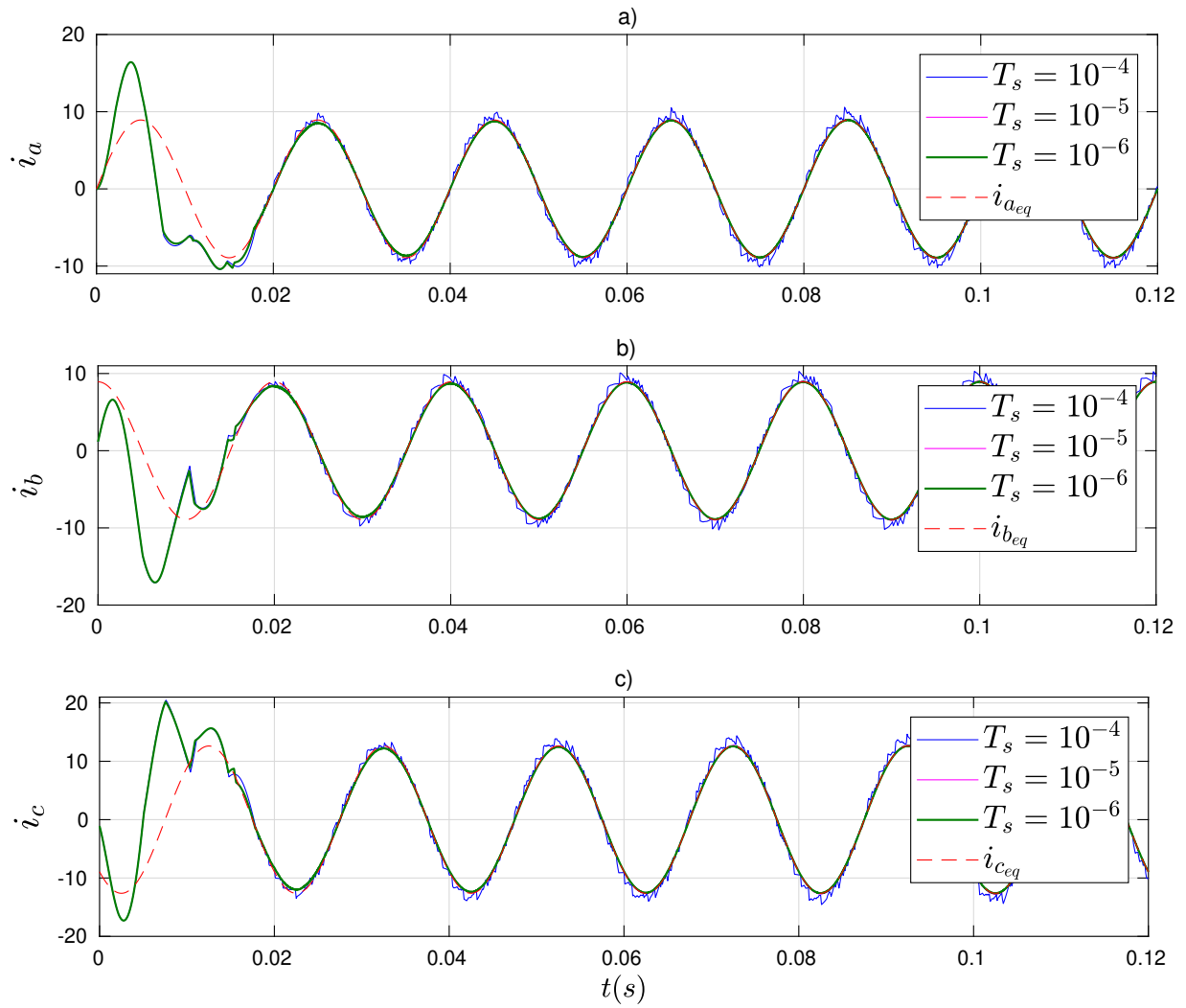


Figure 4.13: Evolution of the phase currents for different values of sampling time  $T_s$  and for  $\eta = 0.1$ .

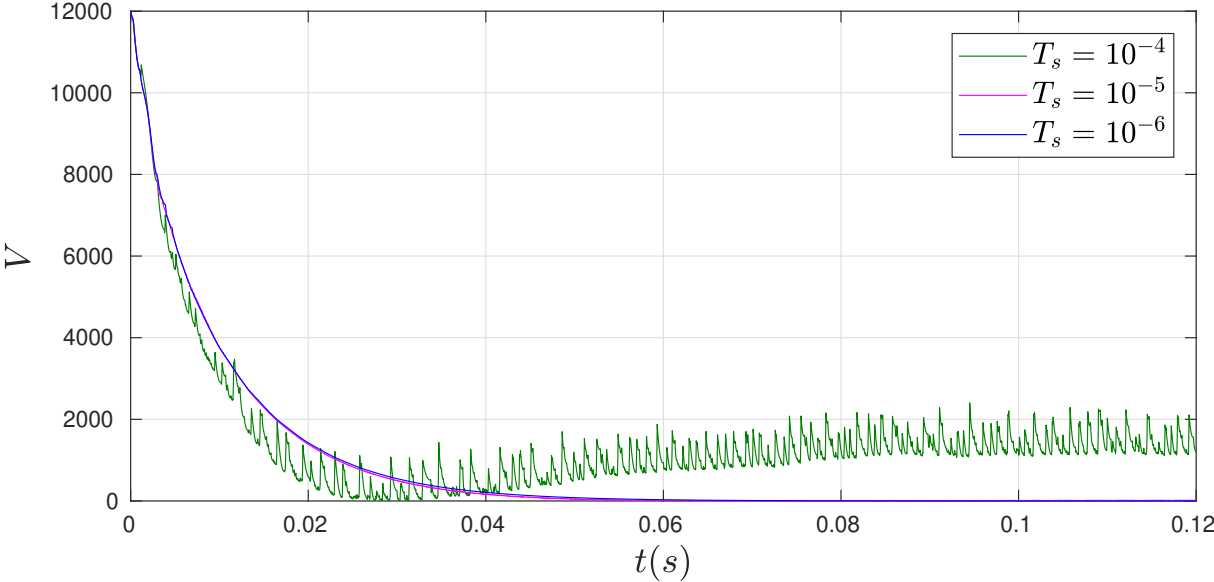


Figure 4.14: Evolution of the Lyapunov function.





# CHAPTER 5

## HYBRID CONTROL FOR DC-AC CONVERTERS

---

### Sommaire

---

<b>5.1</b>	<b>Introduction</b>	<b>73</b>
<b>5.2</b>	<b>DC-AC Converters: Half-bridge inverter</b>	<b>74</b>
5.2.1	Problem formulation	74
5.2.2	A reference model	75
5.2.3	Problem statement	76
5.2.4	Adaptation law	78
5.2.5	Hybrid model and proposed control law	79
5.2.6	Stability of the hybrid system	82
5.2.7	Applications	87
<b>5.3</b>	<b>Conclusions</b>	<b>91</b>

---

### 5.1. Introduction

This chapter deals with the design of control laws for DC-AC converters. Contrary to the previous chapter, the control objective is to design a hybrid control, such that, the output follows a time-varying reference. More precisely, we are interested in designing a hybrid adaptive control law, in order to guarantee a minimum error between the output and the reference. for the half-bridge inverter.

As presented in the previous chapter, since this kind of system exhibits continuous dynamics (current and voltage) and discrete dynamics (switching signals), the goal is to use the hybrid theory presented in Chapter 2, in order to improve performance, as

well as, stability properties. Moreover, as for the boost converter, an adaptive law is added to deal with the variation of the resistance load. The chosen DC-AC converter in this chapter is a half-bridge inverter.

## 5.2. DC-AC Converters: Half-bridge inverter

In this work, we aim at using an accurate model of half-bridge inverters, considering the real nature of the signals. To this end, we extend the results presented in [47], where a hybrid control is designed for the half-bridge inverter considering a constant and known load.

The novelty of this work lies in the design of a hybrid adaptive control for a half-bridge inverter regarding an unknown or perturbed load. A similar problem is considered in [53], where the authors stabilize the output of a DC-DC converter to a desired reference, considering therefore a regulation problem and an unknown load. However, here the problem is different, because we are dealing with a tracking problem. To this end, we transform the problem in an output regulation problem [54][55] and we propose an indirect adaptation mechanism in the hybrid dynamical scheme, in order to adapt the load variations. More precisely, we consider an adaptive law fed by a state observer by assuming that all states are measurable. Then, uniformly locally asymptotically stability is ensured by applying the time-scale separation and by using a singular perturbation analysis.

### 5.2.1. Problem formulation

Let start by rewriting the model of the half-bridge inverter given in equation (2.24), considering the unknown value of resistance  $R_0$ . To this end, let define  $\beta := \frac{1}{R_0} \in [\beta_m, \beta_M]$ , which belongs to the following polytope

$$\Omega := \lambda_{\beta,m}\beta_m + \lambda_{\beta,M}\beta_M, \quad \forall \lambda_{\beta,m}, \lambda_{\beta,M} \in [0, 1],$$

with  $\lambda_{\beta,m} + \lambda_{\beta,M} = 1$ .

And let consider this next assumption

#### ✦ ASSUMPTION 12:

We assume that:

- *Current and voltage are measurable.*
- *All the components are ideal (except the load  $R_0$ ).*
- *The load  $R_0$  is an unknown constant and is assumed to be in the interval  $[R_0^m, R_0^M]$ .*
- *$x_2 = 0$  corresponds to the starting operation mode, and any starting strategy is used to bring our system to  $x_2 \neq 0$ .*

Using definition of  $\beta$  and Assumption 12, then the system (2.24) is rewritten as follows

$$\left\{ \begin{array}{l} \dot{x}(t) = \overbrace{\begin{bmatrix} -\frac{R_{LS}}{L} & -\frac{1}{L} \\ \frac{1}{C_0} & -\frac{\beta}{C_0} \end{bmatrix}}^{A(\beta)} x(t) + \overbrace{\begin{bmatrix} \frac{V_{in}}{L} \\ 0 \end{bmatrix}}^{B_u} u, \\ y(t) = \overbrace{\begin{bmatrix} 0 & 1 \end{bmatrix}}^C x(t), \end{array} \right. \quad (5.1)$$

with  $x(t) = [i_L(t) \ v_C(t)]^T$  is the state vector,  $y(t)$  is the controlled output and  $u = \{-1, 1\}$  is the control input. Note that  $A(\beta)$  is Hurwitz for all  $\beta > 0$ . Moreover, as in the previous work, we assume that the following property is verified.

★ **PROPERTY 5:**

Consider matrix  $A(\beta)$  in (5.1), with  $\beta \in [\beta_m, \beta_M]$ , and a chosen matrix  $Q \in \mathcal{S}^2$ . Then there exists a matrix  $P \in \mathcal{S}^2$  satisfying the two following Lyapunov inequalities:

$$\begin{aligned} A^T(\beta_m)P + PA(\beta_m) + Q &< 0, \\ A^T(\beta_M)P + PA(\beta_M) + Q &< 0. \end{aligned}$$

This property imposes finally a unique Lyapunov function for the polytopic model (5.1). In the next subsection, we propose a desired tracking trajectory, which will be described by a linear time-invariant model.

### 5.2.2. A reference model

The desired trajectory to be tracked by the voltage and the current are given as:

$$\begin{aligned} x_{2e}(t) &:= V_{C_d}(t) = V_{max} \sin(\omega t), \\ x_{1e}(t) &:= i_{L_d}(t) = C_0 \omega V_{max} \cos(\omega t) + \beta V_{max} \sin(\omega t), \end{aligned} \quad (5.2)$$

where  $V_{max}$  and  $\omega$  are respectively the desired amplitude and angular frequency of the voltage applied to the load  $R_0$ . Note that, only  $x_{2e}(t)$  is imposed and  $x_{1e}(t)$  is therefore calculated using equation (5.1), meaning that (5.2) is an admissible trajectory for (5.1). In order to impose a such behavior, let us define the exogenous model, whose the output  $y_d(t)$  is the reference to be followed

$$\left\{ \begin{array}{l} \dot{z}(t) = \Theta z(t), \\ y_d(t) = \Pi(\beta)z(t), \end{array} \right. \quad (5.3)$$

where  $z \in \mathbb{R}^2$  is the state of the exosystem and

$$y_d(t) = \begin{bmatrix} i_{L_d}(t) \\ V_{C_d}(t) \end{bmatrix}, \quad \Theta = \begin{bmatrix} 0 & w \\ -w & 0 \end{bmatrix} \quad \text{and} \quad \Pi(\beta) = \begin{bmatrix} -wC_0 & \beta \\ 0 & 1 \end{bmatrix}.$$

**REMARK 14.** In our case, as  $\beta$  is an unknown parameter, this reference cannot be used directly for the control design. This is the reason why an estimate of  $\beta$ , named  $\hat{\beta}$ , is designed in Section 5.2.4, given via an observer and adaptive control. This estimate should be used to produce the estimated output of the reference model.

$$\hat{y}_d(t) = \Pi(\hat{\beta})z(t), \quad (5.4)$$

with  $\hat{y}_d(t) = \hat{x}_e(t) = [\hat{i}_{L_d}(t) \ \hat{V}_{C_d}(t)]^T$  is the estimated value of the real output of the reference model.

**REMARK 15.** Note that from (5.3) and by considering that  $z(0) = [0 \ V_{max}]^T$ , it is simple to demonstrate that

$$z_1^2(t) + z_2^2(t) = V_{max}^2.$$

Consequently, define the following compact set

$$\Phi = \{(z_1(t), z_2(t)) \in \mathbb{R}^2, \ z_1^2(t) + z_2^2(t) = V_{max}^2\}.$$

Now that, we have described the model and the reference, the problem of tracking for the half-bridge inverter with unknown resistance is stated in the next section.

### 5.2.3. Problem statement

In this work, we are focused on the design of a switching signal  $u \in \{-1, 1\}$  and an adaptive law  $\hat{\beta}$ , which guarantee the two following properties:

1. A suitable trajectory tracking properties of the voltage  $x_2(t)$  to a desired trajectory  $x_{2_e}(t)$ , ensuring asymptotic convergence properties of the error  $e(t)$ , between the state  $x(t)$  and desired tracking trajectory  $y_d(t)$  :

$$\lim_{t \rightarrow \infty} e(t) = 0.$$

where  $e(t) = x(t) - y_d(t)$ .

2. The convergence of the estimation of the load  $\hat{\beta}$  to the real value of  $\beta$ , such that the error between  $y_d(t)$  and  $\hat{y}_d(t)$  converge to zero. meaning that if

$$\lim_{t \rightarrow \infty} \hat{\beta} = \beta, \quad \text{then,} \quad \lim_{t \rightarrow \infty} \hat{y}_d(t) = y_d(t).$$

In the first place, let us rewrite the original system in term of the error between  $x(t)$  and  $y_d(t)$ .

### A. Error dynamics model

Let us define the error state variable  $e(t) = [e_1(t) \ e_2(t)]^T \in \mathbb{R}^2$ , between the state of the model (5.1),  $x(t)$ , and the real output of the reference model,  $y_d(t)$ . Then from equation (5.3), the error equation can be written as:

$$e(t) = x(t) - \Pi(\beta)z(t). \quad (5.5)$$

Furthermore, this error equation can be rewritten as follows:

$$e(t) = x(t) - \Pi(\hat{\beta})z(t) + \Pi(\hat{\beta})z(t) - \Pi(\beta)z(t), \quad (5.6)$$

by defining this new variable

$$\hat{e}(t) = x(t) - \Pi(\hat{\beta})z(t), \quad (5.7)$$

then, the equation (5.6) can then be given by

$$\begin{aligned} e(t) &= \hat{e}(t) + \Pi(\hat{\beta})z(t) - \Pi(\beta)z(t), \\ &= \hat{e}(t) + \begin{bmatrix} 0 & \hat{\beta} - \beta \\ 0 & 0 \end{bmatrix} z(t), \end{aligned} \quad (5.8)$$

The goal is to prove the asymptotic stability of the error  $e(t)$ . To this end, it will be decomposed the problem into two parts:

1. The convergence of  $\hat{\beta}$  to  $\beta$ , which will be ensured by an observer and adaptive control explained in Section 5.2.4.
2. The convergence of the estimated error  $\hat{e}(t)$  towards zero.

In order to find the estimated error dynamics, let us firstly, consider a vector  $\Gamma$ , such that, the following algebraic equation is verified:

$$A(\beta)\Pi(\hat{\beta}) + B\Gamma(\hat{\beta}) = \Pi(\hat{\beta})\Theta, \quad (5.9)$$

A simple calculation shows that,  $\Gamma(\hat{\beta})$  does not depend on  $\beta$  and can be written as:

$$\Gamma(\hat{\beta}) = \begin{bmatrix} -\frac{wL\hat{\beta}}{V_{in}} - \frac{wR_{LS}C_0}{V_{in}} & \left(\frac{1}{L} - C_0w^2 + \frac{R_{LS}\hat{\beta}}{L}\right) \frac{L}{V_{in}} \end{bmatrix}.$$

At this stage, let us consider the estimated error given in (5.7), then the dynamic of this variable is given as:

$$\dot{\hat{e}}(t) = \dot{x}(t) - \Pi(\hat{\beta})\dot{z}(t) - \dot{\hat{\beta}}\Pi'(\hat{\beta})z(t) \quad (5.10)$$

where  $\Pi' = \frac{d\Pi}{d\beta}$ .

Then, by substitution of equation (5.9) in (5.10), we obtain

$$\dot{\hat{e}} = A(\beta)\hat{e} + Bd(\dot{\hat{\beta}}, \hat{\beta}, z), \quad (5.11)$$

where

$$d(\dot{\hat{\beta}}, \hat{\beta}, z) := \left( v(\hat{\beta}, z) - \frac{L}{V_{in}} \dot{\hat{\beta}} z_2 \right), \quad (5.12)$$

with

$$v(\hat{\beta}, z) := u - \Gamma(\hat{\beta})z, \quad (5.13)$$

which is finally a new control input to be designed. Nevertheless, we need to keep in our mind that, the control applied to half-bridge inverter is defined by:

$$u := v + \Gamma(\hat{\beta})z.$$

**REMARK 16.** Note that, if  $\hat{\beta} = \beta$ , then equation (5.4) and (5.9) are the well known "regulator equations" [54][55].

Inspired by [53], we extend the work presented in [30], for model (5.1) with an unknown parameter  $\beta$ . The idea is to design a hybrid adaptive controller that considers the continuous-time dynamics,  $x_1, x_2$ , and the discrete-time dynamic,  $u$ , estimating  $\beta$  in continuous-time, at the same time that  $x_1(t)$  and  $x_2(t)$  converge to a sinusoidal references given by (5.3).

The next section is devoted to the design of an adaptation control law with the aim of estimating the unknown constant  $\beta$ .

#### 5.2.4. Adaptation law

For the purpose of designing an adaptation law, we consider a state observer for the estimated error  $\hat{e}_2$ , and an adaptation law for parameter  $\beta$ , with the following structure

$$\dot{\hat{e}}_2(t) = \frac{1}{C_0}(\hat{e}_1(t) - \hat{\beta}\hat{e}_2(t)) + \alpha(\hat{e}_2(t) - \hat{\hat{e}}_2(t)) \quad (5.14)$$

$$\dot{\hat{\beta}} = g(\hat{e}_2(t), \hat{\hat{e}}_2(t)), \quad (5.15)$$

where  $\hat{\hat{e}}_2(t)$  is the estimated state of  $\hat{e}_2(t)$ ,  $\hat{\beta}$  is the estimated value of  $\beta$  and  $\alpha$  is a positive constant parameter, which represents the convergence speed of the observer.  $g(\cdot)$  is the adaptation law and to achieve a mathematical expression of  $g(\hat{e}_2(t), \hat{\hat{e}}_2(t))$ , let us define the following error variables, considering  $\dot{\hat{\beta}} = 0$

$$\check{e}_2(t) := \hat{e}_2(t) - \hat{\hat{e}}_2(t), \quad \tilde{\beta} := \beta - \hat{\beta} \quad \Rightarrow \quad \dot{\tilde{\beta}} = -\dot{\hat{\beta}} \quad (5.16)$$

Next, from (5.1) and (5.14), we derive the error equation of  $\check{e}_2(t)$

$$\dot{\check{e}}_2(t) = -\frac{\tilde{\beta}}{C_0}\hat{e}_2(t) - \alpha\check{e}_2(t). \quad (5.17)$$

The error model is then rewritten as:

$$\begin{cases} \dot{\check{e}}_2(t) = -\frac{\tilde{\beta}}{C_0}\hat{e}_2(t) - \alpha\check{e}_2(t), \\ \dot{\tilde{\beta}} = -\hat{\beta} \end{cases} \quad (5.18)$$

Now, let us introduce the next candidate Lyapunov function

$$W(\check{e}_2, \tilde{\beta}) = \frac{1}{2} \left( \check{e}_2^2(t) + \frac{\tilde{\beta}^2}{\gamma} \right), \quad (5.19)$$

where  $\gamma$  is a positive scalar. Considering system (5.18),  $W(\check{e}_2, \tilde{\beta})$  is positive definite and radially unbounded. The derivative of  $W$  along the trajectories of (5.18) gives:


$$\dot{W}(\check{e}_2, \tilde{\beta}) = -\alpha\check{e}_2^2(t) - \frac{\hat{e}_2(t)\check{e}_2(t)}{C_0}\tilde{\beta} + \frac{\tilde{\beta}\dot{\tilde{\beta}}}{\gamma} = -\alpha\check{e}_2^2(t) + \tilde{\beta} \left( -\frac{\hat{e}_2(t)\check{e}_2(t)}{C_0} + \frac{\dot{\tilde{\beta}}}{\gamma} \right). \quad (5.20)$$

The adaptation law is now defined by canceling the terms in parentheses, i.e.

$$\dot{\tilde{\beta}} = \frac{\gamma\hat{e}_2(t)\check{e}_2}{C_0}. \quad (5.21)$$

Consequently, by substitution of (5.21) in the second equality of (5.16), the adaptation law is defined as

$$\dot{\hat{\beta}} = -\frac{\gamma\hat{e}_2(t)\check{e}_2(t)}{C_0}. \quad (5.22)$$

 **REMARK 17.** Note that  $\gamma$  defines the adaptation speed, and consequently, if  $\gamma$  is larger, then the adaptation speed comes larger.

Now that we have designed a adaptive control law, we will couple this law with a hybrid control to form a hybrid adaptive control proposed in the next Section.

### 5.2.5. Hybrid model and proposed control law

Now, we model our system under a hybrid dynamic scheme, following the paradigm given in [26]. Wherein

- the continuous-time behavior encompasses the evolution of  $\hat{e}(t)$ ,  $z(t)$ ,  $\hat{e}_2(t)$  and  $\hat{\beta}$ ,
- the discrete-time behavior captures the jump of the switch half-bridge inverter signal  $u \in \{-1, 1\}$ , (through  $v$ ),

We characterize the overall dynamics by the following hybrid model:

$$\mathcal{H} : \left\{ \begin{array}{l} \begin{array}{l} \dot{\hat{e}} \\ \dot{z} \\ \dot{v} \\ \dot{\hat{e}}_2 \\ \dot{\hat{\beta}} \end{array} = f(\xi), \quad \xi \in \mathcal{C}, \\ \begin{array}{l} \hat{e}^+ \\ z^+ \\ v^+ \\ \hat{e}_2^+ \\ \hat{\beta}^+ \end{array} \in G(\xi), \quad \xi \in \mathcal{D}, \end{array} \right. \quad (5.23)$$

where  $\xi = [\hat{e} \ z \ v \ \hat{e}_2 \ \hat{\beta}]$ .  $f(\xi)$  is the *flow* map and contains the continuous dynamics of the system. and  $G(\xi)$  is a *jump* map capturing the switching logic:

$$f(\xi) := \begin{bmatrix} A(\beta)\hat{e} + Bd(\xi), \\ \Theta z \\ -\Gamma(\hat{\beta})\Theta z \\ \frac{1}{C_0}(\hat{e}_1 - \hat{\beta}\hat{e}_2) + \alpha(\hat{e}_2 - \hat{e}_2) \\ -\gamma\hat{e}_2(\hat{e}_2 - \hat{e}_2)/C_0 \end{bmatrix}, \quad (5.24)$$

$$G(\xi) := \begin{bmatrix} \hat{e} \\ z \\ \left( \underset{\substack{v=u-\Gamma(\beta)z \\ u \in \{-1,1\}}}{\operatorname{argmin}} \tilde{e}^T P \left( A(\hat{\beta})\hat{e} + Bd(\xi) \right) \right) - \Gamma(\hat{\beta})z \\ \hat{e}_2 \\ \hat{\beta} \end{bmatrix}, \quad (5.25)$$



where

$$d(\xi) = \left( u - \Gamma(\hat{\beta})z + \frac{\gamma L \hat{e}_2 (\hat{e}_2 - \hat{\hat{e}}_2)}{V_{in} C_0} z_2 \right) \quad (5.26)$$

with  $\alpha$  and  $\gamma$  are positive constant parameters, and  $\tilde{e} = [\tilde{e}_1 \ \tilde{e}_2]$  is defined as follows


$$\begin{cases} \tilde{e}_1 = \hat{e}_1 \\ \tilde{e}_2 = \hat{e}_2 + (e_2 - \hat{\hat{e}}_2). \end{cases} \quad (5.27)$$

Inspired by [30] and as proposed by [53], we select the so-called flow and jump sets

$$\mathcal{C} := \left\{ \xi : \tilde{e}^T P \left( A(\hat{\beta})\hat{e} + Bd(\xi) \right) \leq -\eta \tilde{e}^T Q \tilde{e} \right\}, \quad (5.28)$$

$$\mathcal{D} := \left\{ \xi : \tilde{e}^T P \left( A(\hat{\beta})\hat{e} + Bd(\xi) \right) \geq -\eta \tilde{e}^T Q \tilde{e} \right\}, \quad (5.29)$$

with  $\eta \in (0, 1)$  as for the boost and NPC converters, is tunned parameter.

 **REMARK 18.** To achieve the control objectives, i.e. reach the desired equilibrium,  $\hat{e} = 0$ , the proposed control generates arbitrary fast switching in the steady-state, therefore the desired equilibrium is achieved in a Filippov sense. But from a practical point of view, the switching frequency must present a minimal dwell-time between consecutive switches. Moreover, as for the boost converter, a time- or space-regularization can be added in the closed-loop in order to reduce the switching frequency at the expense of the performances (See Chapter 6)

 **PROPOSITION 4:**

*The hybrid system (5.23)–(5.29) satisfies the basic hybrid conditions given in Assumption 3. Then, applying Theorem 1, we can conclude that the hybrid system (5.23)–(5.29) is well-posed.*

Now, let us define the following compact attractor for the system (5.23)–(5.29):

$$\mathcal{A} := \{ \xi : \hat{e} = 0, \ z \in \Phi, \ u \in \{-1, 1\}, \ \hat{\hat{e}}_2 = \hat{e}_2, \ \hat{\beta} = \beta \}. \quad (5.30)$$

Indeed, we are interested in uniform stability and convergence to a set where  $\hat{e} = 0$ ,  $\hat{\beta} = \beta$ , and  $\hat{\hat{e}}_2 = \hat{e}_2$ , whatever the value of  $z \in \Phi$  and  $u \in \{-1, 1\}$ . The Section 5.2.6 is dedicated to prove the stability of the hybrid system (5.23)–(5.29).

Let now comment the choice of matrices  $P$  and  $Q$ . As in section A, these matrices are selected following some optimization criteria given in (5.31) for a hybrid system (5.23)–(5.29). Specifically, we use [30, Theorem 2], where some LQ performance level is guaranteed, for example: response time, reduce the dissipated energy, current peak

among others. To this end let take the following cost function to get any LQ performance level.

$$J = \min_u \sum_{k \in \text{dom}_j(\xi)} \int_{t_k}^{t_{k+1}} \frac{\rho}{R_0} (v_c(\tau, k) - v_{Cd})^2 + R(i_L(\tau, k) - i_{Ld})^2 d\tau \quad (5.31)$$

with  $\rho$  is a positive scalar.

On the other hand, we find that the suboptimal-LQ performance level corresponds to increase of switching in the transient time, which can increase the dissipated energy. Therefore, the choice of  $\eta$  decides a trade-off between any LQ performance level and switching frequency as shown in Figure 4.7.

### 5.2.6. Stability of the hybrid system

This section is dedicated to prove stability of the hybrid system (5.23)–(5.29). Note that, the observer and adaptation dynamics are given (5.14) and (5.22) respectively. Stability properties of this adaptation are stated in the following lemma:

**\* LEMMA 5:**

*Consider the system (5.1), and assume that its solutions are bounded. The extended observer (5.14)–(4.33) has the following properties:*

- i) The estimated states  $\hat{e}_2(t)$ ,  $\hat{\beta}$  are bounded.*
- ii)  $\lim_{t \rightarrow \infty} \hat{e}_2(t) = \check{e}_2(t)$ .*
- iii)  $\lim_{t \rightarrow \infty} \hat{\beta}(t) = \beta$ ,*

*Proof.* The observer error and the adaptive law equations are fully defined from (5.14) and (5.22), and stability properties of these equations follow from the Lyapunov function  $W$  defined above in (5.19). Note that with the choice (5.21), we obtain

$$\dot{W}(\check{e}_2, \tilde{\beta}) = -\alpha \check{e}_2^2$$

and from standard Lyapunov arguments, it follows that the error variable  $\check{e}_2$  and  $\tilde{\beta}$  are bounded. In addition, by LaSalle invariant principle and from Assumption 12, we easily conclude that  $\check{e}_2 \rightarrow 0$ , which implies from (5.21) that  $\tilde{\beta} \rightarrow 0$ . Likewise from (5.17), and concluding from  $\check{e}_2 \rightarrow 0$  that  $\dot{\check{e}}_2 \rightarrow 0$ , we get  $\tilde{\beta} \rightarrow 0$ .  $\square$

Consider now the quadratic Lyapunov function  $V$  for all system (5.23)–(5.25) as

$$V(\hat{e}, \check{e}_2, \tilde{\beta}) = W(\check{e}_2, \tilde{\beta}) + \hat{e}^T P \hat{e} \quad (5.32)$$

with  $W(\check{e}_2, \tilde{\beta})$  is defined in (5.19). The derivative of this equation a long the trajectories of the system (5.23)–(5.25) is given by

$$\dot{V} = -\alpha \check{e}_2^2 + 2\hat{e}^T P (A(\beta)\hat{e} + Bd(\xi)) \quad (5.33)$$

with the expression of  $d(\xi)$  is given in equation (5.26).

To prove that a such function is negative definite, is very complicated. This is why, to prove that the hybrid system (5.23)–(5.29) is SPAS, we apply singular perturbation analysis presented in section 3.5.1 and assuming that there are slow time-continuous variables,  $\xi_r := (\hat{e}, z, v)$ , and fast time-continuous variables,  $\xi_f := (\hat{e}_2, \hat{\beta})$ , then we apply singular perturbation analysis to establish the stability properties. For this, we will rewrite the complete system in singular perturbation form.

### A. Singular perturbed form

In order to put the system above in the standard singular perturbation form, let define  $\nu := \frac{1}{\alpha}$ ,  $\bar{\gamma} := \frac{\gamma}{C_0}$  and then, we can rewrite the hybrid scheme (5.23)–(5.25) as follows:

$$\mathcal{H}_p : \left\{ \begin{array}{l} \begin{bmatrix} \dot{\hat{e}} \\ \dot{z} \\ \dot{v} \\ \nu \dot{\hat{e}}_2 \\ \nu \dot{\hat{\beta}} \end{bmatrix} = \begin{bmatrix} A(\beta)\hat{e} + Bd(\xi) \\ \Theta z \\ -\Gamma(\hat{\beta})\Theta z \\ \frac{\nu}{C_0} (\hat{e}_1 - \hat{\beta}\hat{e}_2) + (\hat{e}_2 - \hat{\hat{e}}_2) \\ -\nu\bar{\gamma}\hat{e}_2 (\hat{e}_2 - \hat{\hat{e}}_2) \end{bmatrix}, \quad \xi \in \mathcal{C}, \\ \begin{bmatrix} \hat{e}^+ \\ z^+ \\ v^+ \\ \hat{e}_2^+ \\ \hat{\beta}^+ \end{bmatrix} \in \begin{bmatrix} \hat{e} \\ z \\ \left( \underset{\substack{v=u-\Gamma(\hat{\beta})z \\ u \in \{-1,1\}}}{\operatorname{argmin}} \tilde{e}^T P (A(\hat{\beta})\hat{e} + Bd(\xi)) \right) - \Gamma(\hat{\beta})z \\ \hat{e}_2 \\ \hat{\beta} \end{bmatrix}, \quad \xi \in \mathcal{D}, \end{array} \right. \quad (5.34)$$

with  $\xi = [\hat{e} \ z \ v \ \hat{e}_2 \ \hat{\beta}]$ .

Note that the fast variables directly impact the behavior of the slow variables.

In order to fulfill a singular perturbation analysis, we will check the assumptions given in section 3.5.1.

## B. Regularity of “manifold” and the fast sub-system

The fast sub-system can be written as

$$\mathcal{H}_p : \begin{cases} \begin{bmatrix} \nu \dot{\hat{e}}_2(t) \\ \nu \dot{\hat{\beta}} \\ \dot{\hat{e}}_2^+(t) \\ \dot{\hat{\beta}}^+ \end{bmatrix} = \begin{bmatrix} \frac{\nu}{C_0} (\hat{e}_1(t) - \hat{\beta} \hat{e}_2(t)) + (\hat{e}_2(t) - \hat{\hat{e}}_2(t)) \\ -\nu \bar{\gamma} \hat{e}_2(t) (\hat{e}_2(t) - \hat{\hat{e}}_2(t)) \\ \hat{e}_2(t) \\ \hat{\beta} \end{bmatrix}, & \xi_f \in \mathcal{C}, \\ \begin{bmatrix} \hat{e}_2^+(t) \\ \hat{\beta}^+ \end{bmatrix} \in \begin{bmatrix} \hat{e}_2(t) \\ \hat{\beta} \end{bmatrix}, & \xi_f \in \mathcal{D}, \end{cases} \quad (5.35)$$

where  $\xi_f = [\hat{e}_2(t) \hat{\beta}]$ . The “manifold” corresponds to the quasi-steady-state equilibrium manifold of classical singular perturbation theory [36], that means when  $\nu \rightarrow 0^+$ , then

$$\begin{aligned} \hat{e}_2 - \hat{\hat{e}}_2 &= 0 \\ \beta - \hat{\beta} &= 0. \end{aligned} \quad (5.36)$$

Note that  $\beta - \hat{\beta} = 0$  comes the fact that  $\dot{\hat{\beta}} = -\hat{\beta}$  in (5.16). As (5.36) is continuous, we can take that the manifold is empty outside of  $\mathcal{C}$ , letting take the following set-valued:

$$\mathcal{M}(e_2(t)) := \begin{cases} \begin{bmatrix} \hat{e}_2(t) \\ \beta \end{bmatrix} & e_2(t) \in \mathcal{C} \\ 0 & e_2(t) \notin \mathcal{C}. \end{cases}$$

where  $\hat{e}(t) = [\hat{e}_1(t) \hat{e}_2(t)]^T$ . Note that  $\mathcal{M}$  is outer semi-continuous, locally bounded and nonempty.

From Lemma 5, the fast sub-system is locally asymptotically stable. Now, we substitute this solution in (5.34), obtaining the reduced model or just the slow model, presented in the next sub-section.

### C. Stability for reduced system

The reduced system is the system (5.23)–(5.25) in the manifold  $\mathcal{M}$ , which is

$$\mathcal{H}_r : \begin{cases} \begin{bmatrix} \dot{\hat{e}}(t) \\ \dot{z}(t) \\ \dot{v} \end{bmatrix} = \begin{bmatrix} A(\beta)\hat{e}(t) + Bv \\ \Theta z(t) \\ -\Gamma(\hat{\beta})\Theta z(t) \end{bmatrix}, & \xi_r \in \mathcal{C}(\mathcal{M}), \\ \begin{bmatrix} \hat{e}^+(t) \\ z^+(t) \\ v^+ \end{bmatrix} \in \begin{bmatrix} \hat{e}(t) \\ z(t) \\ \left( \underset{\substack{v=u-\Gamma(\hat{\beta})z \\ u \in \{-1,1\}}}{\operatorname{argmin}} \tilde{e}^T(t)P(A(\beta)\hat{e}(t) + Bv) \right) - \Gamma(\beta)z(t) \end{bmatrix}, & \xi_r \in \mathcal{D}(\mathcal{M}), \end{cases} \quad (5.37)$$

where  $\xi_r = (\hat{e}(t), z(t), v)$ . Note that, there is not jump in  $\mathcal{M}$ , therefore the reduced system ignores  $\hat{e}_2$  and  $\hat{\beta}$  when determining jumps.

According to equation (5.36), implying that:

$$\begin{aligned} \hat{e}_2(t) &= \hat{\hat{e}}_2(t) \\ \beta &= \hat{\beta}, \end{aligned} \quad (5.38)$$

and replacing them in the expression of  $d(\hat{\beta}, \hat{\beta}, z)$ , we have

$$d(\beta, z(t)) := u - \Gamma(\beta)z(t) = v(\beta, z(t)) \quad (5.39)$$

According to remark 16, and in order to satisfy the constraint on the value of  $u$  (i.e.  $u \in \{-1, 1\}$ ), the following assumption must be hold.

✦ **ASSUMPTION 13:**

There exist two functions of time  $\lambda_1, \lambda_{-1} \in [0, 1]$  satisfying  $\lambda_1 + \lambda_{-1} = 1$ , such that the following equation holds:

$$\sum_{\substack{i=-1 \\ i \neq 0}}^1 \lambda_i (A(\beta)\hat{e}_e(t) + Bv_i(\beta, z(t))) = 0.$$

with  $\hat{e}_e(t) = 0$  is the desired equilibrium for the error. Hence by substitution  $\hat{e}_e(t) = 0$  in the last equality, we obtain

$$\lambda_1 - \lambda_{-1} - \Gamma(\beta)z(t) = 0. \quad (5.40)$$

🔗 **REMARK 19.** It is important to understand that in Assumption 13, the solution  $\hat{e}(t) = 0$  is obtained in the sense of Krasovskii solution. Indeed the signal  $u = \lambda_1 - \lambda_{-1}$ , is a periodic sequence of arbitrarily small period  $T$ , spending a time equal to  $\lambda_1 T$  in mode  $u = 1$ , and  $\lambda_{-1} T$  in mode  $u = -1$ .

Now, we invoke the lemma presented in [30], which is important to prove the stability properties.

**\* LEMMA 6:**

Consider matrices  $P, Q \in \mathcal{S}^2$  satisfying Property 5. Then for each  $\hat{e}(t) \in \mathbb{R}^2$ ,

$$\min_{i \in [-1, 1]} \tilde{e}^T(t) P (A(\beta) \hat{e}(t) + B v_i(\beta, z(t))) \leq -\tilde{e}^T(t) Q \tilde{e}(t).$$

🔗 **REMARK 20.** We note here that for  $\eta \in (0, 1)$  then

$$-\tilde{e}^T(t) Q \tilde{e}(t) < -\eta \tilde{e}^T(t) Q \tilde{e}(t).$$

Note that the switching frequency is reduced if  $\eta \rightarrow 0$  and, it is increased if  $\eta \rightarrow 1$ , as has been proved in [30].

☀ **THEOREM 8.** Consider Assumption 12, 13, Lemma 6 and matrices  $P, Q \in \mathcal{S}^2$  satisfying Property 5. Then attractor (5.30) is Semiglobally Practically Asymptotically Stable (SPAS) for hybrid system (5.23)–(5.29).

### D. Stability of the boundary layer

The boundary layer is given by

$$\mathcal{H}_{bl} := \begin{cases} \dot{\xi}_r = 0 \\ \nu \dot{\hat{e}}_2(t) = \frac{\nu}{C_0} (\hat{e}_1(t) - \hat{\beta} \hat{e}_2) + (\hat{e}_2(t) - \hat{\hat{e}}_2(t)) \\ \nu \dot{\hat{\beta}} = -\nu \gamma \hat{e}_2(t) (\hat{e}_2(t) - \hat{\hat{e}}_2(t)) \end{cases} \quad \xi \in \mathcal{C} \cap r\mathbb{B}$$

with  $r\mathbb{B}$  a closed ball of radius  $r$ . Note that the boundary layer system ignores the jumps, and during flows  $\xi_r$  remains constant.

In order to evaluate the stability of the boundary layer, let us consider the error equations of  $\mathcal{H}_{bl}$  and given also in (5.16), and let us take as particular solution  $\hat{e}_{2_{bl}} \in \mathbb{R}$  equal to a constant value. Then, we need to evaluate the fast sub-system (5.35) and re-scale time  $t$  to  $\tau = (t - t_0)/\nu$ , getting

$$\begin{aligned} \frac{d}{d\tau} \check{e}_2(t) &= -\frac{\nu}{C_0} \tilde{\beta} \hat{e}_{2_{bl}} - \check{e}_2(t) \\ \frac{d}{d\tau} \tilde{\beta} &= \frac{\nu}{C_0} \gamma \hat{e}_{2_{bl}} \check{e}_2(t). \end{aligned}$$

Then, the stability property can be established using the Lyapunov function given in (5.19). Note that, in this case, the derivative of  $W$  along the trajectories in the boundary layer, is relative to  $\tau$ , instead of ordinary time  $t$ .

$$\frac{d}{d\tau}\kappa(t) = J\kappa(t)$$

with  $\kappa(t) = [\check{e}(t) \tilde{\beta}]^T$

$$J = \begin{pmatrix} -1 & -\frac{\nu}{C_0}\hat{e}_{2bl} \\ -\frac{\nu}{C_0}\gamma\hat{e}_{2bl} & 0 \end{pmatrix}.$$

Therefore, we can define the next property:

★ **PROPERTY 6:**

By replacing  $\nu := 1/\alpha$ , then the real part of the eigenvalues of  $J$ , for  $\hat{e}_{2bl} \in \{\mathbb{R} \setminus \{0\}\}$  are all strictly negative, i.e.

$$\begin{aligned} \lambda_1 &= \Re \left\{ \left( -1 + \sqrt{1 - 4\frac{\gamma}{\alpha^2 C_0^2} \hat{e}_{2bl}^2} \right) / 2 \right\} < 0 \\ \lambda_2 &= \Re \left\{ \left( -1 - \sqrt{1 - 4\frac{\gamma}{\alpha^2 C_0^2} \hat{e}_{2bl}^2} \right) / 2 \right\} < 0 \end{aligned}$$

*Proof of Theorem 8:* From 4 and the analysis given in proposition B, C and D, we prove the Semiglobally Practically Asymptomatic stability SPAS of attractor (4.60). ■

🔗 **REMARK 21.** In order to ensure a singular perturbation form, we need to establish that the response time of the slow subsystem,  $t_R(A(\beta))$ , are larger than the fast subsystem time response. For that, we select  $\gamma = C_0\alpha$  and

$$\alpha \gg \max \left\{ \frac{1}{t_R(A(\beta))} \right\} \text{ for } \beta \in [\beta_m, \beta_M].$$

🔗 **REMARK 22.** We have proved the convergence of  $\hat{\beta}$  to  $\beta$  and the convergence of the estimated error  $\hat{e}(t)$  towards zero. Then the convergence of the error  $e(t)$  to zero is ensured. Meaning that the state  $x(t)$  converges asymptotically toward the desired reference  $y_d(t)$  given in (5.3).

Finally, our control scheme is illustrated by some simulations, given in the next section.

### 5.2.7. Applications

In this section, we perform some simulations using MATLAB/Simulink by exploiting the HyEQ Toolbox [37] to verify the properties of the closed loop (5.23)–(5.29). Let consider, for these simulations, the parameters given in Table 5.1.

Parameter	Convention	Value	Units
DC input voltage	$V_{in}$	96	V
Reference peak voltage	$V_{max}$	$220\sqrt{2}$	V
Nominal angular frequency	$\omega$	$100\pi$	rad/s
Nominal load resistance	$R_0$	240	$\Omega$
Estimated series resistance	$R_{LS}$	2	$\Omega$
Inductor	L	50	mH
Output capacitor	$C_0$	200	$\mu F$

Table 5.1: Simulation parameters

$$R_0 = 240\Omega \in [120, 360]\Omega \Leftrightarrow \beta = 0.0042 \in [0.0028, 0.0083], \quad (5.41)$$

which corresponds to  $\pm 50\%$  of variation with respect to the nominal value of  $R_0$ .

The desired trajectories are defined as

$$x_e = \begin{bmatrix} i_{L_d}(t) \\ v_{C_d}(t) \end{bmatrix} = \begin{bmatrix} 19.5 \sin(100\pi t + 86^\circ) \\ 220\sqrt{2} \sin(100\pi t) \end{bmatrix}.$$

Considering [30, theorem 2], let take the following cost function to get any LQ performance level.

$$J = \min_u \sum_{k \in \text{dom}_j(\xi)} \int_{t_k}^{t_{k+1}} \frac{\rho}{R_0} (v_c(\tau, k) - v_{C_d})^2 + R (i_L(\tau, k) - i_{L_d})^2 d\tau \quad (5.42)$$

with  $\rho = 1000$ , and for a chosen matrix

$$Q = \begin{bmatrix} R_{LS} & 0 \\ 0 & \frac{\rho}{R_0} \end{bmatrix},$$

for satisfying property 5, we take

$$P = \begin{bmatrix} 21.6862 & 0.1721 \\ 0.1721 & 0.0888 \end{bmatrix}.$$



Finally, in order to avoid arbitrary fast switching, we introduce practically a sampling time  $T_s = 10^{-6}s$  in order to avoid a Zeno behavior. Moreover, from (5.1), (5.2) and the convex combination  $u = \lambda_1 - \lambda_{-1}$  with  $\lambda_1 + \lambda_{-1} = 1$ , we get to stabilize  $e(t)$  around 0 in Filippov sense, with  $\lambda_1 = 0.5 + 0.036 \sin(100\pi t) + 0.32 \cos(100\pi t)$ , satisfying the condition (5.40). Furthermore, we take  $\eta = 0.1$  which corresponds to a sub-optimal value that guarantees a trade-off between performance level and switching frequency, as shown in [30].

We select the convergence speed of the observer state,  $\alpha$ , according to Remark 11. Thus, we need to satisfy  $\max\{30, 40\} \ll \alpha$ . For this issue, we choose  $\alpha = 200$  and  $\alpha = 400$ . Moreover,  $\gamma = C_0\alpha$ .

Finally, we force two load changes, in the transient time at  $t = 0.001s$  and in the steady state at  $t = 0.01s$ , changing  $\beta$  of  $\pm 50\%$ . From  $\beta = 2.8 \cdot 10^{-3}$  ( $R_0 = 360\Omega$ ) to  $\beta = 8.3 \cdot 10^{-3}$  ( $R_0 = 120\Omega$ ) at  $t = 0.001s$  and from  $\beta = 8.3 \cdot 10^{-3}$  ( $R_0 = 120\Omega$ ) to  $\beta = 2.8 \cdot 10^{-3}$  ( $R_0 = 360\Omega$ ) at  $t = 0.01s$ .

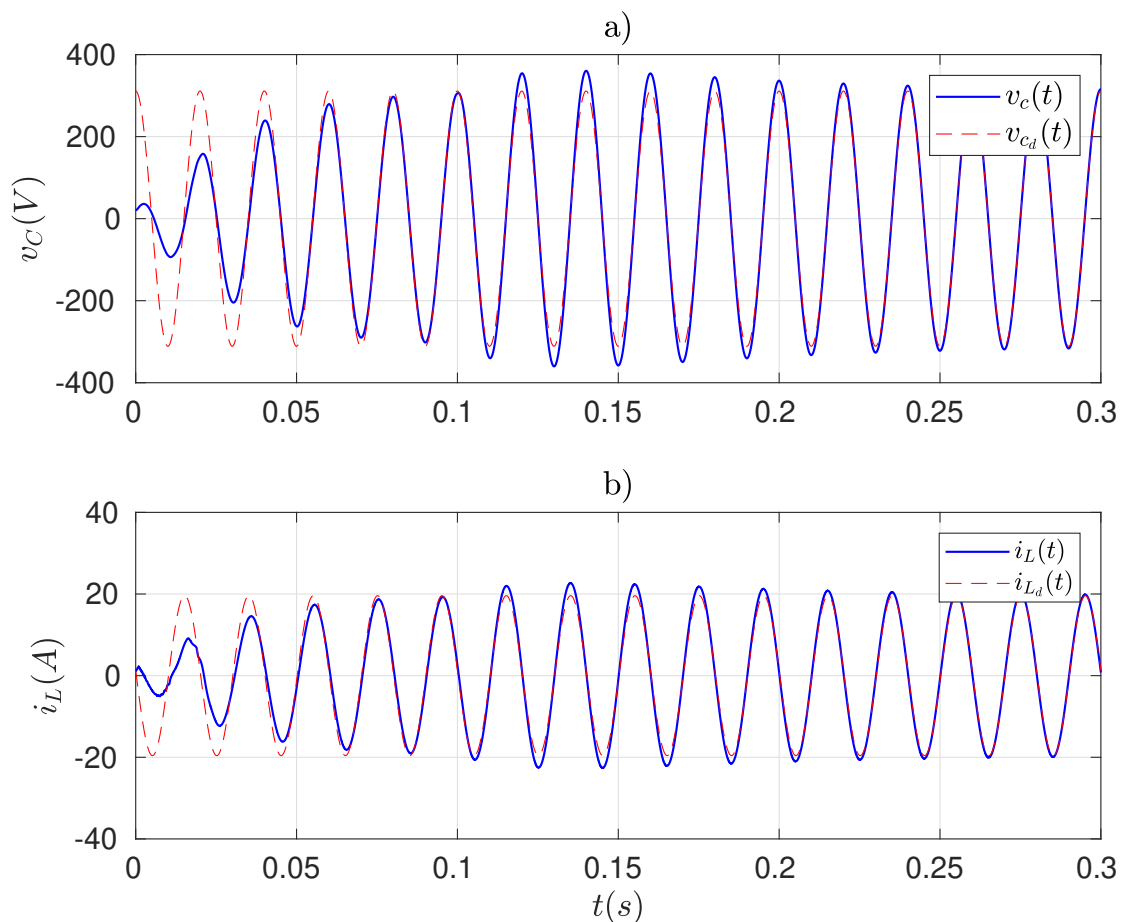
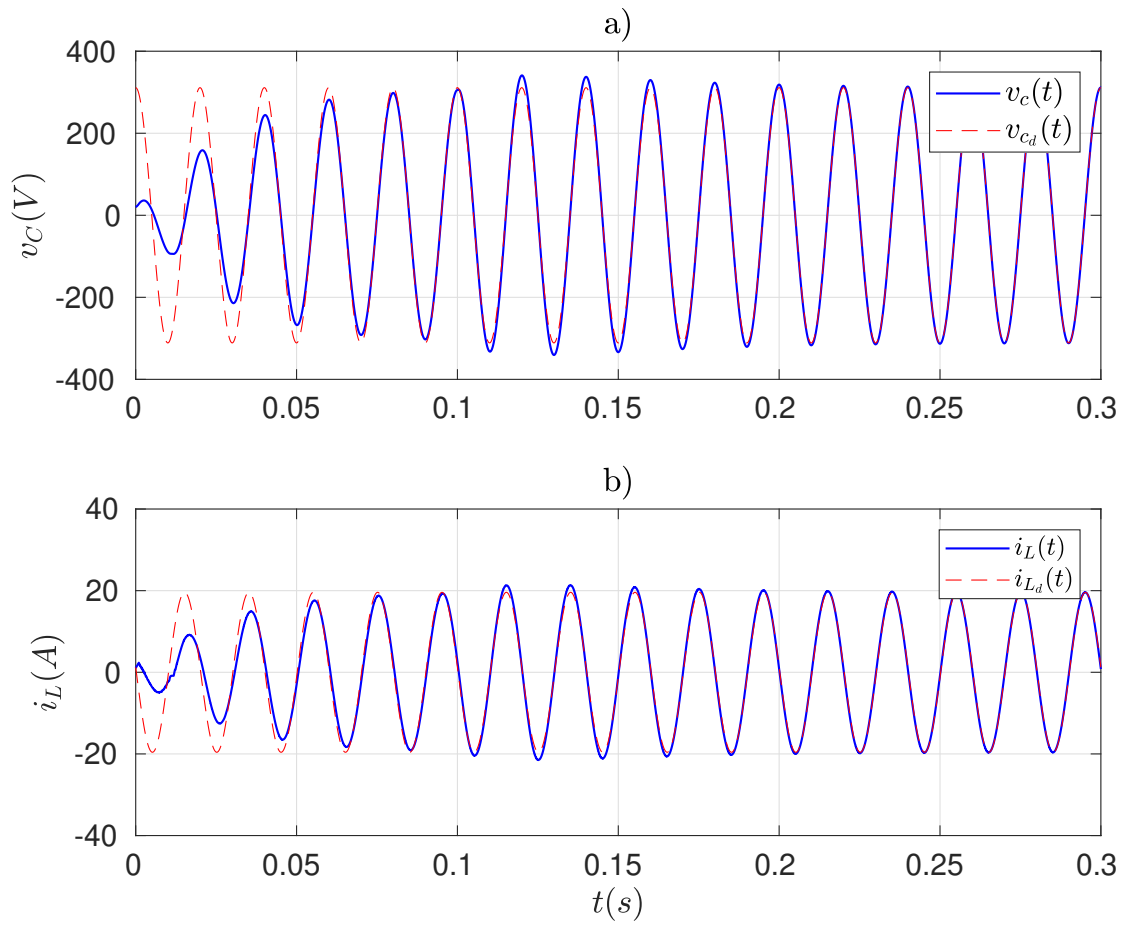


Figure 5.1: Evolution of voltage and current for  $\alpha = 200$ .

Figure 5.2: Evolution of voltage and current for  $\alpha = 400$ .

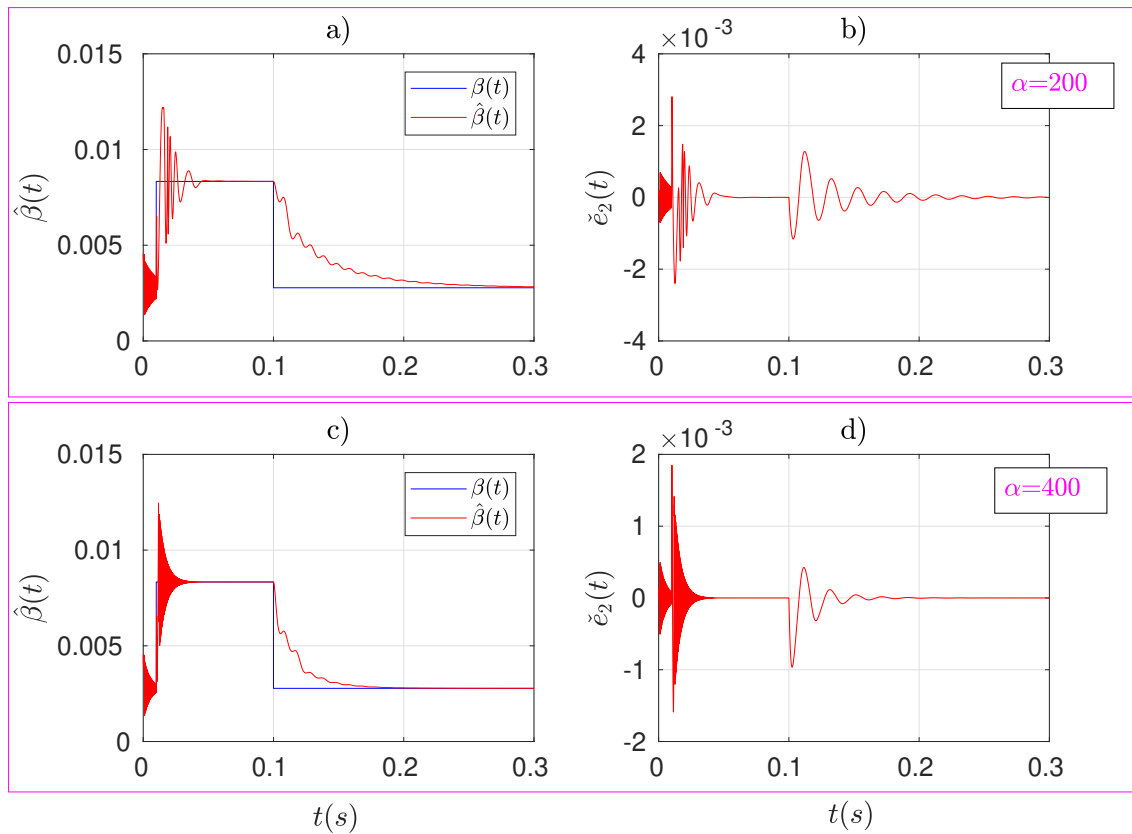


Figure 5.3: Evolution of the estimation of  $\beta$  and the error  $\check{e}_2$  for  $\alpha = 200$  and for  $\alpha = 400$ .

Figures 5.1 and 5.2 show the evolution of the voltage and current for  $\alpha = 200$  and for  $\alpha = 400$ , respectively. In both cases, the states converge to their corresponding references. For  $\alpha = 400$ , the convergence of the state is faster than for  $\alpha = 200$ . On the other hand, Figure 5.3 shows the evolution of  $\hat{\beta}$  and  $\check{e}_2$ , under the load change of  $\beta$  in the transient time ( $t=0.001s$ ) and in the steady state ( $t=0.01s$ ), respectively. The simulations in Figure 5.3 a) and Figure 5.3 b) are performed for a value of  $\alpha = 200$  and Figure 5.3 c) and Figure 5.3 d) are done using  $\alpha = 400$ . Note as  $\alpha$  larger is, the convergence of  $\hat{\beta}$  to  $\beta$  faster is. Similar performance is obtained with the error  $\check{e}_2$ . Therefore, these figures illustrate Theorem 8 statement.

## 5.3. Conclusions

We have proposed a hybrid adaptive control for a half-bridge inverter with unknown resistive load, which guarantees the robustness of the convergence of the states toward the desired trajectories. The interest of such approach is the use of a hybrid control scheme that considers the continuous-time dynamics as well as the discrete-time dynamics for the control, avoiding the use of an averaged control signal. An indirect adaptive control is proposed to estimate the unknown resistive load. Finally, SPAS of

the full system is proven by using a standard singular perturbation analysis.

## CHAPTER 6

# PRACTICAL STABILISATION OF HYBRID SYSTEM WITH DWELL-TIME GUARANTEES

---

### Sommaire

---

<b>6.1 Problem formulation</b> . . . . .	<b>95</b>
<b>6.2 Practical global results using space- or time- regularization</b> . . . . .	<b>96</b>
6.2.1 Space regularization . . . . .	99
6.2.2 Time regularization . . . . .	100
<b>6.3 Illustrative example</b> . . . . .	<b>103</b>
<b>6.4 Conclusions</b> . . . . .	<b>108</b>

---

The power converters addressed in this manuscript can be modeled as Switched Affine Systems (SASs), as mentioned in Section 2.3. In this chapter, we will deal with the problem of practical stabilisation of operating points for SASs, ensuring a minimum dwell-time and an admissible chattering around the operating point.

In the previous chapters, we provide an appealing switching strategy guaranteeing *asymptotic* stability of the operating point, which is also an equilibrium for the average dynamics (Assumption 8, Assumption 9 in chapter 4 and Assumption 13 in chapter 5). However, that results can generate arbitrarily fast switching. Indeed, the equilibriums,  $x_e$ , considered for the DC-DC converter, AC-DC converter and DC-AC converter, are not the equilibriums in the sense of Caratheodory but in the sense of Krasovskii. It means that the equilibrium is obtained at a price of an infinity frequency switching for the control. As a consequence, asymptotic stabilisation of the operated point is not possible if only a finite switching rate is allowed. Hence, the fact that  $x_e$  is not a common equilibrium implies that arbitrarily fast switching is needed by

any asymptotic stabilizer as the solutions approach  $x_e$ . Other solutions, discussed in the context of peculiar applications of switching systems such as power converters, see [56, 57, 58], aim at ensuring a dwell-time associated with an admissible chattering around the operating point. Another interesting line of work is discussed in [57], which focuses on the practical stabilisation of a family of power converters that can be modeled as switching systems with all the affine dynamics in a Hamiltonian form, see also [59]. Inspired by the physical insight coming from power converters, the authors also define the set of admissible operating points having a similar form in terms of equilibrium of the average dynamics, as used in [32]. Then, asymptotic stability is guaranteed without ensuring any dwell-time between consecutive switches.

Summarizing the above, control of switched systems can exhibit *transient chattering* (or lack of dwell time guarantees) possibly due to the presence of sliding modes in the proposed controller and, then, are bounded to unavoidable *steady-state chattering* when approaching the operating point. While the first problem can be avoided by a suitable control action, the second one requires resorting to practical (rather than asymptotic) stability guarantees. Hence, here we are interested in the practical stabilization of operating points for switching systems. Important features of the proposed control strategy are the following ones:

1. stabilization of an (arbitrarily small) set around the operating point  $x_e$  whose size can be adjusted by design parameters;
2. a positive minimal dwell time between consecutive switches during the transient and steady-state response, which can be adjusted by the design parameters, to warrant practical implementability,
3. trade-off knobs (design parameters) that can be suitably adjusted to favor dwell-time properties versus performance guarantees (an LQ cost for the transient phase and the size of the stabilized set for the steady-state phase).

Without loss of generality, we focus here in a SAS for a DC-DC converters, with constant parameters (Chapter 2). Then, let rewrite the model of this class of SAS as:

$$\begin{aligned} \dot{x} &= A_u x + B, & x(0) &= x_0 \\ y &= Cx, \end{aligned} \tag{6.1}$$

where the control input  $u := \{0, 1\}$  is the switching signal, assigning a specific desired mode among the possible ones at each time. Moreover, in dynamics (6.1),  $x \in \mathbb{R}^n$  is the state,  $y \in \mathbb{R}^p$  is a performance output, and  $A_i$  and  $B$  have suitable dimensions for all  $i \in \{0, 1\}$  given in Chapter 2, equation (2.3). The hybrid control of this system was proposed in Section 4.3.2, considering arbitrary switching in steady-state.

To deal with this practical implementation problem, we guarantee a positive dwell time by modifying (regularizing) the chattering controllers using either space or time regularization techniques, where the former enforces dwell time using space-based hysteresis logics, and the latter uses instead an explicit timer inhibiting switches up to some guaranteed dwell time.

By casting the practical stabilization problem using the recent hybrid framework of Chapter 3, we show that time and space regularizations are two variations of a central result, consisting in our Lemma 7 in Section 6.2, which provides an elegant and unified view of the two approaches. To the best of our knowledge, such a unified view, and the distinction between transient and steady-state chattering avoidance has not been proposed before, but only scattered results.

## 6.1. Problem formulation

We aim to provide feedback strategies determining  $u$  such that practical stabilisation of an operating point  $x_e \in \mathbb{R}^n$  for switched systems is achieved while satisfying requirements 1), 2) and 3) of the introduction. To this end, as in chapter 4 and 5, we make the following standard assumption (see [32, 60, 35, 61]).

✦ **ASSUMPTION 14:**

Given  $\Lambda := \{\lambda \in [0, 1] \mid \sum_{i=0}^1 \lambda_i = 1\}$ , there exists  $\lambda \in \Lambda$ , such that

$$\sum_{i=0}^1 \lambda_i (A_i x_e + B) = 0, \quad \text{and} \quad \sum_{i=0}^1 \lambda_i A_i \text{ is Hurwitz.} \quad (6.2)$$

✦ **DEFINITION 6.1.1:** The set of admissible operating points  $\Omega_e \subset \mathbb{R}^n$  is given by

$$\Omega_e := \{x_e \in \mathbb{R}^n \mid \exists \lambda \in \Lambda \text{ satisfying (6.2)}\}. \quad (6.3)$$

Hence,  $x_e \in \Omega_e$  if it is an equilibrium point for the averaged dynamics

$$\dot{x} \in F(x) := \left\{ \sum_{i=0}^1 \lambda_i (A_i x + B) \mid \lambda \in \Lambda \right\}, \quad (6.4)$$

and a stability condition is satisfied on the corresponding convex dynamics. See also [57, 32, 35, 60] and the discussion in Remark 3. While requirement  $x_e \in \Omega_e$  may appear to be non-restrictive for stabilizability of  $x_e$  from  $u$ , it is already known that this condition is not necessary even for the case of SLSs with  $N = 2$ ,  $a_1 = a_2 = 0$  and  $x_e = 0$ , as commented in [62, Section 3.4.2]. The average dynamics can be perceived as the result of arbitrarily fast switching and as the solution of the differential inclusion (6.4). Such generalizations are well characterized in the context of hybrid inclusions of [26], by way of solutions corresponding to the so-called hybrid arcs. Here, we adopt that

framework and discuss properties of those hybrid arcs for hybrid formulations of SAS (6.1).

More specifically, we address the following problem: *Given the SAS (6.1), for each  $x_e \in \Omega_e$  design a feedback law for the switching signal  $u$  that globally asymptotically stabilizes an arbitrarily small neighborhood of  $x_e$  by suitably adjusting the design parameters (in other words, a parametric feedback that practically stabilizes  $x_e$ ), while satisfying requirements 2) and 3) discussed in the introduction.*

Consider (6.1),  $x_e \in \Omega_e$  and  $\lambda_e \in \Lambda$  satisfying (6.2). We select two matrices  $P$  and  $Q$  as follows

★ **PROPERTY 7:**

There exist  $P$  and  $Q \in \mathcal{S}^n$  satisfying

$$\left( \sum_{i=1}^N \lambda_{e,i} A_i^T \right) P + P \left( \sum_{i=1}^N \lambda_{e,i} A_i \right) + 2Q \leq 0. \quad (6.5)$$

Clearly due to  $\sum_{i=1}^N \lambda_{e,i} A_i$  being Hurwitz matrices  $P, Q$  satisfying Property 7 always exist. Note that Property 7, which can be already found in [61] and in the recent work [63], imposes less restrictive assumptions than the one proposed in the previous chapters, which corresponds to a special case.

## 6.2. Practical global results using space- or time- regularization

The hybrid controls proposed in Chapter 4 and 5, can provide arbitrarily fast switching as the solution approaches  $x_e$ . In particular, given an initial condition in  $\mathcal{A}$  given in equation (4.13), one see that the hybrid dynamics (4.7)–(4.10) has at least one solution that keeps jumping onto  $\mathcal{A}$  without flowing. Infinitely fast switching is not desirable in terms of energy efficiency and reliability in many applications, such as power converters, because every switch dissipates energy and reduces the switch lifespan. For this reason, we propose a redesign of the hybrid law, aiming at reducing the number of switches when  $\tilde{x} = x - x_e$  is close to zero, and avoiding infinitely fast switching. This goal is reasonable for the proposed law, because it is possible to show that away from  $\mathcal{A}$ , during *transients*, our control law already enjoys a desirable property of positive dwell time between switches, as long as Assumption 14 and Property 7 hold. To do so, we change system (4.7)–(4.10) with shorthand notation  $\mathcal{H} := (f, G, \mathcal{C}, \mathcal{D})$ , for a non-negative scalar  $\varepsilon$ , to the redesigned system:



$$\mathcal{H}_\varepsilon := (f, G, \mathcal{C}_\varepsilon, \mathcal{D}_\varepsilon) \quad (6.6a)$$

$$\mathcal{C}_\varepsilon := \mathcal{C} \cup \{(x, u) : V(x - x_e) \leq \varepsilon\} \quad (6.6b)$$

$$\mathcal{D}_\varepsilon := \mathcal{D} \cap \{(x, u) : V(x - x_e) \geq \varepsilon\}, \quad (6.6c)$$

with  $V$  is the candidate Lyapunov function given as

$$V(\tilde{x}) := \frac{1}{2}|\tilde{x}|_P^2 := \frac{1}{2}\tilde{x}^T P \tilde{x}. \quad (6.7)$$

A useful practical dwell-time property for  $\mathcal{H}$  is then established next. Lemma 7 below is a nontrivial consequence of the fact that Zeno solutions can only occur at the equilibrium  $x_e$  for the hybrid closed loop. The ensuing dwell-time results are the key to prove the properties of the regularized dynamics of this section.

**\* LEMMA 7:**

*There exists a positive scalar  $T^*$  such that for each  $0 < T \leq T^*$ , there exists a scalar  $\varepsilon > 0$  such that all solutions to  $\mathcal{H}$  jumping from set  $\mathcal{D}_\varepsilon$  flow for at least  $T$  ordinary time units after the jump, before reaching again set  $\mathcal{D}_\varepsilon$ . Moreover, as  $T$  tends to zero, we have that  $\varepsilon$  tends to zero as well.*

*Proof.* To prove the lemma, it is enough to fix any positive scalar  $\varepsilon = \varepsilon^*$  in (6.6) and show that there exists  $T^*$  such that all solutions starting from  $\mathcal{D}_{\varepsilon^*}$  flow for at least  $T^*$  ordinary time units after the jump before reaching set  $\mathcal{D}$ . The rest of the lemma follows trivially from the fact that smaller values of  $\varepsilon < \varepsilon^*$  are associated with the solutions starting in  $\mathcal{D}_{\varepsilon^*}$  (already characterized by  $T^*$ ) plus additional solutions starting in the compact set  $\overline{\mathcal{D}_\varepsilon \setminus \mathcal{D}_{\varepsilon^*}}$ , that enjoy a dwell-time property because any jump from this set maps to the interior of the flow set (and then one can consider the minimum flowing time over this compact set of initial conditions). Without loss of generality we can impose that the dwell time  $T$  converge to zero as  $\varepsilon$  converges to zero, thereby defining the function  $\varepsilon$  discussed in the lemma.

Let us then fix a scalar  $\varepsilon = \varepsilon^*$  in (6.6) and first notice that any solution jumping from  $\mathcal{D}_{\varepsilon^*}$  at time  $(t_j, j - 1)$  satisfies, before and after the jump:

$$|\tilde{x}(t_j, j)|_Q^2 := \tilde{x}^T Q \tilde{x} \geq q_m |\tilde{x}|^2 \geq \frac{q_m}{p_M} V(\tilde{x}) \geq \frac{q_m \varepsilon^*}{p_M} =: 2\varepsilon_Q, \quad (6.8)$$

where the dependence on  $(t, j)$  has been omitted at the right-hand side, and where we denoted by  $q_m$  and  $q_M$  the minimum and maximum eigenvalues of  $Q$ , respectively, and by  $p_M$  the maximum eigenvalue of  $P$ . Define now the function  $\chi(\tau) := 2\varepsilon_Q - |\tilde{x}(t_j + \tau, j)|_Q^2$  and notice that (6.8) implies  $\chi(0) \leq 0$ . Consider now the flow dynamics in equation (4.8) and introduce scalars  $a = A_u x_e + B$ , to get

$$\dot{\tilde{x}} = A_u x + B = A_u \tilde{x} + a, \quad (6.9)$$

so that we may characterize the variation of  $\chi$  as:

$$\dot{\chi} = -2\tilde{x}^T Q(A_u \tilde{x} + a) \leq \kappa_1 |\tilde{x}|_Q^2 + \kappa_2 |\tilde{x}|_Q, \quad (6.10)$$

where  $\kappa_1 := 2\frac{q_M}{q_m} \max_{u \in \bar{N}} |A_u|$  and  $\kappa_2 := 2\frac{q_M}{\sqrt{q_m}} \max_{u \in \bar{N}} |b_u|$ . Using now  $|\tilde{x}|_Q^2 \leq |\chi| + 2\varepsilon_Q$ , which also gives  $|\tilde{x}|_Q \leq \sqrt{|\chi|} + \sqrt{2\varepsilon_Q}$ , because  $|\chi|$  and  $\varepsilon_Q$  are both non-negative, we get the bound:

$$\begin{aligned} \dot{\chi}(\tau) &\leq \kappa_1 (|\chi(\tau)| + 2\varepsilon_Q) + \kappa_2 (\sqrt{|\chi(\tau)|} + \sqrt{2\varepsilon_Q}) \\ &= \kappa_1 |\chi(\tau)| + \kappa_2 \sqrt{|\chi(\tau)|} + \kappa_3, \quad \forall \tau \leq t_{j+1} - t_j, \end{aligned} \quad (6.11)$$

where  $\kappa_3 = 2\kappa_1 \varepsilon_Q + \kappa_2 \sqrt{2\varepsilon_Q} > 0$ . Denote by  $\phi$  the solution to the differential equation induced by (6.11) starting at zero. This solution is continuous by definition, and strictly increasing because  $\kappa_i > 0$  for all  $i = 1, 2, 3$ . Then there exists  $T_1$  such that  $\phi(T_1) = \varepsilon_Q$  and from standard comparison theory, and recalling that  $\chi(0) \leq 0$  (by (6.8)), we have  $\chi(\tau) \leq \varepsilon_Q$  for all  $\tau \leq T_1$ , which implies

$$|\tilde{x}(t_j + \tau, j)|_Q^2 = 2\varepsilon_Q - \chi(\tau) \geq \varepsilon_Q, \quad \forall \tau \leq T_1. \quad (6.12)$$

Consider now equation (4.17) and define the function <sup>1</sup>

$$\varsigma(\tilde{x}) := \frac{\tilde{x}^T (A_u \tilde{x} + a)}{|\tilde{x}|_Q^2} + 1,$$

which, from (4.17) clearly satisfies  $\varsigma(\tilde{x}(t_j, j)) \leq 0$  after the jump from  $\mathcal{D}_{\varepsilon^*}$ . We prove below the existence of  $T^*$  such that

$$\varsigma(\tilde{x}(t_j + \tau, j)) \leq 1 - \eta, \quad \text{for all } \tau \leq T^*, \quad (6.13)$$

which trivially proves  $\tilde{x}(t_j + \tau, j)^T (A_u \tilde{x}(t_j + \tau, j) + b_u) \leq -\eta |\tilde{x}(t_j + \tau, j)|_Q^2$  for all  $\tau \leq T^*$ , which in turn implies that the solution does not belong to  $\mathcal{D}$ , thus completing the proof of the lemma.

To prove (6.13), we proceed again with bounding the derivative of  $\varsigma$ . Straightforward derivations provide, along flowing solutions according to (4.8):

$$\begin{aligned} \dot{\varsigma} &= -\frac{2\tilde{x}^T P(A_u \tilde{x} + a)\tilde{x}^T Q(A_u \tilde{x} + a)}{|\tilde{x}|_Q^4} \\ &\quad + \frac{\tilde{x}^T (PA_u + A_u^T P)A_u \tilde{x} + \tilde{x}^T (2A_u^T P + PA_u)a + a^T Pa}{|\tilde{x}|_Q^2} \\ &\leq \varsigma_1 + \varsigma_2 \frac{1}{|\tilde{x}|_Q} + \varsigma_3 \frac{1}{|\tilde{x}|_Q^2}, \end{aligned}$$

<sup>1</sup>To avoid overloading notation, the hybrid time is only specified on the  $\tilde{x}$  component, but the state variable  $u$  should be evaluated at the same hybrid time in the derivations at the end of the proof of Lemma 7.

where  $\varsigma_1, \varsigma_2, \varsigma_3$  are sufficiently large positive scalars (and where we used  $|\tilde{x}| \leq \frac{1}{\sqrt{q_m}}|\tilde{x}|_Q$  in several places). Consider now any time  $\tau \leq T_1$ , and use bound (6.12) to obtain  $\dot{\varsigma} \leq \varsigma_1 + \varsigma_2 \varepsilon_Q^{-1/2} + \varsigma_3 \varepsilon_Q^{-1}$ , which, together with  $\varsigma(\tilde{x}(t_j, j)) \leq 0$ , and integrating  $\dot{\varsigma}$ , immediately gives (6.13) for  $T^* := \min\{T_1, T_2\}$ , where  $T_2 := \frac{1-\eta}{\varsigma_1 + \varsigma_2 \varepsilon_Q^{-1/2} + \varsigma_3 \varepsilon_Q^{-1}}$ .  $\square$

Lemma 7 ensures that a positive dwell time holds if solutions remain sufficiently far from  $\mathcal{A}$ . Then we have two possibilities to modify our control law to ensure that dwell time is enjoyed by solutions. One of them corresponds to replace the jump set  $\mathcal{D}$  by the restricted version in  $\mathcal{D}_\varepsilon$  (we call it space regularization) and forcing solutions to flow in  $\mathcal{D} \setminus \mathcal{D}_\varepsilon$  (this is called space regularization and is addressed in Section 6.2.1), and the other one corresponds to force solutions not to jump unless some dwell time has expired (this is called time regularization and is addressed in Section 6.2.2). Then, it makes sense to introduce the following  $\varepsilon$ -inflated version of attractor  $\mathcal{A}$ :

$$\mathcal{A}_\varepsilon := \{(\tilde{x}, u) : V(\tilde{x}) \leq \varepsilon, u \in \bar{N}\}, \quad (6.14)$$

which evidently reduces to  $\mathcal{A}$  as  $\varepsilon$  tends to zero. *Practical stabilization* of  $\mathcal{A}$  comprises finding a parametric control law (whose parameter is  $\varepsilon$ ) such that for each sufficiently small value of  $\varepsilon$  a subset of  $\mathcal{A}_\varepsilon$  is UGAS for the closed loop. This is done in the next sections.

### 6.2.1. Space regularization

Based on Lemma 7, for any value of a positive scalar  $\varepsilon$ , let us consider the space-regularized version of  $\mathcal{H} = (f, G, \mathcal{C}, \mathcal{D})$  given in (6.6). The regularized dynamics are clearly motivated by the fact that jumps are forbidden when solutions are  $\varepsilon$ -close to the attractor.

Mainly using Lemma 7 the following desirable results are enjoyed by hybrid system  $\mathcal{H}_\varepsilon$ .

**THEOREM 9.** *Consider point  $x_e$  and a vector  $\lambda_e$  satisfying Assumption 14 and matrices  $P$  and  $Q \in \mathcal{S}^n$  satisfying Property 7. The following hold:*

1. *for any positive scalar  $\varepsilon$ , set  $\mathcal{A}_\varepsilon$  in (6.14) is UGAS for dynamics  $\mathcal{H}_\varepsilon$  in (6.6);*
2. *set  $\mathcal{A}$  is globally practically asymptotically stable for (6.6), with respect to parameter  $\varepsilon$ ;*
3. *There exists  $T > 0$  such that all solutions to  $\mathcal{H}_\varepsilon$  enjoy a  $T$ -dwell-time property, namely given any solution  $\varphi$  to  $\mathcal{H}_\varepsilon$ , all  $(t, j) \in \text{dom } \varphi$  satisfy  $t \geq \frac{j}{T} - 1$ .*

*Proof.* First notice that sets  $\mathcal{C}_\varepsilon$  and  $\mathcal{D}_\varepsilon$  are both closed. Indeed,  $\mathcal{C}_\varepsilon$  is the union of two closed sets and  $\mathcal{D}_\varepsilon$  is the intersection of two closed sets. Then, due to the properties

of  $f$  and  $G$ , system  $\mathcal{H}_\varepsilon$  satisfies the hybrid basic condition presented in chapter 3 and we may apply several useful results pertaining to well-posed hybrid systems.

*Proof of item 3).* This item follows in a straightforward way from Lemma 7. Indeed, solutions to  $\mathcal{H}_\varepsilon$  can only jump from  $\mathcal{D}_\varepsilon$ . Any such solution  $\varphi$  flows for at least  $T$  time after each jump, before reaching again  $\mathcal{D}_\varepsilon$ , which clearly implies  $t + 1 \geq \frac{j}{T}$  (where the “1” takes care of the initial condition), as to be proven.

*Proof of item 1).* Consider the following Lyapunov function candidate:

$$V_\varepsilon(\tilde{x}) = \max\{V(\tilde{x}) - \varepsilon, 0\}, \quad (6.15)$$

which is clearly positive definite with respect to  $\mathcal{A}_\varepsilon$  and radially unbounded. Since outside set  $\mathcal{A}_\varepsilon$  the hybrid dynamics  $\mathcal{H}_\varepsilon$  coincides with the one of  $\mathcal{H}$ , then equations (4.14) and (4.15) hold for any  $(\tilde{x}, u)$  not in  $\mathcal{A}_\varepsilon$ , which implies that

$$\langle \nabla V_\varepsilon(\tilde{x}), f(x, u) \rangle < 0 \quad \forall \tilde{x} \in \mathcal{C}_\varepsilon \setminus \mathcal{A}_\varepsilon \quad (6.16)$$

$$V_\varepsilon(\tilde{x}^+) - V_\varepsilon(\tilde{x}) = 0, \quad \forall \tilde{x} \in \mathcal{D}_\varepsilon \setminus \mathcal{A}_\varepsilon \quad (6.17)$$

Moreover, from the property established in item 3), all complete solutions to  $\mathcal{H}_\varepsilon$  must flow for some time, and therefore from (6.16), we have that no solution can keep  $V_\varepsilon$  constant and non-zero. UGAS of  $\mathcal{A}_\varepsilon$  by applying the nonsmooth invariance principle in [64], also using the well posedness result established at the beginning of the proof.

*Proof of item 2).* The proof follows in a straightforward way from the previous item, after noticing that given any neighborhood  $\mathcal{I}$  of  $\mathcal{A}$ , there exists a small enough  $\varepsilon > 0$  such that  $\mathcal{A}_\varepsilon \subset \mathcal{I}$ .  $\square$

### 6.2.2. Time regularization

Based on Lemma 7, for any value of  $T < T^*$ , we may introduce the following additional state variable  $\tau$  to dynamics (4.7):

$$\mathcal{H}_{\varepsilon_T} : \begin{cases} \begin{cases} \begin{bmatrix} \dot{x} \\ \dot{u} \end{bmatrix} = f(x, u), \\ \dot{\tau} = r\left(\frac{\tau}{T}\right), \end{cases} & (x, u) \in \mathcal{C}_{\varepsilon_T} \\ \begin{cases} \begin{bmatrix} x^+ \\ u^+ \end{bmatrix} \in G(x, u), \\ \tau^+ = 0, \end{cases} & (x, u) \in \mathcal{D}_{\varepsilon_T}, \end{cases} \quad (6.18a)$$

where  $r(s) := \min\{1, 2 - s\}$ , for all  $s \geq 0$  and the jump and flow sets are the following time-regularized versions of  $\mathcal{C}$  and  $\mathcal{D}$  in (4.7)–(4.10):

$$\begin{aligned}\mathcal{C}_{\varepsilon_T} &:= \mathcal{C} \times [0, 2T] \cup \{(x, u, \tau) : \tau \in [0, T]\} \\ \mathcal{D}_{\varepsilon_T} &:= \mathcal{D} \times [T, 2T].\end{aligned}\tag{6.18b}$$

The above regularization is clearly motivated by the fact that jumps are forbidden when the timer  $\tau$  is too small, namely not enough time has elapsed since the last jump. Then all solutions are forced to flow for at least  $T$  ordinary time after each jump. Note also that function  $r$  at the right-hand side of equation (6.18a) allows a solution to flow forever while ensuring that timer  $\tau$  remains in a compact set.

Before proceeding any further, we emphasize that forcing a solution to flow regardless of whether it belongs to  $\mathcal{D}$  or not, may lead to an increase of function  $V$ . It is useful to quantify how much increase  $V$  can experience from the set where  $V(\tilde{x}) \leq \varepsilon_T$  (let recall  $\varepsilon_T := \varepsilon$ , being  $\varepsilon$  introduced in Lemma 7). To this end, we exploit the affine nature of the dynamics and observe that along solutions of (6.18) we have  $\dot{V}(\tilde{x}) \leq |\tilde{x}| |P| |\dot{\tilde{x}}| = |\tilde{x}| |P| |\dot{\tilde{x}}| \leq |\tilde{x}| |P| (\kappa_1 |\tilde{x}| + \kappa_2) \leq 2\alpha V(\tilde{x}) + 2\beta \sqrt{V(\tilde{x})}$ , where  $\alpha$  and  $\beta$  are large enough positive scalars and where we used positive definiteness of  $P$  and the sector growth condition  $|\dot{\tilde{x}}| = |\dot{x}| \leq |A_u(x - x_e)| + |A_u x_e + a_u| \leq \kappa_1 |\tilde{x}| + \kappa_2$  (which clearly holds for some  $\kappa_1 > 0$  and  $\kappa_2 > 0$ ). Proceeding as in [65, page 203], we obtain along any solution  $\phi$  satisfying  $(t, j) \in \text{dom } \phi$  and  $(t + T, j) \in \text{dom } \phi$ ,

$$\begin{aligned}\sqrt{V(\phi(t + \tau, j))} &\leq e^{\alpha\tau} \sqrt{V(\phi(t, j))} + \beta \int_0^\tau e^{\alpha s} ds \\ &= e^{\alpha\tau} \sqrt{V(\phi(t, j))} + \frac{\beta}{\alpha} (e^{\alpha\tau} - 1), \quad \forall \tau \in [0, T].\end{aligned}$$

Therefore, assuming that  $V(\phi(t, j)) \leq \varepsilon_T$ , we obtain for all  $\tau \in [0, T]$ ,

$$V(\phi(t + \tau, j)) \leq \varepsilon_T(T) := 2e^{2\alpha T} \varepsilon_T + \frac{2\beta^2}{\alpha^2} (e^{\alpha T} - 1)^2.\tag{6.19}$$

This bound motivates the introduction of the following set:

$$\mathcal{E}_T := \{(\tilde{x}, u, \tau) : V(\tilde{x}) \leq \varepsilon_T(T), u \in \bar{N}, \tau \in [0, 2T]\},\tag{6.20}$$

which enjoys the nice property of shrinking to  $\mathcal{A}_\varepsilon \times \{0\}$ , as  $T$  converges to zero.

Mainly using Lemma 7 the following desirable results are enjoyed by hybrid system  $\mathcal{H}_{\varepsilon_T}$  in (6.18).

☀ **THEOREM 10.** *Consider point  $x_e$  and a vector  $\lambda_e$  satisfying Assumption 14 and matrices  $P \in \mathbb{R}^{n \times n}$  and  $Q \in \mathbb{R}^{n \times n}$  satisfying Property 7. The following holds:*

1. *all solutions to  $\mathcal{H}_{\varepsilon_T}$  enjoy a dwell-time property corresponding to  $T$ ;*

2. for any positive scalar  $T < T^*$ , there exists a compact set  $\mathcal{A}_\varepsilon \times [0, 2T] \subset \mathcal{E}_T$ , which is UGAS for dynamics  $\mathcal{H}_{\varepsilon_T}$  in (6.18);
3. set  $\mathcal{A} \times \{0\}$  is globally practically asymptotically stable for (6.18), with respect to parameter  $T$  (namely as long as  $T$  is sufficiently small, the UGAS set  $\mathcal{A}_\varepsilon \times [0, 2T]$  characterized in the previous item can be made arbitrarily close to  $\mathcal{A} \times \{0\}$ ).

*Proof.* Similar to the proof of Theorem 9 we start by noticing that hybrid system (6.18) enjoys the hybrid basic conditions of [26, As. 6.5], because sets  $\mathcal{C}_{\varepsilon_T}$  and  $\mathcal{D}_{\varepsilon_T}$  are both closed and  $f$  and  $G$  enjoy desirable properties. Then we may apply several useful results pertaining well-posed hybrid systems (specifically, in the proof of item 2 below).

*Proof of item 1.* The dwell-time property of solutions follows in a straightforward way from the fact that solutions are forced to not jump until the timer variable  $\tau$  has reached the value  $T$ . Since  $\dot{\tau} = 1$  for all  $\tau \leq T$ , then all solutions flow for at least  $T$  ordinary time after each jump (because  $\tau^+ = 0$  across jumps).

*Proof of item 2.* Consider the two hybrid systems  $\mathcal{H}_\varepsilon$  and  $\mathcal{H}_{\varepsilon_T}$  in (6.6) and (6.18), respectively. For any positive value of  $T < T^*$ , we have shown in the proof of item 1 of Theorem 9 that it suffices to pick  $\varepsilon_T = \varepsilon$  (coming  $\varepsilon$  from Lemma 7) to obtain UGAS of the attractor  $\mathcal{A}_\varepsilon$  in (6.14) and a dwell time of  $T$  for all solutions to  $\mathcal{H}_\varepsilon$ . Since the  $(x, u)$  dynamics of  $\mathcal{H}_\varepsilon$  and  $\mathcal{H}_{\varepsilon_T}$  coincide, except for the dwell-time restriction on  $\mathcal{H}_{\varepsilon_T}$ , the above mentioned dwell-time property of solutions to  $\mathcal{H}_\varepsilon$  ensures that (possibly after an initial flow of at most  $T$  ordinary time) the  $(x, u)$  component of each solution to  $\mathcal{H}_{\varepsilon_T}$  remaining outside  $\mathcal{A}_\varepsilon \times [0, 2T]$ , coincides with a solution to  $\mathcal{H}_\varepsilon$ , therefore any such solution to  $\mathcal{H}_{\varepsilon_T}$  must approach  $\mathcal{A}_\varepsilon \times [0, 2T]$ , which is a strict subset of  $\mathcal{E}_T$  in (6.20). Two things may happen then. Either the solution approaches  $\mathcal{A}_\varepsilon \times [0, 2T]$  without ever reaching it, so it eventually remains in  $\mathcal{E}_T$ , or it reaches  $\mathcal{A}_\varepsilon \times [0, 2T]$  and may then be forced to flow by the dwell-time logic of  $\mathcal{H}_{\varepsilon_T}$ . However, in this last case we get from bound (6.19) that such a solution cannot flow outside  $\mathcal{E}_T$ . As a consequence,  $\mathcal{E}_T$  is uniformly attractive and reaches in finite time by all solutions, in addition to being strongly forward invariant for  $\mathcal{H}_{\varepsilon_T}$ .

We now use the well-posedness property established at the beginning of the proof to exploit a number of regularity results from [26, Ch. 6 & 7]. Denote by  $\Omega(\mathcal{E}_T)$  the  $\omega$ -limit set of  $\mathcal{E}_T$  (see [26, Def. 6.23]) and note that it cannot be empty, and must satisfy  $\Omega(\mathcal{E}_T) \subset \mathcal{E}_T$ , because  $\mathcal{E}_T$  is bounded and strongly forward invariant. Then using again strong forward invariance of  $\mathcal{E}_T$  we get boundedness of all solutions starting from  $\mathcal{E}_T$  and we may apply [26, Prop. 6.26] to obtain that  $\Omega(\mathcal{E}_T)$  is compact, nonempty, uniformly attractive from  $\mathcal{E}_T$ , and strongly forward invariant. Since  $\mathcal{E}_T$  is also uniformly attractive, we may then apply a global version<sup>2</sup> of [26, Prop. 7.5] applied to the compact

<sup>2</sup>A global version of [26, Prop. 7.5] is trivially obtained by establishing its hypotheses for any arbitrary positive value of  $\mu$ .



attractor  $\Omega(\mathcal{E}_T)$ , to conclude global asymptotic stability of  $\Omega(\mathcal{E}_T)$ , which is equivalent to UGAS from [26, Th 3.40 & Th 7.12].

*Proof of item 3.* Item 3 follows in a straightforward way by recalling from Lemma 7 that  $\varepsilon$  converges to zero as  $T$  goes to zero, and then that also  $\varepsilon(T)$  in (6.19) enjoys the same property. As a consequence, set  $\mathcal{E}_T$  in (6.20) shrinks to  $\mathcal{A} \times \{0\}$  as  $T$  goes to zero, and since we established in item 2 that  $\mathcal{A}_\varepsilon \times [0, 2T] \subset \mathcal{E}_T$  for all  $T > 0$ , we can make  $\mathcal{A}_\varepsilon \times [0, 2T]$  arbitrarily close to  $\mathcal{A} \times \{0\}$  by selecting  $T$  sufficiently small.  $\square$

### 6.3. Illustrative example

The two hybrid control schemes developed in Section 6.2.1 (space regularization) and 6.2.2 (time regularization) are tested on a boost converter model (2.3). The considered nominal values are:  $V_{in} = 100V$ ,  $R = 2\Omega$ ,  $L = 500\mu H$ ,  $C_o = 470\mu F$  and  $R_o = 50\Omega$ . The desired equilibrium point is chosen as  $x_e = [3 \quad 120]^T$ . Assumption 14 is therefore satisfied with  $\lambda_e = [0.22 \quad 0.78]$ .

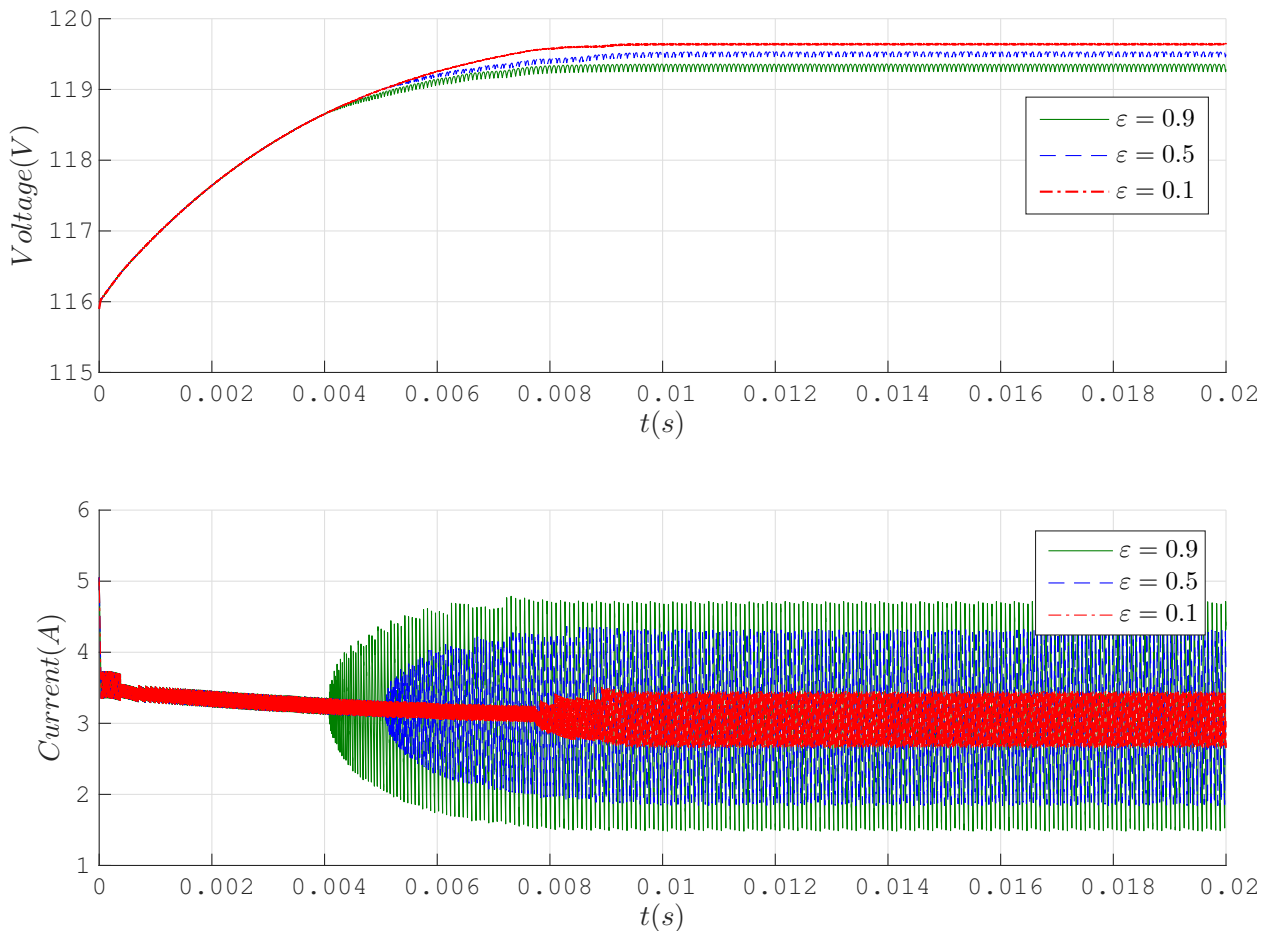


Figure 6.1: Evolution of the states for different values of  $\varepsilon$ .

Fig. 6.1 reports voltage and current evolutions for different selections of  $\varepsilon$ . Smaller  $\varepsilon$  is, smaller the set  $\mathcal{A}_\varepsilon$  given by equation (6.14) is. Also we can show the convergence of the states to the desired attractor  $\mathcal{A}_\varepsilon$  with respect to the design parameter  $\varepsilon$ .

Now, we consider a time-regularization, applying Theorem 10. Fig. 6.2 reports voltage and current evolutions for different selections of  $T$ . When  $T$  increases, the number of switches decreases according to Lemma 7. We can show the convergence of the states to the desired attractor.

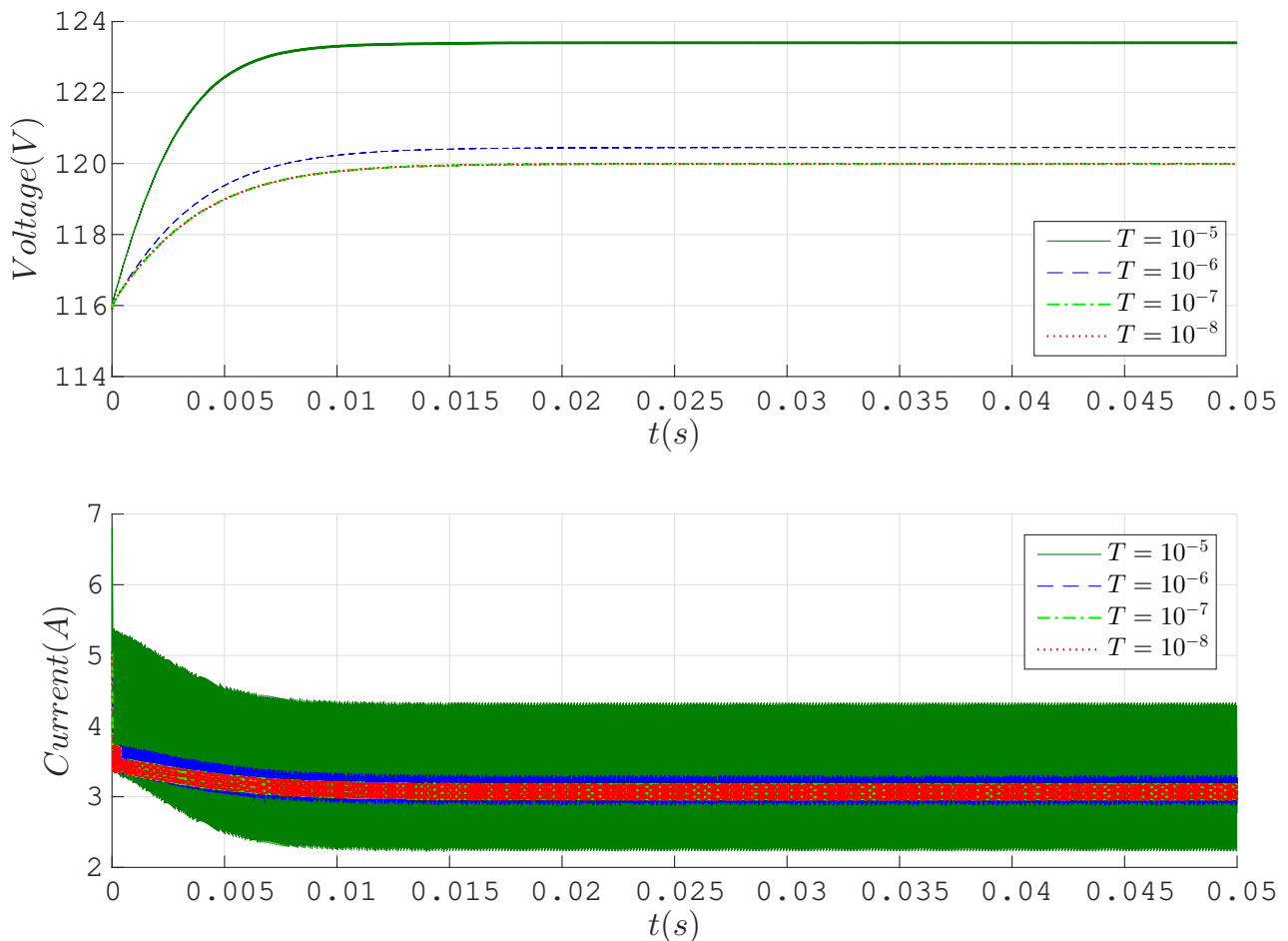


Figure 6.2: Evolution of the states for different values of sampling time  $T$ .

In Figure 6.3 we report on the results of extensive simulation tests, and the arising statistics about the switching frequency. To suitably illustrate the different roles of the “transient” parameter  $\eta$  introduced in Section 4.3.2 and the “steady-state” parameters  $\varepsilon$  and  $T$  introduced in Sections 6.2.1 and 6.2.2, respectively, we select a grid of possible values of  $(\eta, \varepsilon)$  (for the space regularization case, shown in the two upper surfaces), and a grid of possible values of  $(\eta, T)$  (for the time regularization case, shown in the two bottom surfaces). Two large sets of simulations have been carried out using space



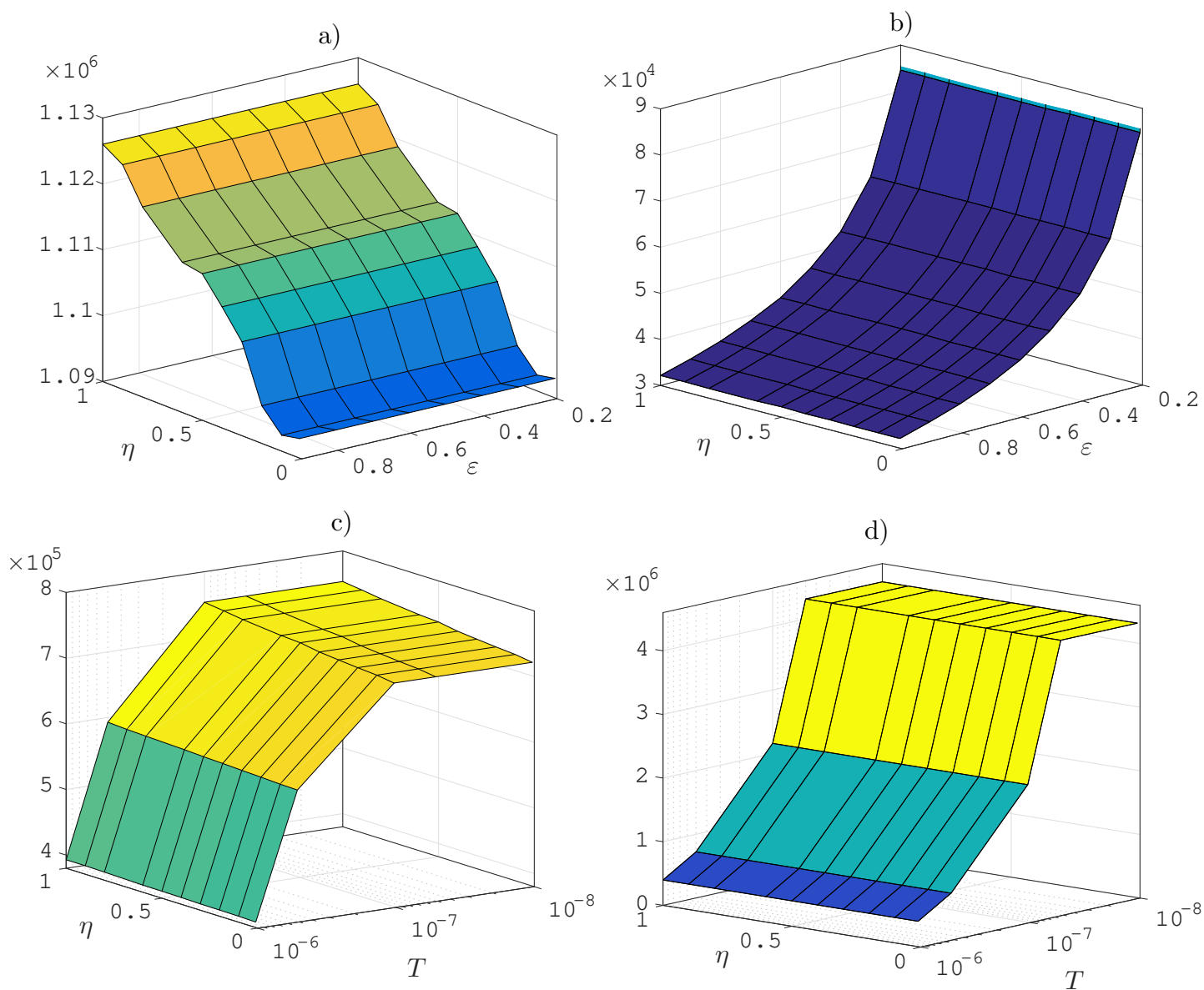


Figure 6.3: Top surfaces: evolution of the switching frequency with space regularization in the transient (left) and at the steady state (right). Bottom surfaces: evolution of the average switching frequency with time regularization in the transient (left) and at the steady state (right).

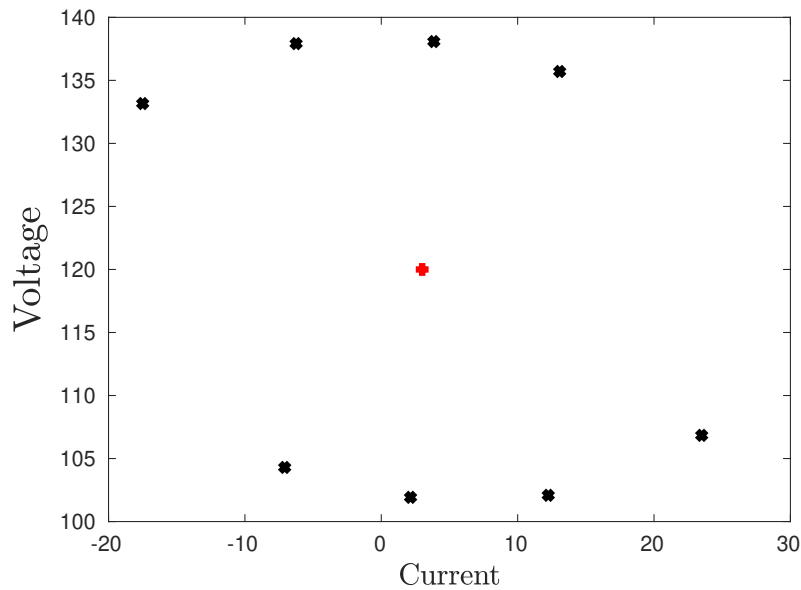


Figure 6.4: The chosen initial conditions.

regularization and time regularization, respectively, leading to Figure 6.3.

Let us first consider the upper surfaces of Figure 6.3 (space regularization). Each point on these surfaces correspond to a pair  $(\eta, \varepsilon)$  and has been generated by first running eight simulations from eight different initial conditions, with good coverage of all the possible directions of the initial error (given in Figure 6.4). These initial conditions all correspond to an initial value of  $V(\tilde{x}(0, 0)) = 200$  (they are all on the same level set of  $V$ ). Each simulation runs for 50 ms and the statistics reported in the left of Figure 6.3 show the average switching frequency in the time domain preceding the first time  $(\bar{t}, \bar{j}) \in \text{dom } \tilde{x}$  when  $V(\tilde{x}(\bar{t}, \bar{j})) \leq \varepsilon$  (when the response is still in the transient phase). The right surface shows instead the response in the remaining portion of each simulation (where the response has reached the steady state).

For example:

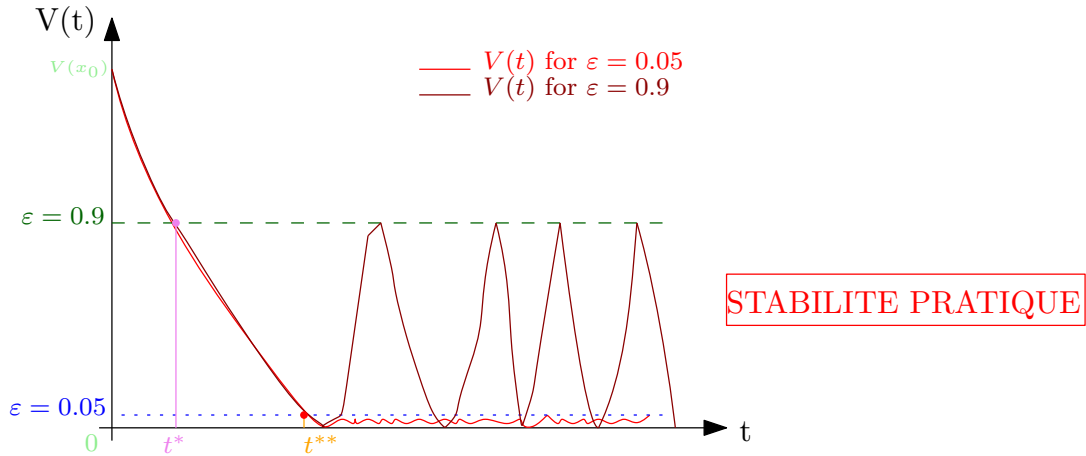


Figure 6.5: Evolution of Lyapunov function for two values of  $\varepsilon$  ( $\varepsilon=0.05$  and  $\varepsilon=0.9$ ).

- $t^*$  is the time dividing the transit-time and steady-state for  $\varepsilon = 0.9$ .
- $t^{**}$  is the time dividing the transit-time and steady-state for  $\varepsilon = 0.05$ .

Each of these statistics represents the number of switches normalized by the length of the interval, averaged over the eight simulated solutions. We may appreciate the fact that the steady-state parameter  $\varepsilon$  has no effect on the transient switching frequency and has significant effect on the steady-state switching frequency. The converse holds for the transient parameter  $\eta$ , which is shown to have an effect on the transient switching frequency.

Time regularization is instead used in the lower surfaces of Figure 6.3, corresponding to a grid of selections of the two parameters  $(\eta, T)$ , where for each point on the grid eight simulations from the same initial conditions as in the previous case, are performed. For this second case, a rough indication of the expiration of the transient phase has been performed by detecting the smallest time  $(\bar{t}, \bar{j})$  when  $V(\tilde{x}(\bar{t}, \bar{j})) \leq 1$  namely it is 200 times smaller than the initial condition), and transient statistics (providing the lower left surface of Figure 6.3) is the averaged switching frequency over hybrid times up to  $t = \bar{t}/2$ , whereas the steady-state statistics (providing the lower right surface of Figure 6.3) are computed by focusing on hybrid times after  $\frac{3}{2}\bar{t}$  and until the end of the simulation run. The resulting two lower plots of Figure 6.3 confirm the same trends as in the space regularization case, even though here the steady-state tuning knob is given by scalar  $T$ .

Figure 6.6 shows the evolution of the Lyapunov function (6.7) with space regularization (left) and time regularization (right) for the same initial condition and different selections of the steady-state parameters  $\varepsilon$  and  $T$ . In the left plot, we may see that as  $\varepsilon$  is decreased, the solution comes closer to the operating point  $x_e$  but, as noticed in Section 4.3.2, the price to pay for such proximity is a high average switching frequency (indeed,  $x_e$  is not an equilibrium for the two dynamics of the switching scheme). Con-

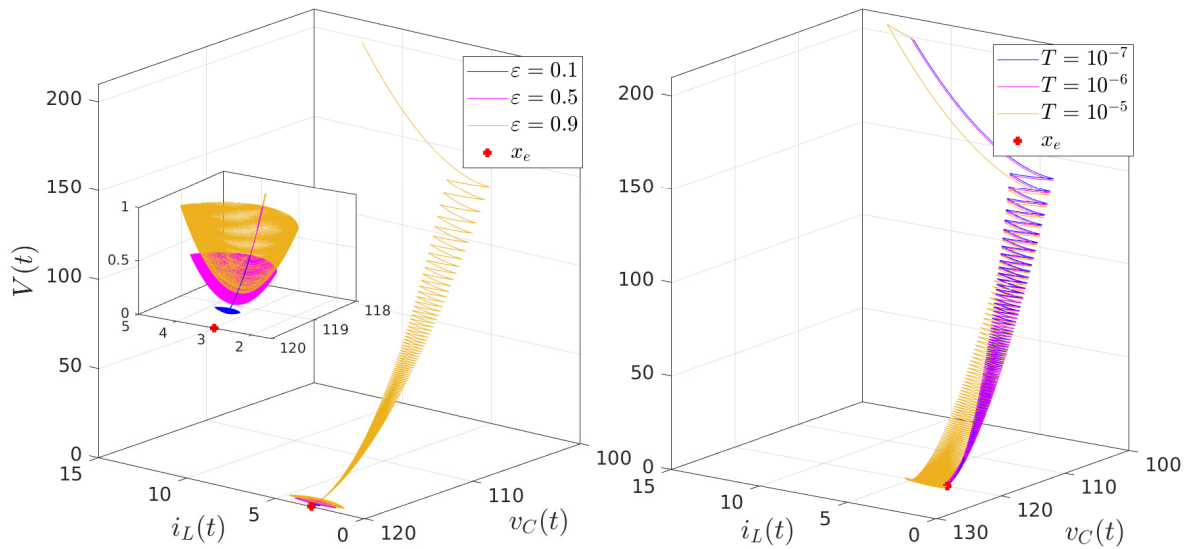


Figure 6.6: Lyapunov function  $V(\tilde{x})$  with space regularization (left) and with time regularization (right).

versely, for larger values of  $\varepsilon$ , the number of jumps decreases and, as expected, the error between  $x$  and  $x_e$  increases. Similarly, for the right plot of Figure 6.6, smaller values of  $T$  provide solutions that remain increasingly close to  $x_e$  exhibiting a large switching frequency, and vice-versa, the solutions exhibit a Zeno behavior when  $x \rightarrow x_e$ . Indeed, the number of jumps increases when  $\varepsilon$  is small (respectively, when  $T$  is small). When  $\varepsilon$  is large, (respectively, when  $T$  is large), the number of jumps decreases and as expected, the error between  $x$  and  $x_e$  increases, as we can see in Fig. 6.6. Hence, for practical reasons, it appears reasonable that a straight trade off between the number of jumps and error should be found.

## 6.4. Conclusions

In this chapter, we have dealt with practical stabilization of operating points for the power converters addressed in this thesis (which can be modeled as switched affine systems) by using a hybrid controller that performs a trade off between minimum dwell time and the size of the asymptotically stable set. Practical asymptotic stability is obtained by two design strategies, involving space- and time-regularization for SASs with constant parameters. Each one of these strategies is associated to a convenient tuning knob that may be used to perform a trade-off between the dwell time and the magnitude of the steady-state oscillations around the operating point. The switching frequency during the transient phase of the response can also be adjusted using another convenient knob, as seen in Chapter 4. This result can be easily applied

## 6.4. CONCLUSIONS

---

to DC-AC and AC-DC converters. The proposed construction has been numerically illustrated on a boost converter example.



## CHAPTER 7

# CONCLUSIONS AND PERSPECTIVES

---

### 7.1. Conclusions

In this dissertation, a hybrid modeling of power converters is used to design efficient control laws. Indeed, unlike many works in the literature, we propose to design some control laws taking into account both of continuous-time dynamics of the voltages and the currents and discrete-time nature of the switches. As a matter of fact, it appears that the hybrid dynamical framework given in [26] can be a suited manner of designing the control laws. Based on this formulation, some control results have been designed and listed:

1. The regulation of the output voltage of the boost converter and the one of the NPC converter, while considering the real nature of the electronic signals. The systems are controlled by managing the switched states. Thus, the stability and optimality of the hybrid closed loop are provided by using the hybrid dynamical system theory. Due to the character of the solution, which can be generalized in the sense of Filippov, the desired point is obtained with an arbitrarily fast switching, which makes the practical implementation impossible.
2. Following the main ideas developed in Chapter 5, we have proposed a hybrid control law for the half-bridge inverter, in the aim that the states track the desired sinusoidal references. As noticed in the previous item, This control law makes the system switch infinitely (Zeno phenomena) when  $x \rightarrow x_e$ .
3. To deal with the arbitrarily fast switching induced by the control, we guarantee a positive dwell time by modifying (regularizing) the chattering controllers using either space- or time-regularization techniques, where the former enforces dwell time using space-based hysteresis logics, and the latter uses instead an explicit timer inhibiting switches up to some guaranteed dwell time. Each one of these strategies is associated to a convenient tuning knob that may be used to

perform a trade-off between the dwell time and the magnitude of the steady-state oscillations around the operating point.

## 7.2. Perspectives

The development of this thesis has also generated several questions from different point of view and can be listed as:

- From theoretical point of view
  - For the NPC converter, to solve the problem of the time-varying system, a polytopic representation are proposed in order to embed the time-varying system into an uncertain model, which can be tackled easily by the proposed methodology. But one knows that this approach may be conservative and one wonder if it is possible to find a hybrid control law by taking the original model.
  - In this thesis, all the dynamical matrices are Hurwitz, which is realistic since it represents dynamics of the electronic circuit, which are at least asymptotic stable. A future work is to extend our approach to a larger class of systems including unstable open loop systems.
  - Extend this work on another complex converters, to cite some:
    - ◇ The boost inverter is composed by two DC-DC boost converters connected with a load which makes the closed loop nonlinear time-varying hybrid model and make a such system tracks a sinusoidal reference is a hard task.
    - ◇ Three-phase five-level NPC Converters are complex system because of the number of the state of the switches, which are important compared to rectifier and these will make the control design complex since find a common Lyapunov function for all theses combinations can be hard or even impossible.
- From practical point of view,
  - Altogether, the results presented in this manuscript remain theoretical results. As future works, the experimental implementation of the proposed hybrid controls could be done, following for instance the work of [66].



# Bibliography

---

- [1] N. Mohan and T. M Undeland. *Power electronics: converters, applications, and design*. John wiley & sons, 2007.
- [2] J. G. Kassakian, M. F. Schlecht, and G. C. Verghese. *Principles of power electronics*. adisson-wesley, publishing company, 1992.
- [3] H. Shu-hung Chung, H. Wang, F. Blaabjerg, and M. Pecht. *Reliability of power electronic converter systems*. Institution of Engineering and Technology, 2015.
- [4] M. H Rashid. *Power electronics handbook*. Butterworth-Heinemann, 2017.
- [5] G. Spagnuolo, G. Petrone, S. V. Araujo, C. Cecati, E. Friis-Madsen, E. Gubia, D. Hissel, M. Jasinski, W. Knapp, M. Liserre, P. Rodriguez, R. Teodorescu, and P. Zacharias. Renewable energy operation and conversion schemes: A summary of discussions during the seminar on renewable energy systems. *IEEE Industrial Electronics Magazine*, 4(1):38–51, March 2010.
- [6] T. M Undeland and W. P Robbins. *Power electronics: converters, applications and design*. Wiley, 2003.
- [7] S. Bacha, I. Munteanu, A. Iuliana Bratcu, et al. Power electronic converters modeling and control. *Advanced textbooks in control and signal processing*, 454:454, 2014.
- [8] T. G. Habetler and R. G. Harley. Power electronic converter and system control. *Proceedings of the IEEE*, 89(6):913–925, 2001.
- [9] J. Linares-Flores, A. Hernández Méndez, C. García-Rodríguez, and H. Sira-Ramírez. Robust nonlinear adaptive control of a boost converter via algebraic parameter identification. *IEEE Transactions on Industrial Electronics*, 61(8):4105–4114, Aug 2014.

- 
- [10] D.C. Lee, G.M. Lee, and K.D. Lee. Dc-bus voltage control of three-phase ac/dc pwm converters using feedback linearization. *IEEE Transactions on Industry Applications*, 36(3):826–833, May 2000.
- [11] H. El Fadil and F. Giri. Backstepping based control of pwm dc-dc boost power converters. In *2007 IEEE International Symposium on Industrial Electronics*, pages 395–400, June 2007.
- [12] K. B. Liu and C. S. Fann. Reducing output current ripple of power supply with component replacement. *Proceedings of EPAC. Lucerne, Switzerland, 2004*.
- [13] N. Mohan. *Power electronics: a first course*. Wiley, 2011.
- [14] D. M. Huynh, Y. Ito, S. Aso, K. Kato, and K. Teraoka. New concept of the dc-dc converter circuit applied for the small capacity uninterruptible power supply. In *2018 International Power Electronics Conference (IPEC-Niigata 2018 -ECCE Asia)*, pages 3086–3091, May 2018.
- [15] M. Junaid and B. Singh. Analysis and design of buck-boost converter for power quality improvement in high frequency on/off-line ups system. In *2014 IEEE International Conference on Power Electronics, Drives and Energy Systems (PEDES)*, pages 1–7, Dec 2014.
- [16] D. Li and X. Ruan. A high efficient boost converter with power factor correction. In *2004 IEEE 35th Annual Power Electronics Specialists Conference (IEEE Cat. No.04CH37551)*, volume 2, pages 1653–1657 Vol.2, June 2004.
- [17] T. H. Priya, A. M. Parimi, and U. M. Rao. Performance evaluation of high voltage gain boost converters for dc grid integration. In *2016 International Conference on Circuit, Power and Computing Technologies (ICCPCT)*, pages 1–6, March 2016.
- [18] S. Sinha, Vinayak, A. Gullapalli, S. S. John, and S. Kundu. Dc dc boost converter for thermoelectric energy harvesting. In *2018 International Conference on Current Trends towards Converging Technologies (ICCTCT)*, pages 1–4, March 2018.
- [19] M. Kermadi, Z. Salam, and E. M. Berkouk. An adaptive sliding mode control technique applied in grid-connected pv system with reduced chattering effect. In *2017 IEEE Conference on Energy Conversion (CENCON)*, pages 180–185, Oct 2017.
- [20] T. Ghennam, O. Bouhali, D. Maizi, E. M. Berkouk, and B. Francois. Theoretical study and experimental validation of a wind energy conversion system control with three-level npc converters. In *2012 XXth International Conference on Electrical Machines*, pages 2178–2183, Sep. 2012.
-

- [21] A. Nabae, I. Takahashi, and H. Akagi. A new neutral-point-clamped pwm inverter. volume IA-17, pages 518–523, Sept 1981.
- [22] J. Bordonau, M. Cosan, D. Borojevic, H. Mao, and F. C. Lee. A state-space model for the comprehensive dynamic analysis of three-level voltage-source inverters. In *Power Processing and Electronic Specialists Conference 1972*, volume 2, pages 942–948 vol.2, June 1997.
- [23] F. Umbria, F. Gordillo, and F. Salas. Model-based npc converter regulation for synchronous rectifier applications. In *IECON 2014 - 40th Annual Conference of the IEEE Industrial Electronics Society*, pages 4669–4675, Oct 2014.
- [24] F. Blaabjerg, R. Teodorescu, M. Liserre, and A. V. Timbus. Overview of control and grid synchronization for distributed power generation systems. *IEEE Transactions on Industrial Electronics*, 53(5):1398–1409, Oct 2006.
- [25] H. Akagi, Y. Kanazawa, and A. Nabae. Generalized theory of the instantaneous reactive power in three-phase circuits. *Proceedings of the International Power Electronics Conference-IEEJ IPEC-Tokyo'83*, pages 1375–1386, 1983.
- [26] R. Goebel, R.G. Sanfelice, and A.R. Teel. *Hybrid Dynamical Systems: modeling, stability, and robustness*. Princeton University Press, 2012.
- [27] R. G. Sanfelice and A. R. Teel. On singular perturbations due to fast actuators in hybrid control systems. *Automatica*, 47(4):692–701, 2011.
- [28] R. Goebel and A. R. Teel. Solutions to hybrid inclusions via set and graphical convergence with stability theory applications. *Automatica*, 42(4):573–587, 2006.
- [29] P. Kokotovic, H. K. Khali, and J. O'reilly. *Singular perturbation methods in control: analysis and design*, volume 25. Siam, 1999.
- [30] C. Albea Sanchez, G. Garcia and L. Zaccarian. Hybrid dynamic modeling and control of switched affine systems: application to DC-DC converters. In *54th IEEE Conference on Decision and Control*, Osaka, Japan, December 2015. An extended version is available in: <https://hal.archives-ouvertes.fr/hal-01220447v3/document>.
- [31] S. Mariéthoz, S. Almér, M. Bâja, A.G. Beccuti, D. Patino, A. Wernrud, J. Buisson, H. Cormerais, T. Geyer, H. Fujioka, et al. Comparison of hybrid control techniques for buck and boost dc-dc converters. *IEEE Trans. on Control Systems Technology*, 18(5):1126–1145, 2010.
- [32] G. S. Deaecto, J. C. Geromel, F.S. Garcia, and J.A. Pomilio. Switched affine systems control design with application to DC-DC converters. *IET control theory & applications*, 4(7):1201–1210, 2010.

- 
- [33] L. Martínez-Salamero, G. Garcia, M. Orellana, C. Lahore, B. Estibals, C. Alonso, and C.E. Carrejo. Analysis and design of a sliding-mode strategy for start-up control and voltage regulation in a buck converter. *IET Power Electronics*, 6(1):52–59, 2013.
- [34] C. Prieur, A. R. Teel, and L. Zaccarian. Relaxed persistent flow/jump conditions for uniform global asymptotic stability. *IEEE Trans. on Automatic Control*, 59(10):2766–2771, October 2014.
- [35] D. Liberzon and A.S. Morse. Basic problems in stability and design of switched systems. *IEEE Control Systems Magazine*, 19(5):59–70, 1999.
- [36] H. K. Khalil. *Nonlinear Systems*. Prentice Hall, third edition edition, 2002.
- [37] R. G. Sanfelice, D. Copp, and P. A Nanez. A toolbox for simulation of hybrid systems in Matlab/Simulink: Hybrid equations (HyEQ) toolbox. In *Hybrid Systems: Computation and Control Conference*, 2013.
- [38] K. Al-Haddad H. Kanaan and F. Fnaiech. Modelling and control of three-phase/switch/level fixed-frequency pwm rectifier: state-space averaged model. *IEE Proceedings - Electric Power Applications*, 152(3):551–557, May 2005.
- [39] A. Yazdani and R. Iravani. A generalized state-space averaged model of the three-level NPC converter for systematic dc-voltage-balancer and current-controller design. *IEEE Transactions on Power Delivery*, 20(2):1105–1114, April 2005.
- [40] Y. Zhang Y. Zhang T. Lu, Z. Zhao and L. Yuan. A novel direct power control strategy for three-level pwm rectifier based on fixed synthesizing vectors. In *2008 International Conference on Electrical Machines and Systems*, pages 1143–1147, Oct 2008.
- [41] Y. Cho I. Won and K. Lee. Predictive control algorithm for capacitor-less inverters with fast dynamic response. In *2016 IEEE International Conference on Power and Energy (PECon)*, pages 479–483, Nov 2016.
- [42] L. Xie X. Li Z. Liu, F. Gao and L. Xie. Predictive functional control for buck dc-dc converter. In *The 27th Chinese Control and Decision Conference (2015 CCDC)*, pages 320–325, May 2015.
- [43] D. Kalyanraj and S. L. Prakash. Design of sliding mode controller for three phase grid connected multilevel inverter for distributed generation systems. In *2016 21st Century Energy Needs - Materials, Systems and Applications (ICTFCEN)*, pages 1–5, Nov 2016.
-

- [44] L. Hou Z. Liu X. Zheng, K. Qiu and C. Wang. Sliding-mode control for grid-connected inverter with a passive damped lcl filter. In *2018 13th IEEE Conference on Industrial Electronics and Applications (ICIEA)*, pages 739–744, May 2018.
- [45] H. A. Bouziane M. B. Debbat and R. B. Bouiadjra. Sliding mode control of two-level boost dc-dc converter. In *2015 4th International Conference on Electrical Engineering (ICEE)*, pages 1–5, Dec 2015.
- [46] C. S. Sachin and S. G. Nayak. Design and simulation for sliding mode control in dc-dc boost converter. In *2017 2nd International Conference on Communication and Electronics Systems (ICCES)*, pages 440–445, Oct 2017.
- [47] C. Albea Sanchez, O. Lopez Santos, D.A. Zambrano Prada, F. Gordillo, and G. Garcia. Hybrid control scheme for a half-bridge inverter. *IFAC-PapersOnLine*, 50(1):9336–9341, 2017.
- [48] J. D. Barros and J. F. Silva. Optimal predictive control of three-phase npc multi-level converter for power quality applications. *IEEE Transactions on Industrial Electronics*, 55(10):3670–3681, Oct 2008.
- [49] J. F. A. Silva J. D. Barros and E. G. A. Jesus. Fast-predictive optimal control of npc multilevel converters. *IEEE Transactions on Industrial Electronics*, 60(2):619–627, Feb 2013.
- [50] V. Utkin Y. Alsmadi and L. Xu. Sliding mode control of ac/dc power converters. In *4th International Conference on Power Engineering, Energy and Electrical Drives*, pages 1229–1234, May 2013.
- [51] C. Albea Sanchez, G. Garcia, S. Hadjeras, M.W.P.M.H. Heemels, and L. Zaccarian. Practical stabilisation of switched affine systems with dwell-time guarantees. 2017. Report.
- [52] Z. Galias and X. Yu. Discretization effects in single input delayed sliding mode control systems. In *2013 European Conference on Circuit Theory and Design (ECCTD)*, pages 1–4, Sept 2013.
- [53] S. Hadjeras, C. Albea. Sanchez, and G. Garcia. Hybrid adaptive control of the boost converter. In *2017 IEEE 56th Annual Conference on Decision and Control (CDC)*, pages 5720–5725, Dec 2017.
- [54] B.A. Francis. The linear multivariable regulator problem. *SIAM Journal on Control and Optimization*, 15(3):486–505, 01 1977.

- 
- [55] A. Serrani, A. Isidori, and L. Marconi. Semi-global nonlinear output regulation with adaptive internal model. *IEEE Transactions on Automatic Control*, 46(8):1178–1194, Aug 2001.
- [56] M. Senesky, G. Eirea, and T.J. Koo. Hybrid modelling and control of power electronics. In *Hybrid Systems: Computation and Control*, volume 2623 of *Lecture Notes in Computer Science*, pages 450–465. Springer Berlin Heidelberg, 2003.
- [57] J. Buisson, P.Y. Richard, and H. Cormerais. On the stabilisation of switching electrical power converters. In *Hybrid Systems: Computation and Control*, volume 3414 of *Lecture Notes in Computer Science*, pages 184–197. Springer Berlin Heidelberg, 2005.
- [58] T. A.F. Theunisse, J. Chai, R.G. Sanfelice, and W.P. Heemels. Robust global stabilization of the dc-dc boost converter via hybrid control. *IEEE Trans. on Circuits and Systems I: Regular Papers*, 62(4):1052–1061, 2015.
- [59] G. Escobar, A.J. Van Der Schaft, and R. Ortega. A hamiltonian viewpoint in the modeling of switching power converters. *Automatica*, 35(3):445–452, 1999.
- [60] L. Hetel and E. Fridman. Robust sampled-data control of switched affine systems. *IEEE Trans. on Automatic Control*, 58(11):2922–2928, 2013.
- [61] Z. Sun. A robust stabilizing law for switched linear systems. *International Journal of Control*, 77(4):389–398, 2004.
- [62] D. Liberzon. *Switching in systems and control*. Birkhauser, 2003.
- [63] L. Hetel and E. Bernuau. Local stabilization of switched affine systems. *IEEE Transactions on Automatic Control*, 60(4):1158–1163, 2015.
- [64] A. Seuret, C. Prieur, S. Tarbouriech, A.R. Teel, and L. Zaccarian. A non-smooth hybrid invariance principle applied to robust event-triggered design. *Submitted to IEEE Transactions on Automatic Control*. See also: <https://hal.archives-ouvertes.fr/hal-01526331/>, 2017.
- [65] H.K. Khalil. *Nonlinear systems, vol. 3*. Prentice Hall, 2002.
- [66] A. Sferlazza, L. Martínez-Salamero, C. Albea Sanchez, G. Garcia, and C. Alonso. Min-type control strategy of a dc-dc synchronous boost converter. *IEEE Transactions on Industrial Electronics*, 2019.